



University of
Stavanger

Faculty of Science and Technology

MASTER'S THESIS

Study program/ Specialization: Offshore Technology – Marine and Subsea Technology	Spring semester, 2015 Open / Restricted access
Writer: Sandra Djupevåg Eri (Writer's signature)
Faculty supervisor: Professor Arnfinn Nergaard	
Thesis title: Analysis of Operability in Installing Heavy Subsea Modules	
Credits (ECTS): 30	
Key words: - Vessel operability - Heavy subsea modules - Splash zone - Monohull - Twin-hull	Pages: 72 + enclosure: 21 Stavanger, 09.06.2015

Abstract

Today (2015) subsea technology is a big part of the oil and gas industry. New subsea solutions are developed rapidly and large components that previously were placed on a platform are now being moved subsea towards the vision of a complete subsea processing facility. In order to ensure high operability of the subsea systems, it is essential to be able to perform marine lifting operations of subsea structures all year. This implies that high operability and large lifting capacity of the vessels are necessary.

This report deals with how the weight of subsea modules affects the vessel operability during installation operations. Subsea installation operations, from a typical 145 meter long construction vessel, have been analyzed, and limiting operational seastates for installation of three heavy subsea modules are defined. To evaluate the vessel's ability to install the subsea modules, the marine dynamics program OrcaFlex has been used. The analysis is based on lifting the modules through the splash zone. Estimation of vessel operability and probability of experiencing a sufficiently long weather window for the operation period are conducted. Furthermore, a qualitative comparison study of monohull and twin-hull vessels has been performed to get an indication of whether they can compete on the same market.

The operability of the vessel has been calculated for installation of a module weighing 289 tons, 400 tons and 600 tons. Results from the feasibility study revealed that installation of the two lightest modules could be achieved in high seastates with high operability in North Sea environment. For installation of the heaviest module, the limiting seastate was reduced significantly, with a lower operability as consequence. The limiting seastate and operability for installation of the mentioned modules can be seen in table 1.1.

Table 1.1: Limiting seastate and operability for installation of three heavy subsea modules

Installation of module weighing	Limiting seastate, H_s [m]	Total operability [%]
289 tons	4.5	94.6
400 tons	4.0	92.6
600 tons	3.0	86.2

The qualitative comparison study revealed that the seastate is the limiting factor when performing subsea installation operations, and that the vessel motions are of less significance. Although a semi-submersible has favorable motion characteristics, it will not obtain a higher operability than a comparable monohull vessel. Furthermore, semi-submersibles generally have a higher lightship weight and they have a more complex structure compared to monohulls, which results in a higher cost of lightship weight per unit from the shipyard.

Acknowledgement

This master thesis was written during spring semester of 2015 at the Faculty of Science and Technology at the University of Stavanger. The work has been limited to the period between January - June 2015.

First of all, I would like to express my gratitude to my adviser, Professor Arnfinn Nergaard, for his support, guidance and encouragement throughout the entire work of my thesis.

Secondly, I would like to thank Adekunle Orimolade and Dreng Viki for their help and advice towards learning the simulation program OrcaFlex.

Next, I would like to thank Gretha Rosland (Statoil ASA), Jarle Marius Solland (Statoil ASA), Arild Ramstad (Statoil ASA), Johannes Eldøy (Salt Ship Design) and Margareth Gram (Salt Ship Design) for taking the time to meet and discuss the project with me in the early phase of its development.

I would also like to thank my parents, Kjell Eri and Anne Kari Djupevåg, my sister Marie Djupevåg Eri and my brother Gaute Djupevåg Eri for helping me during my years of study and for always being supportive of me.

Lastly I would like to thank my boyfriend Torstein Eldøy for his encouragement and support during my work with this thesis.

Sandra Djupevåg Eri
University of Stavanger
June 2015

Table of Contents

ABSTRACT	I
ACKNOWLEDGEMENT	II
TABLE OF CONTENTS	III
LIST OF FIGURES	VI
LIST OF TABLES	IX
ABBREVIATIONS	XI
NOMENCLATURE	XII
1 INTRODUCTION	1
1.1 Background	1
1.2 Objective	1
1.3 Limitations	2
1.4 Organization of the Thesis	3
2 BACKGROUND INFORMATION	4
2.1 Market Forecast	4
2.2 Subsea Production Systems	5
2.3 Subsea Installation	6
2.3.1 Lift off From Deck	7
2.3.2 Lowering Through the Wave Zone	8
2.3.3 Landing on the Seabed	8
3 STATE OF THE ART	9
3.1 Processing on the Seabed	9
3.1.1 Today’s Achievements Related to Subsea Processing	9
3.1.1.1 Boosting	10
3.1.1.2 Separation	10
3.1.1.3 Water Injection	11
3.1.1.4 Gas Compression	11
3.1.2 Future: The Statoil “ Subsea Factory”	12
3.2 Vessels	13
3.2.1 Monohull	14
3.2.2 Twin-Hull	16
4 FEASIBILITY STUDY – INSTALLATION OF HEAVY MODULE	20
4.1 Dynamic Analysis	20

4.1.1	Installation Vessel	20
4.1.2	Subsea Structures	22
4.1.2.1	Hydrodynamic Added Mass	22
4.1.2.2	Mass Moment of Inertia	26
4.1.2.3	Displaced Volume of Water	26
4.1.2.4	Drag, Inertia and Slam	27
4.1.3	Lifting Wire	29
4.1.4	Environment	29
4.1.4.1	Wave Spectrum	30
4.1.4.2	Significant Wave Height and Zero-Up-Crossing Period	32
4.2	Operational Criterion	33
4.2.1	Slack Sling Criterion	33
4.2.2	Capacity Check	34
4.2.3	Operational Criterion Dynamic Analysis	37
4.3	Dynamic Analysis Result	39
4.3.1	Effective Tension in Different Wave Direction	39
4.3.2	Effective Tension in Different Significant Wave Height	41
4.3.3	Highest and Lowest Effective Tension in Lifting Wire	42
4.3.3.1	Module 289 tons	43
4.3.3.2	Module 400 tons	44
4.3.3.3	Module 600 tons	45
4.3.4	Limiting Seastates	46
4.4	Vessel Operability	48
4.5	Evaluation of Weather Window	50
4.5.1	Weather Restricted and Unrestricted Operation	50
4.5.2	Operation Reference Period	50
4.5.3	Probability of Acceptable Weather Window	51
4.5.3.1	Not Including Uncertainty in Weather Forecast	52
4.5.3.2	Including Uncertainty in Weather Forecast	53
4.6	Discussion and Main Findings Feasibility Study	56
5	QUALITATIVE COMPARISON - MONOHULL VS. TWIN-HULL	58
5.1	Motion Behavior and Operability	58
5.2	Lightship Weight Comparison	60
5.2.1	Monohull	61
5.2.2	Twin-hull	63

5.3 Discussion and Main Findings Qualitative Comparison.....	64
6 CONCLUSION	66
7 FURTHER WORK	67
8 REFERENCES.....	68

APPENDIX A - INPUT ORCAFLEX

APPENDIX B - HIGHEST AND LOWEST EFFECTIVE TENSION IN LIFTING WIRE
OBTAINED FROM ORCAFLEX

APPENDIX C - WEATHER STATISTICS

APPENDIX D - VESSEL DATA CALCULATION

List of Figures

Figure 2.1: Production forecast for the NCS up to 2030 (NPD, 2015)	4
Figure 2.2: Total number of cumulative subsea wells installed since 1990 (Helix Energy Solutions, 2015)	4
Figure 2.3: Åsgard subsea compressor station (Hedne, 2013), (Davies, Ramberg, Økland, & Rognhø, 2013).....	6
Figure 2.4: Subsea installation phases (Nielsen, 2012).....	7
Figure 3.1: Worldwide locations for subsea pumping, compression, separation and water injection systems (Intecsea, 2014)	9
Figure 3.2: Subsea factory existing components (Davies et al., 2013)	13
Figure 3.3: Far Saga (Nordhal, 2002).....	14
Figure 3.4: Viking Neptun (Reachsubsea, 2015)	15
Figure 3.5: Seven Arctic (Subsea 7, 2014).....	15
Figure 3.6: Normand Maximus (Solstad, 2015).....	16
Figure 3.7: SWATH (left side) and semi-submersible (right side) vessel (Hovland, 2007)	17
Figure 3.8: Twin-hull offshore support and construction vessels (Marinetraffic, 2015), (Gusto MSC, 2009), (Norsk kystfart, 2002)	17
Figure 3.9: Q4000 semi-submersible (Marinetraffic, 2015)	18
Figure 3.10: Semi-submersible intervention vessel Q7000 (Helix Energy Solutions, 2013)	19
Figure 3.11: CSS Derwent (Hallin, 2014).....	19
Figure 4.1: Vessel motion characteristics in a coordinate system (Rawson & Tupper, 2001).....	21
Figure 4.2: Wave directions with respect to vessel	22
Figure 4.3: Hydrodynamic added mass (Sakar & Gudmestad, 2010).....	25

Figure 4.4: Drag force on a structure (Subsea 7, 2010).....	27
Figure 4.5: Slamming load on a structure (Subsea 7, 2010)	28
Figure 4.6: Irregular waves (Journee and Maissie, 2001)	30
Figure 4.7: Effect of peak shape parameter for $H_s=4\text{m}$, $T_p=8\text{s}$ (DNV-RP-H103 p.18, 2014).....	31
Figure 4.8: Lifting through the splash zone (Subsea 7, 2010).....	37
Figure 4.9: Highest effective tension versus depth of submergence when installing a module weighing 289t in $H_s=2.5\text{m}$, in heading 165° , 180° and 190°	40
Figure 4.10: Lowest effective tension versus depth of submergence when installing a module weighing 289t in $H_s=2.5\text{m}$, in heading 165° , 180° and 190°	40
Figure 4.11: Highest effective tension versus depth of submergence for all significant wave heights in heading 165° , when installing a module weighing 289t.....	41
Figure 4.12: Lowest effective tension versus depth of submergence for all significant wave heights at heading 165° , when installing a module weighing 289t.....	42
Figure 4.13: Probability of acceptable weather window for installing the different modules through out the year, not included uncertainty in weather	53
Figure 4.14: Operation periods (DNV-OS-H101 p. 29, 2011).....	53
Figure 4.15: Probability of acceptable weather window for installing the different modules through out the year, included uncertainty in weather	55
Figure 5.1: RAO for heave, wave heading 0° (Moss Maritime, 2002)	59
Figure 5.2: Wave energy versus wave period North Sea (Gudmestad, 2014)	59
Figure 5.3: Vessel displacement weight breakdown	60
Figure 5.4: Lightship weight versus ship length based on Hovland's (2007) curve, monohull vessels	62
Figure 5.5: DWT and LSW monohull vessels (Marinetraffic.com, 2015), (Subsea 7, 2014), (Solstad, 2015), (Hovland, 2007).....	62

Figure 5.6: Some typical small semi-submersible design with lightship weight and displacement (Clauss et al., 1992), (Kaltvedt, 2014), (Diamond Offshore, 2014), (Schepman & Santen, 1991)	63
Figure 5.7 Displacement versus lightship weight, monohull and twin-hull vessels	64

List of Tables

Table 1.1: Limiting seastate and operability for installation of three heavy subsea modules.....	I
Table 2.1: Weight and dimensions of typical subsea structures (Wang et al., 2012).....	5
Table 4.1: Subsea modules for installation operation	22
Table 4.2: Added mass coefficient (DNV-RP-H103 p.148, 2014)	24
Table 4.3: Added mass for different submergence levels in z-direction.....	25
Table 4.4: Common wave spectra in different regions (Gudmestad, 2014).....	31
Table 4.5: Average values experiment data JONSWAP wave spectrum (DNV-RP-H103 p.18, 2014)	31
Table 4.6: Significant wave height and corresponding zero-up-crossing periods and peak periods	33
Table 4.7: Highest and lowest allowable effective tension for installation of a module weighing 289t.....	38
Table 4.8: Highest and lowest allowable effective tension for installation of a module weighing 400t.....	38
Table 4.9: Highest and lowest allowable effective tension for installation of a module weighing 600t.....	38
Table 4.10: Upper limit criterion, highest effective tension in lifting line [kN] - module 289t.....	43
Table 4.11: Lower limit criterion, lowest effective tension in lifting line [kN] - module 289t	44
Table 4.12: Upper limit criterion, highest effective tension in lifting line [kN] - module 400t.....	44
Table 4.13: Lower limit criterion, lowest effective tension in lifting line [kN] - module 400t	45
Table 4.14: Upper limit criterion, highest effective tension in lifting line [kN] - module 600t.....	46
Table 4.15: Lower limit criterion, lowest effective tension in lifting line [kN] - module 600t	46

Table 4.16: Limiting design seastates – installation module weighing 289t.....	47
Table 4.17: Limiting design seastates – installation module weighing 400t.....	47
Table 4.18: Limiting design seastates – installation module weighing 600t.....	47
Table 4.19: Operable seastates in the North Sea for installation of a module weighing 289t.....	48
Table 4.20 Operable seastates in the North Sea for installation of a module weighing 400t.....	49
Table 4.21: Operable seastates in the North Sea for installation of a module weighing 600t.....	49
Table 4.22: α -factors for waves, level B highest forecast (DNV-OS-H101 p. 32, 2011).....	54
Table 4.23: Design significant wave height, α -factor factor and operational criteria.....	54

Abbreviations

AHC	Active Heave Compensated
CFD	Computational Fluid Dynamics
CSS	Compact Semi Submersible
DAF	Dynamic Amplification Factor
DNV	Det Norske Veritas
DWT	Dead Weight Tonnage
ESP	Electrical Submersible Pump
IMR	Inspection Maintenance and Repair
LSW	Light Ship Weight
MHS	Module Handling System
NCS	Norwegian Continental Shelf
NPD	Norwegian Petroleum Directorate
NPV	Net Present Value
OCV	Offshore Construction Vessel
PSV	Platform Supply Vessel
RAO	Response Amplitude Operator
ROV	Remotely Operated Vehicle
RSWI	Raw Sea Water Injection
SPIV	Subsea Processing Intervention Vessel
SWL	Safe Working Load
SWATH	Small Waterplane Area Twin Hull

Nomenclature

A_{33}	Added mass in heave for perforated structure
A_{33o}	Added mass for flat plate
A_{33s}	Solid added mass
A_p	Area of submerged part of object projected on a horizontal plane
A_s	Slam area
A_{wire}	Effective cross section area of wire
a	Short side of the structure normal to flow direction
B	Vessel breadth
b	Long side of the structure normal to flow direction
C_A	Hydrodynamic added mass coefficient
C_b	Block coefficient
C_{D_x}	Hydrodynamic drag coefficient x-direction
C_{D_y}	Hydrodynamic drag coefficient y-direction
C_{D_z}	Hydrodynamic drag coefficient z-direction
C_F	Fill factor for wire rope
C_M	Hydrodynamic inertia coefficient
c	Damping
D	Wire diameter
D	Vessel depth
d	Duration of operation
E	Modulus of rope elasticity
$F_{dynamic}$	Minimum dynamic force in wire
F_{static}	Static force in wire when the structure is partly or fully submerged, but the flooding has not yet started

g	Acceleration of gravity
H_s	Significant wave height
h	Height of object
I_x	Mass moment of inertia around x-axis
I_y	Mass moment of inertia around y-axis
I_z	Mass moment of inertia around z-axis
$K_{1,2}$	Constant for specific ship type
k	System stiffness
k_{wire}	Wire stiffness
L	Length of wire
L	Length of the underwater form of vessel
M	Weight of module in air
m	Object mass
OP_{LIM}	Design criteria
OP_{WF}	Operational criteria
$P(d)$	Probability of a weather window greater than the duration of the operation
p	Perforation rate
$S(\omega)$	Wave energy spectrum
T_C	Estimated maximum contingency time
T_{POP}	Planned operation period
T_p	Peak period
T_R	Operation reference period
T_z	Zero-up-crossing period
V	Volume of displaced water
V_R	Reference volume
W_s	Steel weight

X	Displacement amplitude
x	Length of module
y	Width of module
z	Height of module
z	Position function of object
z_h	Solution of the homogeneous equation
z_p	Solution of the particular equation
\ddot{z}	Acceleration
\dot{z}	Velocity
α	Alpha factor
β	Mean duration of weather window below threshold
λ	Factor between height of object and area of submerged part
ρ_o	Density of object
ρ_w	Density of seawater
∇	Displaced volume of water
ω	Angular Frequency
γ	Peak shape parameter
σ_a	Spectral width parameter a
σ_b	Spectral width parameter b
θ	Phase angle

1 Introduction

In this chapter, background and objective of the thesis are given, followed by its limitations. Lastly a description of the organization of the report is presented.

1.1 Background

Over the last decade subsea technology has become an important part of the oil and gas industry. New subsea solutions are developed rapidly and large components that previously were placed on a platform are now being moved subsea towards the vision of a complete subsea processing facility.

Today (2015) Offshore Construction Vessels (OCV) performs most of the subsea installation operations, and the largest OCVs on the market have a lifting capacity of 400 tons. However, this past year Toisa, Subsea 7, DOF Subsea and Technip have ordered vessels with crane capacity from 600 to 900 tons.

In order to ensure high operability of a subsea system, it is essential to be able to install and replace modules all year. As the quantity and weight of subsea modules increase, high operability and large lifting capacity of the installation vessels are required.

1.2 Objective

The main objective of this thesis is to study subsea installation operations from a typical 145 meter long construction vessel. Installation of three different subsea structures will be considered, in order to study how the weight of the module affect the vessel's ability to perform the operation. The goal is to define limiting seastates for the operations, and further evaluate the vessel operability and probability of experiencing a sufficiently long weather window for the operation. Another objective is to perform a qualitative comparison of monohull and twin-hull vessels, where the goal is to get an indication of whether they can compete on the same market.

Secondary objectives will be as follows:

- Establish an overview of monohull and twin-hull vessels on the subsea lifting market
- Simulate splash zone lifting operations performed by a typical 145 meter long OCV for installation of a subsea module weighing 289 tons, 400 tons and 600 tons
- Study the forces that act on the subsea modules at different levels of submergence during the installation operations
- Study how wave direction and height influence the installation operations
- Define limiting seastates for installation of the three subsea modules
- Calculate total vessel operability for installation of the three subsea modules

- Determine the probability of experiencing an acceptable weather window for the operation to be carried out in all twelve months, with and without accounting for uncertainty in the weather
- Compare monohull construction vessels and semi-submersibles in order to get an indication of whether they can compete on the same market

1.3 Limitations

The marine dynamics program OrcaFlex, developed by Orchina, was used to simulate installation operations of three subsea structures. The dynamic analysis was performed in a simplified manner. The splash zone phase was considered the most critical phase of the operation, thus determining the operational seastate. There is, however a possibility that other phases of the installation operation may be more critical.

Only vertical relative motion between the subsea module and water was accounted for in the dynamic analysis. Other modes of motions were disregarded. Furthermore, it was assumed that the motion of the crane tip was fixed and that it followed the motion of the vessel. This means that in the analysis, the stiffness of the crane and Active Heave Compensated (AHC) effects were not accounted for.

The effect of swells was not accounted for in the dynamic analysis. A swell is a long relatively low wind generated wave that has moved away from the storm that generated it. During the installation operation the vessel was approaching the waves head sea. Swells with different directions, especially from beam side, could cause heavy roll accelerations. Therefore, if swells were included in the analysis, the vessel operability could possibly have been reduced.

Hydrodynamic loads acting on the subsea module were estimated according to a simplified method developed by Det Norske Veritas (DNV) (DNV-RP-H103 p.61, 2014). This method gives conservative estimations of the forces that act on the module during lowering from air down through the wave zone. To estimate the largest allowable force acting on the module during the operation, a dynamic amplification factor value was assumed to be equal to 1.75, with respect to the static weight of the subsea module.

Simulations were performed for significant wave heights up to 5 meters, corresponding zero-up-crossing periods and wave headings +/- 15° head seas. Response Amplitude Operators (RAO) for a typical 145 meter long OCV were imported to OrcaFlex, and the analysis was based on this vessel.

1.4 Organization of the Thesis

Chapter 2 will present background information for the thesis. An understanding of why it is an important topic will be established by presenting a brief overview of the subsea market forecast. Subsea processing will be presented and some examples with respect to size and weight of installed structures will be given. The phases of a subsea installation operation will also be described.

In chapter 3, state of the art subsea processing structures, and monohull and twin-hull vessels on the subsea installation market will be presented.

In chapter 4, a feasibility study will be carried out on installation of heavy subsea modules performed by a typical 145 meter long OCV. This will include dynamic analyses of three installation operations. A description will be given of how the installation scenario was modeled using OrcaFlex software, which parameters were used for the simulations, and how they were calculated. Operational requirements will be established, and a presentation of the forces that act on the modules during the operations will be given. Lastly, an evaluation of vessel operability and probability of a sufficient weather window will be presented. The result of the analysis will be presented and discussed.

Chapter 5 will include a qualitative comparison of monohull construction vessels and semi-submersibles. Motion behavior and lightship weight of the two vessel types will be presented. The results of the analysis will be presented and discussed.

In chapter 6, main findings and concluding remarks will be presented. Chapter 7 will present recommendations for future work.

2 Background Information

In this chapter, background for the thesis is given. The chapter is divided into three sections, where the first section, section 2.1 looks at the market forecast for the subsea industry. Section 2.2 gives an explanation of subsea production systems and introduces some examples with respect to size and weight of installed structures. The last section of this chapter, section 2.3 addresses subsea installation operations.

2.1 Market Forecast

According to the Norwegian Petroleum Directorate (2015) (NPD), 20% of the resources on the Norwegian Continental Shelf (NCS) are not yet discovered. In 2014, 90 discoveries were made on the NCS, and it is expected that 68 of these discoveries will be developed as subsea solutions. In figure 2.1 below the production forecast up to 2030 for the NCS is shown.

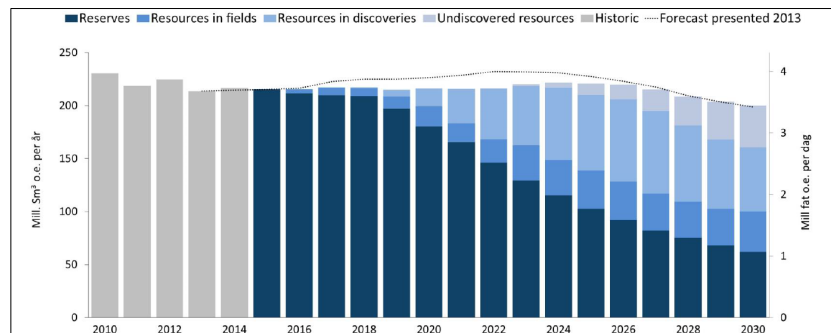


Figure 2.1: Production forecast for the NCS up to 2030 (NPD, 2015)

Extraction of hydrocarbons from subsea applications has increased significantly in the last 15 years. In 1978 there were a total of 140 operational subsea wells worldwide. Today it has exceeded a number of 5000 (DNV, 2014). Figure 2.2 below shows the total cumulative number of subsea wells installed worldwide since 1990.

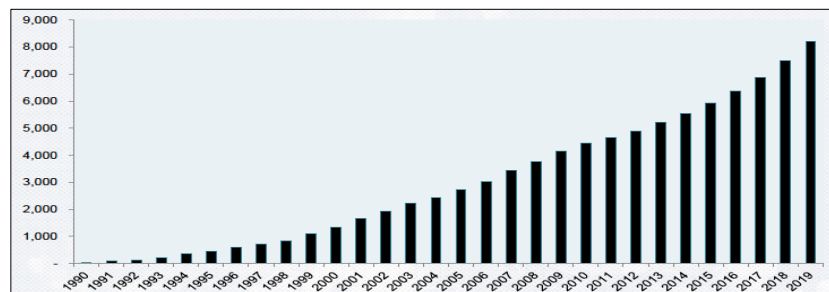


Figure 2.2: Total number of cumulative subsea wells installed since 1990 (Helix Energy Solutions, 2015)

Quest Offshore Resources predicts that by 2019 the total number of subsea wells will exceed 8000 (Helix Energy Solutions, 2015).

2.2 Subsea Production Systems

The world's first subsea production system was installed in the Gulf of Mexico at a water depth of 16.7 meters in 1961. Since then, the subsea application has continued to grow (Moreno-Trejo, 2012). The first subsea development on the NCS, Ekofisk, started to produce in 1971 at a water depth of 67 meters (DNV, 2014).

The term “subsea production system” refers to production equipment that is installed on the seabed for the purpose of extracting hydrocarbons from a reservoir. Moreno-Trejo (2012) defines a subsea production system as:

“An arrangement of subsea components, equipment or facilities installed on the seabed to produce oil and gas fields. It includes equipment on the seabed, such as components, structures, valves, processing equipment, control or monitoring devices, as well as underwater interventions services such as, installation, inspections, maintenance, modification or upgradation and removal services needed to assure functional and technical performance of the system.”

A result of development in the subsea industry is that subsea modules are becoming larger. Structures that have been installed on the seabed vary in size, weight and shape. Table 2.1 below shows weight and dimensions of some typical subsea structures. The presented numbers are approximations.

Table 2.1: Weight and dimensions of typical subsea structures (Wang et al., 2012)

Subsea structure	Weight [t]	Dimension (l×b×h)(Ø×h) [m]
Processing modules	200 - 400	Up to (15×15×18)
Pumping modules	5 - 50	(1×1×1.5) - (5×5×6)
Subsea trees	10 - 70	Up to (5×5×6)
Template	100 - 400	(10×10×6) - (30×20×7)
Manifolds	50 - 400	(5×5×4) - (25×20×8)
Riser base	50 - 200	Up to (20×20×10)
Suction pile	40 - 200	(4.5×15) - (10×30)

Another more concrete example regarding weight and dimensions of subsea structures is the subsea compressor station that will be installed at the Åsgard field in 2015. The subsea compressor station includes two parallel compression trains. Each of the two compressor trains contains an inlet and anti-surge cooler module, a scrubber module, a compressor module, a pump module and a discharge cooler module. Figure 2.3 shows the weight and dimensions of these modules, including the compressor template and manifold station.

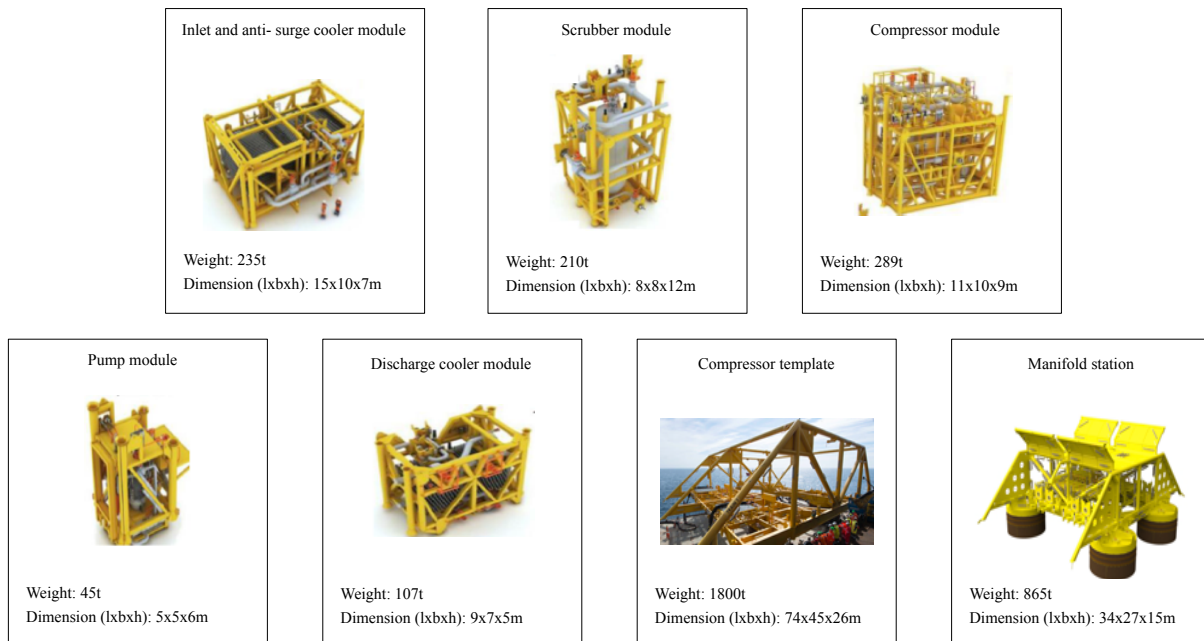


Figure 2.3: Åsgard subsea compressor station (Hedne, 2013), (Davies, Ramberg, Økland, & Rognhø, 2013)

By comparing table 2.1 and the numbers in figure 2.3 it can be seen that many of the structures that will be installed at the Åsgard field are larger than typical processing modules, templates and manifolds today.

2.3 Subsea Installation

As a result of the growing number of subsea installations, marine lifting operations of subsea structures have become very common. According to DNV-RP-H103 (2014) section 3.1.2, a subsea installation can be divided into the following main phases:

1. Lift off from deck
2. Lift in air and maneuvering object clear of transportation vessel
3. Lowering through wave zone
4. Further lowering down to sea bed
5. Positioning and landing

During planning of a subsea installation, these phases have to be carefully examined (DNV-RP-H103 p. 31, 2014). By analyzing the various phases, maximum allowable seastate for when the structure can be installed safely may be determined (Sarkar & Gudmestad, 2010). Typically the operational limitations are expressed in terms of significant wave height, H_s and peak period, T_p . Lift off from deck, lowering through the wave zone and landing the structure on the seabed are considered to be the most challenging phases. Figure 2.4 shows an illustration of the five phases of a subsea installation operation.

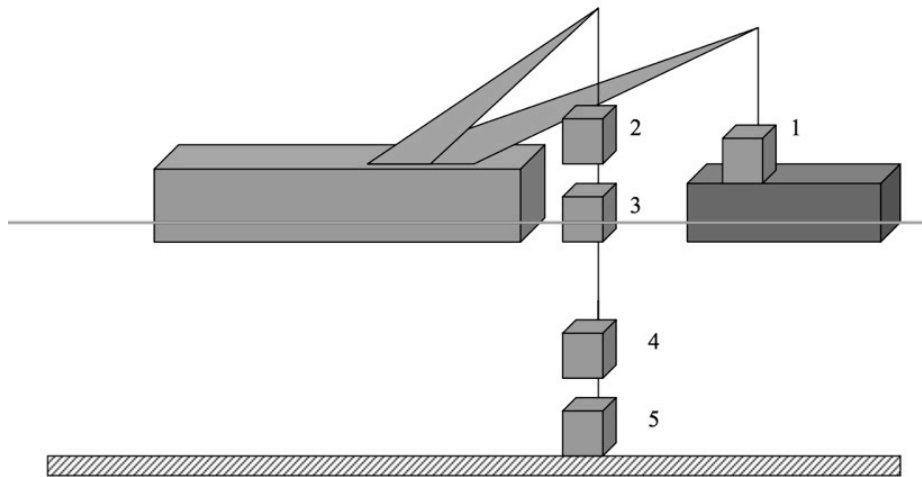


Figure 2.4: Subsea installation phases (Nielsen, 2012)

This section is further divided into three sub-sections, where the most critical phases of a subsea installation operation are enlightened. In the first section, section 2.3.1, lift off from deck is described. Section 2.3.2 describes lowering the structure through the wave zone. Landing the structure on the seabed is described in section 2.3.3.

2.3.1 Lift off From Deck

A lifting operation often includes a transport vessel, a crane vessel and the lifted structure. The crane vessel and the transport vessel have different motion characteristics and will be affected by the waves accordingly (DNV-RP-H103 p. 137, 2014).

During lift off, it is important that the structure is raised fast enough to avoid collision between the transport vessel and the lifted object. A collision could cause large damage on the structure, transport vessel and/or the crane. Another important factor is to avoid snap loads in crane wire during hoop-up. Snap loads can be large compared to the static load of the object. To avoid snap loads, there must be sufficient slack in the wire when hooking to the equipment, so that a full heave amplitude of the vessel is allowed. Furthermore, it is essential that the timing of the lift off is carefully planned and that the crane wire is kept vertical to minimize pendulum motion of the structure once being lifted off (Gudmestad, 2014).

Prior to lift off from deck, following operational aspects shall be evaluated (DNV-RP-H103 p. 137, 2014):

- Clearance between lifted object and crane boom
- Clearance between crane boom and any other object
- Clearance between the lifted object and any other object
- Clearance between the underside of the lifted object and grillage or seafastening structure on the transport vessel/barge

The clearance must be calculated based on design environmental conditions, expected duration of the operation and operational procedures. For clearance between the lifted object or transport vessel and the crane vessel or crane boom, motions of the crane vessel and transport vessel shall be considered in the calculations (DNV-RP-H103 p. 137, 2014).

2.3.2 Lowering Through the Wave Zone

During a splash zone lifting operation the object being lifted will be exposed to the transition from lift in air to lift in water, and a number of forces are present and have to be accounted for. When the structure enters the water it will be exposed to slamming impact forces that could damage the structure, further hydrodynamic drag and added mass forces will influence the dynamic response of the system. Varying buoyancy and hydrodynamic forces may result in snap loads in lifting wire. These forces are generated as a result of the relative motion between the lowered structure and the water particles (DNV-RP-H103 p. 69, 2014).

According to Sarkar and Gudmestad (2010), lowering through the wave zone is the phase that creates the largest forces in the hoisting system for subsea lifting operations, thus represent the maximum allowable design seastate for the operation. In this thesis, the focus will be on the phase of lowering the structure through the splash zone.

2.3.3 Landing on the Seabed

Landing the structure on the seabed is also considered one of the most critical phases of a subsea installation operation. Oscillating motion of the structure may result in collision forces when it hits the seabed, this can cause large damage on the lifted object. In addition to collision forces between structure and seabed, there is an increased risk for slack sling conditions and large dynamic forces in the lifting wire when the operation goes from a free end system to a fixed end system (DNV-RP-H103 p. 99, 2014).

3 State of the Art

In this chapter, state of the art subsea processing equipment and vessels used for the purpose of installation and retrieval of subsea modules is given.

This chapter is divided into two sections. In section 3.1 processing on the seabed is presented. In section 3.2 monohull and twin-hull vessels are presented.

3.1 Processing on the Seabed

This section is further divided into two sub-sections. Section 3.1.1 describes today's achievements related to subsea processing. Section 3.1.2 regards the future vision of a subsea factory on the seabed.

3.1.1 Today's Achievements Related to Subsea Processing

Subsea processing is divided into four applications: boosting, separation systems, water injection and gas compression (Davies, Ramberg, Bakke, & Jensen, 2010). By looking at Norway's portfolio of developed subsea processing units, it is clear that Norway is one of the leading countries in the world in the subsea industry (Infield, 2011). Figure 3.1 below shows worldwide locations for projects related to subsea processing.



Figure 3.1: Worldwide locations for subsea pumping, compression, separation and water injection systems (Intecsea, 2014)

This section has been divided into four sub-sections. Section 3.1.1.1 describes seabed boosting. Section 3.1.1.2 describes seabed separation. Water injection is described in section 3.1.1.3, and section 3.1.1.4 describes seabed gas compression.

3.1.1.1 Boosting

Subsea boosting is the most applied seabed processing technology. The subsea pump is usually applied to increase pressure and flow rates from mature fields and fields that have long tie back distance (Infield, 2011).

The pumps are mainly categorized as either positive displacement pumps or rotodynamic pumps. For the positive displacement pumps, twin-screw pumps are most widespread. For the rotodynamic pumps, the most widely used are the helico-axial and centrifugal models (Infield, 2011).

The twin-screw pump features counter-rotating screws to enclose and pump the fluid from the suction end to the discharge end. This model is often used when the pumping conditions contain high gas volume fractions, varying inlet conditions, and when the possibility for slugging formation in the riser is high (Infield, 2011). In 1994, the world's first electrically driven multiphase twin-screw pump was installed at the Prezioso field in the Mediterranean Sea. This technology was also installed at Lyell field in the North Sea in 2006, and the King field in GOM in 2008 (Intecsea, 2014).

The multiphase helico-axial pump manufactured by OneSubsea is capable of handling high gas volume fractions. The pump generates pressure by spinning the fluids at high rotations per minute, using helicon and impellers (Infield, 2011). Today there are a total of 23 helicon-axial subsea pumps in operation worldwide. In 1997 the first centrifugal pump was installed at the Lufeng field in the South China Sea. Another technology, the rotodynamic Electrical Submersible Pump (ESP) mainly manufactured by Baker Hughes and Schlumberger-Reda was first installed in 2002 at the Jubarte field Offshore Brazil. Since then, a total of 30 ESP pumps have been installed in the Gulf of Mexico and offshore Brazil (Intecsea, 2014).

3.1.1.2 Separation

Seabed separation involves separating the oil, gas and water directly at the seabed instead of transporting the well stream all the way to the topside facility. Two-phase separation is the process when the well stream is separated into gas and liquids, and three-phase separation is when the well stream is separated into gas, oil and water (Infield, 2011).

The water to oil ratio increases with the reservoir's life. After some years, it may be cost inefficient to pump all the produced water to the topside facility. When separating water on the seabed, the water is kept from entering the well stream. The backpressure in the well is therefore reduced, resulting in increased oil production. In addition, it is also possible to re-inject the

produced water into the reservoir in order to increase and maintain the preferred well pressure (Infield, 2011).

The seabed separation technology is often combined with the seabed boosting technology. The Troll C field in the Norwegian Sea installed the world's first subsea water injection pump system in 1999, and is currently the longest operating subsea separation system in the world (Intecsea, 2014).

Statoil's Tordis project installed in 2007 was the first of its kind and includes a three-phase separation process (Davies et al., 2013). At the first stage the majority of the gas is extracted. At a later stage the remaining gas, sand and water are separated from the oil stream. The sand and the water are injected back into the reservoir through an injection pump, while the separated oil and gas are boosted by a multiphase pump back to the Gullfaks C platform (Infield, 2011).

Other fields that have taken subsea separation into use are Total's Pazflor in Angola, Shell's Perdido Host in the Gulf of Mexico, Shell's Parque das Conchas BC-10 and Petrobras's Marlim in Campos Basin (Infield, 2011).

3.1.1.3 Water Injection

Water injection may be used to increase or maintain field pressure and production rates. The most conventional method is that the water is processed on a topsides facility, and then re-injected into the reservoir. If a Raw Sea Water Injection (RSWI) system is implemented, the seawater is processed and cleansed on the seabed, and then injected into the reservoir. The topsides facility provides electricity and chemicals necessary for the processing through an umbilical. RSWI may be used when the topsides facility faces challenges related to space and weight, if there is a long step-out distance or there is a requirement for higher injection pressures. Similar technology is also used for subsea separation where the extracted water is processed and re-injected without any topside facility intervention (Infield, 2011).

Statoil's Tyrihans field was the first field where the RSWI system was applied. Two centrifugal pumps with 31 kilometer step-out were installed to provide pressure support and to boost the oil production. On the Tyrihans field it is expected that the total oil recovery will increase by 10% due to this RSWI system. The system was put into operation in March 2013 (Davies et al., 2013).

3.1.1.4 Gas Compression

Subsea gas compression involves a gas compressor being placed at the seabed level on the field or very close to the field. This way the recovery factor from the reservoir is increased compared to if the compressor was placed on a topsides facility. The main factors driving this technology are the discovery of gas fields far from shore, in harsh environments, colder and deeper water, a long step-out distance from the host facility and low reservoir temperature and pressure (Infield, 2011).

The Åsgard field will be the first field in the world to apply the subsea gas compressor technology. Installation of the system is planned to be in mid 2015 (Intecsea, 2014). The subsea compressor station includes two parallel compression trains. Each of the two compressor trains contains an inlet and anti-surge cooler module, a scrubber module, a compressor module, a pump module and a discharge cooler module (Hedne, 2013), as illustrated in figure 2.3. The Gullfaks field is the next field to install subsea gas compressors with planned operation start up in the end of 2015. There are also plans for a subsea gas compressor at the Ormen Lange field. This project has been postponed, and is now planned to be in operation in 2021 (Intecsea, 2014).

3.1.2 Future: The Statoil “ Subsea Factory”

Statoil introduced the concept of a subsea factory at the Underwater Technology Conference in Bergen in 2012. The goal of the concept is to remove the need for topsides processing facilities, thus enabling subsea to shore transport solutions for any remote offshore location. Subsea production and processing development are the key developments in order to realize the vision of a complete factory on the seabed (Davies et al., 2013).

Potential benefits of a subsea factory include production boosting, increased recovery rate, increased Net Present Value (NPV) and reduced surface production, facility cost and weight (Infield, 2011).

No subsea fields are identical and the same subsea solutions may not be implemented on all future fields; therefore it will not be a “one and only subsea factory”. The subsea factory concept can be divided into three sub concepts (Davies et al., 2013):

- The brown field factory
- The green field subsea factory to host
- Subsea factory to market

The brown field factories are old fields that are in decline and need smart solutions to increase recovery and/or accelerate production. Simplified boosting and compression, water separation and injection and power distribution are the technology required. Cost effective Inspection Maintenance and Repair (IMR) solutions are important as the requirement for operability are set high for these fields. The green field subsea factory to host are the fields that today are inaccessible, far from shore, in deep water or in cold environments. A subsea field center, gas treatment and sea water injection are the technology needed. In order to realize this concept, new technology development is essential. Subsea factory to market are developments that are beyond the year 2020. This concept includes processing on the seabed and transporting directly to the potential market without further treatment (Davies et al., 2013).

Throughout many years of developing subsea technology, significant achievements have been made. Major steps towards a subsea factory are already completed.

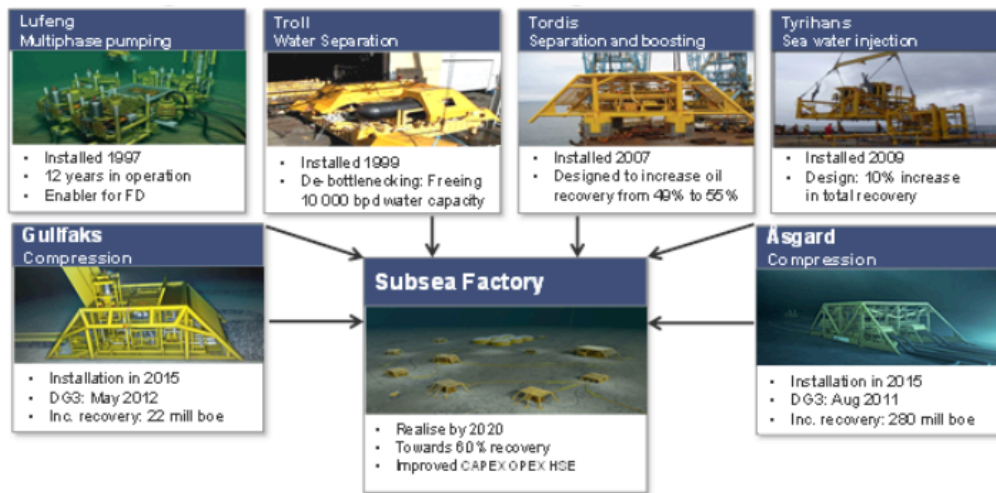


Figure 3.2: Subsea factory existing components (Davies et al., 2013)

Figure 3.2 shows some of the subsea processing units developed by Statoil. This portfolio covers all the major components in a future subsea factory (Davies et al., 2013).

3.2 Vessels

Vessels that are used for subsea installation operations vary depending on factors like weight and size of the structure to be installed, vessel cost, weather forecast, motion compensation of the vessel and availability of the vessel (Moreno-Trejo, 2012).

A variety of specialized vessels for marine services exist. Today most of the installation and retrieval of subsea structures are performed by OCVs or IMR vessels. As the subsea application continue to grow, more equipment is installed on the seabed, the structures may become larger and the environment harsher.

Vessels capable of installing and replacing subsea processing modules are necessary to obtain high availability of a subsea system. These vessels are described by the industry as Subsea Processing Intervention Vessels (SPIV). They shall be capable of working year round in significant wave height of 4.5 meters, and lift modules weighing 400 tons with dimensions 15×12×12 meters (Jahnsen, 2015).

In this thesis, monohull and twin-hull vessels are considered with regards to subsea installation operations. This section is divided into two sub-sections. Section 3.2.1 presents monohull vessels. Section 3.2.2 presents twin-hull vessels.

3.2.1 Monohull

Typical monohull offshore support vessels are survey vessels, IMR vessels and construction vessels. The survey vessel is usually the “lightest” vessel that is a part of an offshore operation. It often assists larger vessels like construction vessels. Installation and transportation of small items and mapping the seabed are its main task. It is more common lately that the survey vessel facilitate larger deck and higher crane capacity to enable the vessel to perform other tasks that come up on short notice, for example light construction and IMR activities (Hovland, 2007).

IMR vessels perform inspection of for example anchor chains, pipelines and platform legs. Replacement of equipment, like valves and chokes, on subsea installations are performed by IMR vessels. Sometimes subsea modules are also replaced by an IMR vessel. Module Handling System (MHS), crane, inspection and working Remotely Operated Vehicles (ROV) are some common systems applied on this vessel (Hovland, 2007).

Far Saga, a Platform Supply Vessel (PSV) was one of the first vessels equipped for the IMR market. The 96 meter long vessel was built in 2000 and modified for the IMR market in 2001 (Hovalnd, 2007). The vessel featured a MHS and was able to launch and recover modules with weight of 30 tons in significant wave height of 3.5 meters. It was also equipped with a main offshore crane of 50 ton capacity, a moonpool with dimensions 6.5×6.5 meters, a working ROV and an inspection ROV (Nordhal, 2002). Far Saga is shown in figure 3.3 below.



Figure 3.3: Far Saga (Nordhal, 2002)

Seven Viking and Edda Fauna are typical IMR vessels on today’s market. Seven Viking has a length of 106.5 meters, and features a 135 ton AHC main deck crane and a 70 ton AHC MHS (Statoil, 2012). The same vessel is today often used for IMR and installation/construction activities, for example if a module needs to be replaced (Moreno-Trejo, 2012).

The construction vessel installs larger structures, for example templates, manifolds and large spool pieces. Large crane, large deck space and loading features are some of its characteristics (Hovland, 2007).

Today the Safe Working Load (SWL) on OCVs is generally limited to 400 tons. In the subsea industry some of the most influential companies are Subsea 7, Technip, Saipem and DOF Subsea. In the fleet of these companies vessels with capacity of 400 tons can be found, Skandi Acergy and Skandi Arctic are two examples. Viking Neptun, designed by Salt Ship Design, shown in figure 3.4 below, was delivered to Eidesvik March 2015. Viking Neptun is representative of a new generation of construction vessels. It has a crane capacity of 400 tons, and the ability to upgrade the SWL on the crane to 600 tons. The overall length is 145.6 meters and it features a working moonpool with dimensions 7.2×7.2 meters (Reachsubsea.com, 2015).



Figure 3.4: Viking Neptun (Reachsubsea, 2015)

As the demand for larger lifting capacity increases, new vessels are ordered. One of them is Seven Arctic that has been ordered by Subsea 7. The vessel is shown in figure 3.5. It has an overall length of 162.3 meters and features a 900 ton AHC offshore crane (Subsea 7, 2014).



Figure 3.5: Seven Arctic (Subsea 7, 2014)

Another new vessel, Normand Maximus, ordered by Solstad and designed by Vard is shown in figure 3.6 below. The vessel has an overall length of 177.9 meters, features a working moonpool with dimensions 9.1×7.2 meters and an AHC main crane of 900 ton capacity. The hull is being built in Romania, while the completion of the construction will be done in Norway (Solstad, 2015).



Figure 3.6: Normand Maximus (Solstad, 2015)

3.2.2 Twin-Hull

Semi-submersibles are multi-hull column stabilized structures. This vessel type has a rectangular platform deck that is supported above the water with vertical columns with small waterplane area, which are connected to longitudinal hulls with interconnecting structural members below the water surface (Clauss, Lehmann & Ostergaard, 1992).

Small Waterplane Area Twin Hull (SWATH) vessel is a twin-hull vessel type on the market. Figure 3.7 shows the difference between a SWATH and a semi-submersible. SWATH vessels have good motion characteristics, a large deck area and moderate speed. Known problems with this design are slamming in the wet deck, and structural challenges like split forces acting on the legs of the vessel. On semi-submersibles, cross bracings are used to handle these forces. However, on SWATH's cross bracings are avoided as the resistance shall be as low as possible (Hovland, 2007).

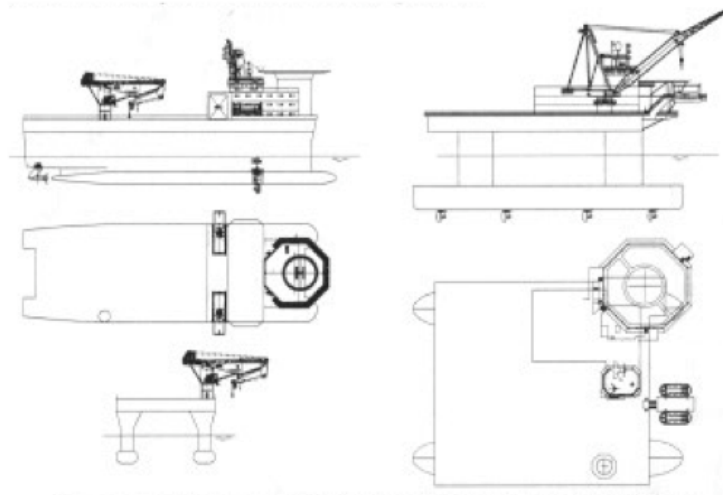


Figure 3.7: SWATH (left side) and semi-submersible (right side) vessel (Hovland, 2007)

The SWATH vessel is not considered robust enough to operate in North Sea environment. Hovland (2007) suggested that a solution for future operations in the North Sea might be a “heavy-SWATH” with low vessel motion, as it may be capable to work in higher seastates than some monohull vessels.

In the 1970’ies and 80’ies a few medium-size semi-submersibles were used for offshore support and construction. Regalia, Semi 2, Seaway Swan and Uncle John shown in figure 3.8 below were some of the semi-submersibles built especially for the purpose of performing maintenance and construction work.

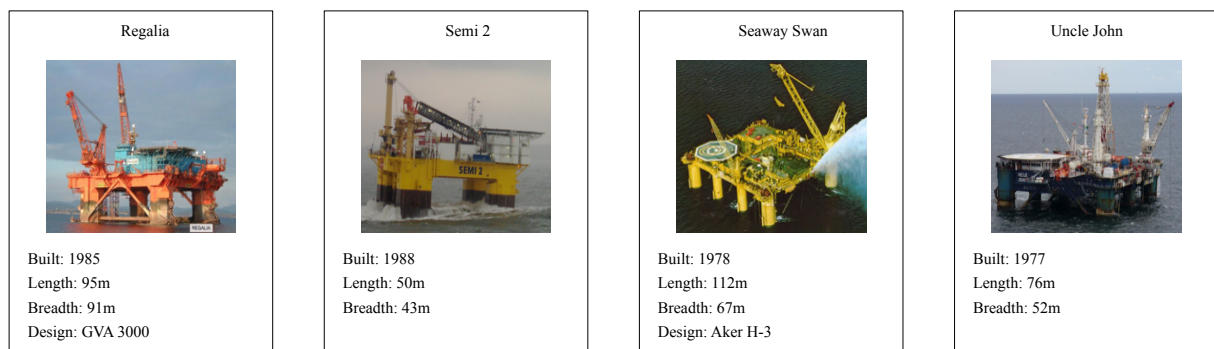


Figure 3.8: Twin-hull offshore support and construction vessels (Marinetraffic, 2015), (Gusto MSC, 2009), (Norsk kystfart, 2002)

The semi-submersible has nearly disappeared from the construction market, and today the semi-submersible is mostly used for drilling activities (Hovland, 2007). However, there are a few semi-submersibles that are especially built for non- drilling activities.

The semi-submersible Q4000 designed by Quantum, shown in figure 3.9, has been in operation since 2002. The vessel is designed to perform multiple tasks: IMR activities, installation of templates and manifolds, installation and recovery of subsea trees and other subsea structures,

installation of pipelines and umbilicals, and field and well decommissioning. The overall length of Q4000 is 95 meters. It is equipped with a moonpool of dimension 11.9×6.4 meters, a 600 ton capacity multipurpose tower and a large deck space with 4000 ton deck loading capacity (Helix Energy Solutions, 2013).

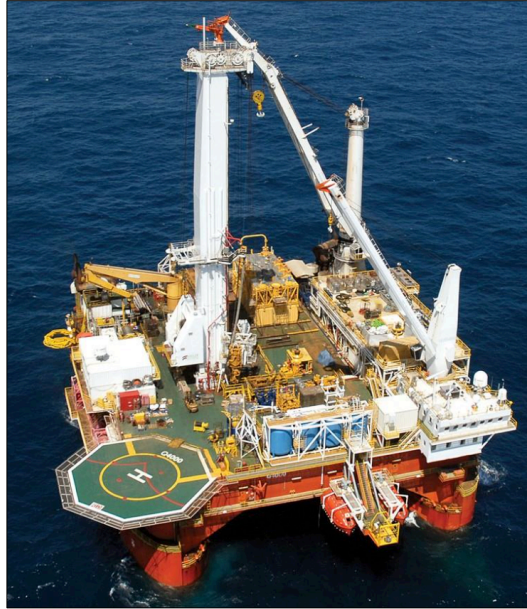


Figure 3.9: Q4000 semi-submersible (Marinetraffic, 2015)

Another semi-submersible, Q5000, is currently under construction and is expected to enter the market in 2015. The design of this vessel is based on Q4000, and is also claimed to be capable of performing a variety of tasks. Q5000 has an overall length of 109 meters, and features a 680 ton capacity multipurpose tower, a moonpool with dimension of 24.7×7.9 meters and a deck load capacity of 4000 tons (Helix Energy Solutions, 2013). When the vessel is completed it will provide well intervention services in the Gulf of Mexico for British Petroleum (Subsea World News, 2015).

Q7000, shown in figure 3.10, is the latest multi service semi-submersible designed by Helix Energy Solutions. This vessel is also a larger and upgraded version of the Q4000 design. Q7000 is currently under construction and is expected to enter the market in 2016. Subsea construction, decommissioning, top hole drilling, coiled tubing operations and twin ROV deployment are some of its features (Gcaptain, 2013). The vessel is designed towards the fast growing subsea market (Helix Energy Solutions, 2013) and will be able to operate in North Sea environment (Gcaptain, 2013).

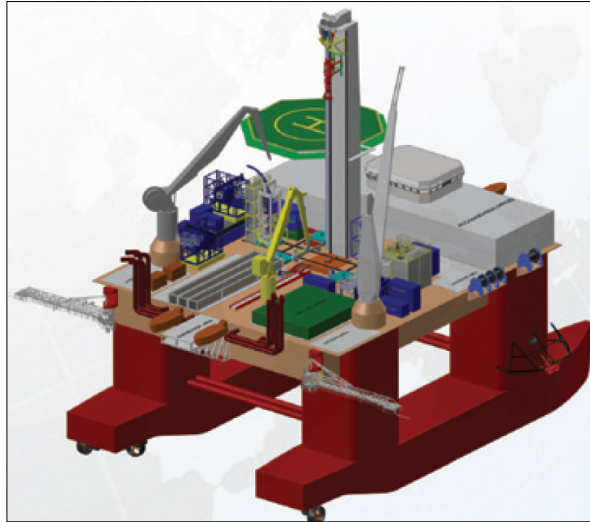


Figure 3.10: Semi-submersible intervention vessel Q7000 (Helix Energy Solutions, 2013)

Another concept on the non-drilling semi-submersible market is the Compact Semi-Submersible (CSS). The CSS concept is developed by Vard and combines the semi-submersible and the monohull vessel features, like the SWATH concept. The result claimed to be a stable working platform with good seakeeping performance (Annual Offshore Support Journal, 2014).

CSS Derwent is a multi-service vessel built for various subsea operations like IMR, well intervention and installation, construction support and recovery of subsea manifolds and trees. The vessel is shown in figure 3.11. It features a moonpool with dimension of 7.4×7.6 meters, a 160 ton capacity MHS and a 120 ton capacity crane. The length of the vessel is 84 meters, and it is equipped with dynamic positioning class 3 and has a transit speed of 10 knots (Hallin, 2014).



Figure 3.11: CSS Derwent (Hallin, 2014)

The former owner, Hallin Marine, cancelled the shipbuilding contract with the yard in the end of 2014. The vessel was sold to PaxOcean who plans to complete the building of CSS Derwent (Sea Ship News, 2014).

4 Feasibility Study – Installation of Heavy Module

In the following chapter, a feasibility study of utilizing a typical 145 meter long OCV to perform installation of heavy subsea structures in the North Sea is performed. Dynamic analyses have been performed in the marine dynamics program OrcaFlex, and maximum operational seastates in which the OCV is able to complete installation are determined. Furthermore, vessel operability is defined and lastly the probability of experiencing a sufficiently long weather window for the operation is calculated.

This chapter is divided in six sections. Section 4.1 presents the dynamic analysis and explains the required input parameters for the modeling and analyses program OrcaFlex. Operational criterions for the three subsea installation operations are described in section 4.2. Results of the dynamic analyses are presented in section 4.3. In Section 4.4, the vessel operability is determined. In section 4.5, the probability of experiencing a sufficient weather window for the operations is calculated. A discussion of the main findings of the feasibility study is presented in section 4.6.

4.1 Dynamic Analysis

The most critical phases for subsea installation operations are when the structure is being lifted off the vessel deck/transporting barge, when it is being lowered through the splash zone and when the object lands on the seabed, as described in section 2.3. According to Sarkar and Gudmestad (2010) the splash zone phase normally gives the expected largest forces in the hoisting system for subsea installation operations.

For the purpose of this analysis the most critical phase of the installation operation was assumed to be when the module is being lowered through the splash zone, thus determining the operational seastate. Analyses were performed for three different subsea structures, for lift over the side of the vessel. Lift over the side of the vessel was chosen because the dimensions of the lifted structures are too large for deployment through moonpool. The subsea structures have dimensions 11×9×10m and weight of 289t, 400t and 600t. Further, the dynamic analyses were performed when the modules were locked in six specific submergence heights, and for all levels, the applied simulation time was 1800s, in accordance with DNV-RP-H103 (2014) section 3.4.3.5.

In this section the input parameters to the simulation program OrcaFlex are described. The section has been divided into four sub-sections. Section 4.1.1 describes the necessary vessel input. Section 4.1.2 describes the input for the subsea structures. Lifting wire parameters are described in section 4.1.3, and section 4.1.4 specifies the environmental conditions.

4.1.1 Installation Vessel

The vessel function in OrcaFlex was used to model an OCV, and the vessel's motion characteristics in waves are required input in order to perform the analysis.

A vessel's motion in waves can be defined by displacement RAO's. Each displacement RAO consists of a pair of numbers that define the vessels response for one particular degree of freedom, wave heading and wave period (OrcaFlex, 2014).

The vessel has six degrees of freedom that are divided into translational and rotational motions. The translational motions include surge along the longitudinal x-axis, sway along the lateral y-axis and heave along the vertical z-axis. The rotational components about these axes are roll, pitch and yaw motions. Surge motion is the longitudinal front to back motion, sway motion is the lateral side-to-side motion and heave motion is the vertical up and down motion. Roll motion is the side-to-side rotational movement, pitch motion is the forward and backward rotational movement and the yaw motion is rotation about the vertical axis. Figure 4.1 illustrates the characteristic vessel motions in a coordinate system (Tupper, 2004).

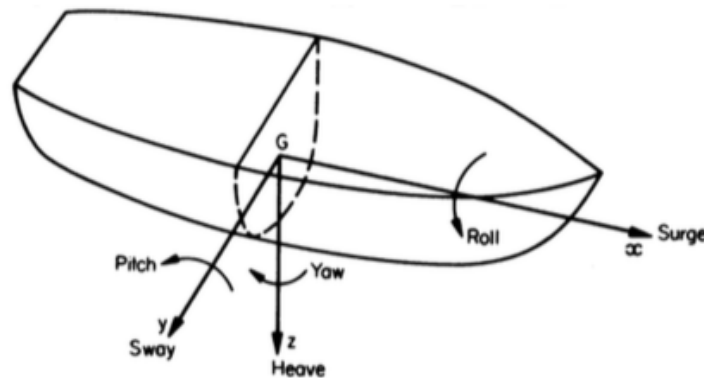


Figure 4.1: Vessel motion characteristics in a coordinate system (Rawson & Tupper, 2001)

Thus the RAO data consist of six amplitude and phase pairs for each wave period and direction. RAO's are usually obtained from either models of ship designs tested in a model basin or from specialist computer programs (OrcaFlex, 2014).

RAO's for all ship motions (surge, sway, heave, roll, pitch and yaw) were imported to OrcaFlex for a typical 145 meter long OCV. A ship design company has provided the RAO's used in this thesis.

Wave direction with respect to the vessel is defined according to OrcaFlex, and is illustrated in figure 4.2. Direction 0° are waves from astern, direction 90° are waves from starboard, direction 180° are waves from head seas and direction 270° are waves from port.



Figure 4.2: Wave directions with respect to vessel

Ships normally perform overside crane lift with waves approaching head seas, but some drifting shall be accounted for. The dynamic analyses were based on waves coming from +/- 15° head seas (DNV-RP-H103 p.64, 2014), and wave headings 165°, 180° and 195° were studied.

4.1.2 Subsea Structures

Subsea modules are geometrically complex structures. However, in order to perform simulations in OrcaFlex, simplifications and assumptions were made. The three subsea structures were simplified to be 6D buoys with the shape of rectangular prisms. The structures have dimensions 11×9×10m and a weight of 289t, 400t and 600t. Weight of 289t was chosen for the lightest module, as this is weight of the heaviest module in the compressor station that will be installed at the Åsgard field. Specifications for the three modules are presented in table 4.1 below.

Table 4.1: Subsea modules for installation operation

Mass in air, M [kg]	Length, x [m]	Width, y [m]	Height, z [m]	Perforation [%]
289000	11	9	10	30
400000				
600000				

Many forces act on a structure when it is lowered through the splash zone. OrcaFlex requires a set of input data for each module in order to account for these loads. A summary of the data input to OrcaFlex is presented in Appendix A.

This section is further divided into four sections. Section 4.1.2.1 presents the equations for calculating hydrodynamic added mass. The equation for calculating mass moment of inertia is given in section 4.1.2.2. Section 4.1.2.3 describes displaced volume of water. Hydrodynamic coefficients for drag, inertia and slam are presented in section 4.1.2.4.

4.1.2.1 Hydrodynamic Added Mass

Added mass is a phenomenon that occurs when water particles move due to movement of a structure with amplitudes that decline away from the structure (Gudmestad, 2014). The mass of the fluid adjacent to the structure will thus be displaced to some degree, depending on the movement of the object relevant to the fluid.

According to DNV-RP-H103 (2014) section 4.6, the value of solid added mass in heave for a three-dimensional non-perforated structure with vertical sides, A_{33s} , can be calculated as shown in equation 4.1-1. However, subsea modules are in most cases perforated to some degree. This was accounted for by introducing equation 4.1-3. In this thesis, a perforation degree of 30% was assumed for the modules.

$$A_{33s} = \left[1 + \sqrt{\frac{1 - \lambda^2}{2 \cdot (1 + \lambda^2)}} \right] \cdot A_{33o} \quad (4.1-1)$$

and

$$\lambda = \frac{\sqrt{A_p}}{h + \sqrt{A_p}} \quad (4.1-2)$$

and

$$A_{33} = A_{33s} \cdot e^{\frac{10-p}{28}} \quad (4.1-3)$$

Where:

A_{33s}	[kg]	Solid added mass (added mass in heave for non-perforated structure)
A_{33}	[kg]	Added mass in heave for perforated structure
A_{33o}	[kg]	Added mass for flat plate with shape equal to the horizontal projected area of the object
λ	[-]	Factor between height of object and area of submerged part
h	[m]	Height of object
A_p	[m ²]	Area of submerged part of object projected on a horizontal plane
p	[%]	Perforation rate

Further, the added mass for a flat plate, A_{33o} , can be calculated as follows:

$$A_{33o} = \rho_w \cdot V_R \cdot C_A \quad (4.1-4)$$

Where:

ρ_w	$[kg/m^3]$	Density of seawater
V_R	$[m^3]$	Reference volume
C_A	$[-]$	Hydrodynamic added mass coefficient

For a rectangular plate the reference volume, V_R , is calculated as:

$$V_R = \frac{\pi}{4} \cdot a^2 \cdot b \quad (4.1-5)$$

Where:




a	$[m]$	Short side of the structure normal to flow direction
b	$[m]$	Long side of the structure normal to flow direction

The drag area of object, A_p , can be written as:

$$A_p = a \cdot b \quad (4.1-6)$$

The hydrodynamic added mass coefficient, C_A , for flat rectangular plates was found by linear interpolation in table 4.2.

Table 4.2: Added mass coefficient (DNV-RP-H103 p.148, 2014)

Body shape		Direction of motion	C_A				V_R
Flat plates	Circular disc 	Vertical	$2/\pi$				$\frac{4}{3} \pi a^3$
	Elliptical disc 	Vertical	b/a	C_A	b/a	C_A	$\frac{\pi}{6} a^2 b$
			∞	1.000	5.0	0.952	
		14.3	0.991	4.0	0.933		
		12.8	0.989	3.0	0.900		
		10.0	0.984	2.0	0.826		
		7.0	0.972	1.5	0.758		
		6.0	0.964	1.0	0.637		
	Rectangular plates 	Vertical	b/a	C_A	b/a	C_A	$\frac{\pi}{4} a^2 b$
			1.00	0.579	3.17	0.840	
			1.25	0.642	4.00	0.872	
			1.50	0.690	5.00	0.897	
			1.59	0.704	6.25	0.917	
			2.00	0.757	8.00	0.934	
			2.50	0.801	10.00	0.947	
			3.00	0.830	∞	1.000	

As seen in table 4.2, the added mass coefficient is decided by the relation b/a , b being the width, and a being the length of the structure. In order to calculate the value for C_A , interpolation can be used:

$$y = y_a + \left(\frac{y_b - y_a}{x_b - x_a} \right) \cdot (x - x_a) \quad (4.1-7)$$

A simplified illustration of hydrodynamic added mass for a submerged rectangular prism can be seen in figure 4.3 below.

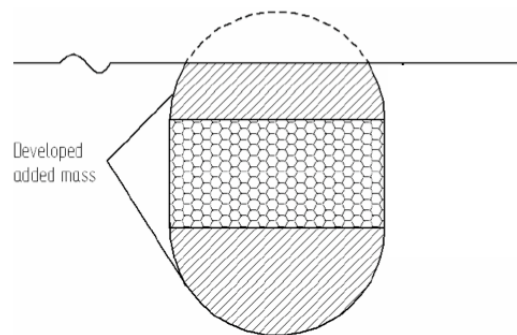


Figure 4.3: Hydrodynamic added mass (Sakar & Gudmestad, 2010)

The hydrodynamic added mass varies according to the structures level of submergence. When the bottom of a rectangular module is located right on the sea surface, the added mass value is equal to the lower half-circle as shown in figure 4.3. As the module is lowered more in to the sea, the added mass value increase. When the whole module is fully submerged the added mass reaches its maximum and stabilizes.

For a module with dimensions $11 \times 9 \times 10$ m and a perforation rate of 30%, the calculated added mass in z-direction for five levels of submergence is presented in table 4.3.

Table 4.3: Added mass for different submergence levels in z-direction

Depth of submergence [m]	Hydrodynamic added mass z-direction [t]
0	223.0
-1	271.7
-5	320.9
-10	345.3
-15	357.3

Depth of submergence is defined as the distance from still water level to the bottom of the module.

4.1.2.2 Mass Moment of Inertia

The mass moment of inertia represents the modules resistance against rotation around any of its three axis. Moment of inertia around x, y and z-axis of a solid rectangular prism can be calculated as:

$$I_x = \frac{1}{12} \cdot M \cdot (y^2 + z^2) \quad (4.1-8)$$

$$I_y = \frac{1}{12} \cdot M \cdot (x^2 + z^2) \quad (4.1-9)$$

$$I_z = \frac{1}{12} \cdot M \cdot (x^2 + y^2) \quad (4.1-10)$$

Where:

I_x	$[kg/m^2]$	Mass moment of inertia around x-axis
I_y	$[kg/m^2]$	Mass moment of inertia around y-axis
I_z	$[kg/m^2]$	Mass moment of inertia around z-axis
M	$[kg]$	Weight of module in air
x	$[m]$	Length of module
y	$[m]$	Width of module
z	$[m]$	Height of module

4.1.2.3 Displaced Volume of Water

The volume of water displaced by the submerged object is required by OrcaFlex in order to determine the submerged weight of the structure. Displaced volume of water can be found by dividing the weight of object in air on the density of the object as shown in equation 4.1-11. In this thesis it was assumed that the modules were made up of steel with a density of 7850kg/m³.

$$\nabla = \frac{M}{\rho_o} \quad (4.1-11)$$

Where:

∇	$[m^3]$	Displaced volume of water
M	$[kg]$	Weight of module in air
ρ_o	$[kg/m^3]$	Density of object

4.1.2.4 Drag, Inertia and Slam

Several forces act on the object as it passes through the splash zone. Hydrodynamic coefficients are applied in OrcaFlex to account for force contribution from drag, inertia and slam.

The drag force on the lifted structure is a result of the flow disturbance and wake close to the object as illustrated in figure 4.4 below. The drag coefficient, C_D , is a function of several parameters such as the Reynolds number for the flow and the roughness of the module (Gudmestad, 2014).

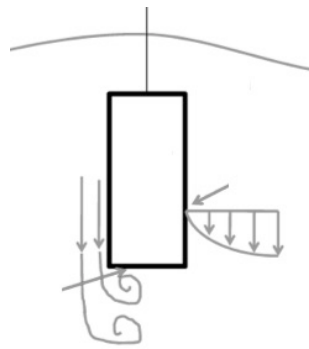


Figure 4.4: Drag force on a structure (Subsea 7, 2010)

The drag coefficient can be difficult to determine without the use of CFD studies or model tests. DNV-RP-H103 (2014) section 4.6.2.4, states that that the drag coefficient for typical subsea structures in oscillatory flow shall be equal or less than 2.5. Therefore the hydrodynamic drag coefficients were assumed to be 2.5 in the dynamic analyses:

$$C_D = C_{D_x} = C_{D_y} = C_{D_z} = 2.5 \quad (4.1-12)$$

Where:

C_{D_x}	$[-]$	Hydrodynamic drag coefficient x-direction
C_{D_y}	$[-]$	Hydrodynamic drag coefficient y-direction
C_{D_z}	$[-]$	Hydrodynamic drag coefficient z-direction

The hydrodynamic inertia coefficient can be written as (DNV-RP-H103 p.10, 2014):

$$C_M = 1 + C_A \quad (4.1-13)$$

Where:

C_M	[-]	Hydrodynamic inertia coefficient
C_A	[-]	Hydrodynamic added mass coefficient

Slamming loads on the lifted object can both damage the structure and contribute to decreased tension in the lifting wire and slings. If the slamming force is higher than the weight of the structure it can cause slack in the slings and lifting wire, which may result in snap loads. Figure 4.5 illustrates slack wire and slamming load on a structure as it is lowered through the splash zone.

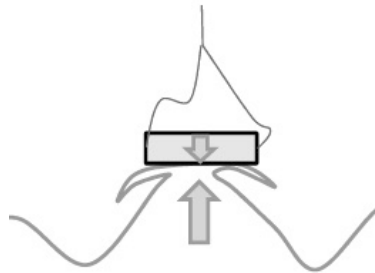


Figure 4.5: Slamming load on a structure (Subsea 7, 2010)

The slam coefficient may be determined by theoretical and/or experimental methods. According to DNV-RP-H103 (2014) section 4.3.5, the slam coefficient shall not be taken as less than 5 for any of the complex structures defined in this thesis, therefore $C_s = 5$ was used in the analyses.

The area of the module that is exposed to slamming may be calculated as:

$$A_s = A_p \cdot (1 - p) \quad (4.1-14)$$

Where:

A_s	$[m^2]$	Slam area
A_p	$[m^2]$	Area of submerged part of object in z-plane
p	[-]	Perforation rate

4.1.3 Lifting Wire

To model the lifting wire, the winch function in OrcaFlex was used. The winch is connected to the construction vessel crane in one end, and at the top of the subsea module (6D buoy) in the other end.

The stiffness of the wire is required input to OrcaFlex, and according to DNV-RP-H103 (2014) section 4.7.6 the stiffness of the wire can be calculated as:

$$k_{wire} = \frac{EA_{wire}}{L} \quad (4.1-15)$$

and:

$$A_{wire} = \frac{\pi D^2}{4} \cdot C_F \quad (4.1-16)$$

Where:

k_{wire}	$[N/m]$	Wire stiffness
E	$[N/m^2]$	Modulus of rope elasticity
A_{wire}	$[m^2]$	Effective cross section area of wire
L	$[m]$	Length of wire
C_F	$[-]$	Fill factor for wire rope
D	$[m]$	Wire diameter

Typical values for a commonly used IWRC steel core wire rope according to DNV-RP-H103 section 4.7.6 are $C_F = 0.58$ and $E = 85 \cdot 10^9 N/m^2$. These values were used to calculate the wire stiffness, in addition the diameter of the wire was assumed to be 0.130m. The calculated wire stiffness becomes 654370kN, and that is the stiffness that was used in the analysis.

4.1.4 Environment

Environmental conditions have large impact on marine operations. The environmental input data to OrcaFlex represent the hydrodynamic forces that act during the subsea installation operation.

This section is further divided into two sections. Section 4.1.4.1 describes the wave specter, while significant wave height, zero-up-crossing period and spectral peak period are defined in section 4.1.4.2.

4.1.4.1 Wave Spectrum

There are various wave theories for regular waves, some of them are; linear airy wave theory, stokes finite amplitude wave theory and cnoidal wave theory. The simplest wave theory is the linear wave theory, this theory applies linearized boundary conditions which forms regular sinusoidal shaped waves (Gudmestad, 2014).

In a real sea there are no regular waves, but a combination of many irregular waves with different periods and different heights (Gudmestad, 2014). To describe irregular sea one can analyze the sum of all waves. Fourier transformation may be applied to do this, where the sum of the sea surface can be seen as linear superposition of many regular sinusoidal waves (Journee and Maissie, 2001). Figure 4.6 shows how linear superposition of sinusoidal waves forms an irregular seastate.

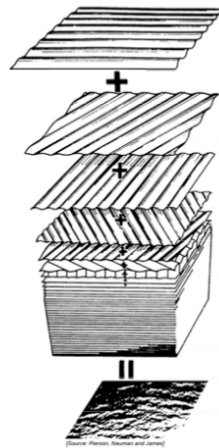


Figure 4.6: Irregular waves (Journee and Maissie, 2001)

The process of Fourier transformation compiles the heights over time to a graph of power spectral density with respect to frequency, also known as a wave spectrum (Carbon Trust, 2006).

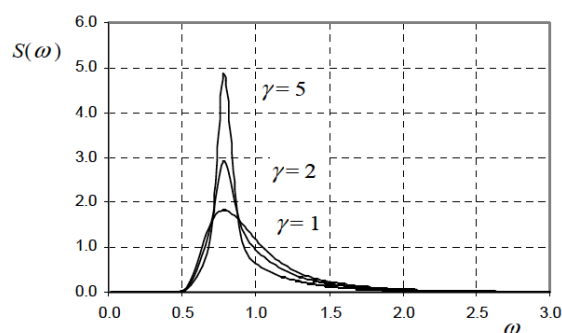
It is hard to describe the exact seastate at various geographical locations. A wave rider buoy can be placed at location and a wave spectrum graph may be produced from the collected data. However, results show that the wave spectra for many locations are similar. Generalization of wave spectrum shape is done by spectral density functions, Pierson-Moskowitz and JONSWAP wave spectra are the most frequently used spectras (Carbon Trust, 2006). Table 4.4 shows the most common wave spectra for various geographical locations.

Table 4.4: Common wave spectra in different regions (Gudmestad, 2014)

Location	Operational	Survival
Gulf of Mexico	Pierson-Moskowitz	Pierson-Moskowitz or JONSWAP
North Sea	JONSWAP	JONSWAP
Northern North Sea	JONSWAP	JONSWAP
Offshore Brazil	Pierson-Moskowitz	Pierson-Moskowitz or JONSWAP
Western Australia	Pierson-Moskowitz	Pierson-Moskowitz
Offshore Newfoundland	Pierson-Moskowitz	Pierson-Moskowitz or JONSWAP
West Africa	Pierson-Moskowitz	Pierson-Moskowitz

For the dynamic lifting analyses the JONSWAP wave spectrum was applied in OrcaFlex to represent irregular sea, as it is the most accurate spectrum for the North Sea. JONSWAP wave spectrum covers sea conditions under development and fully developed wave conditions. This spectrum is developed from wave measurements in the Southern North Sea established during a joint research project named the “Joint North Sea Wave Project”. The peak is more pronounced in the JONSWAP spectrum than in the Pierson-Moskowitz spectrum, which leads to a spectrum that changes in time (Gudmestad, 2014).

The effect of the peak shape parameter can be seen in figure 4.7 below, $S(\omega)$ represent the wave energy spectrum and ω is the wave angular frequency.

Figure 4.7: Effect of peak shape parameter for $H_s=4\text{m}$, $T_p=8\text{s}$ (DNV-RP-H103 p.18, 2014)

Average peak shape parameter and spectral width for the JONSWAP spectrum in the North Sea are shown in table 4.5 below. These are the values that were plotted in OrcaFlex under the wave spectrum section.

Table 4.5: Average values experiment data JONSWAP wave spectrum (DNV-RP-H103 p.18, 2014)

Parameter	Value
Peak shape parameter, γ	3.3
Spectral width parameter, σ_a	0.07
Spectral width parameter, σ_b	0.09

Further all the waves were assumed to approach from the same angle, therefore the wave spreading was conservatively set to zero.

4.1.4.2 Significant Wave Height and Zero-Up-Crossing Period

Significant wave height, H_s , and zero-up-crossing period, T_z , were specified in order for OrcaFlex to create a real sea. Significant wave height is defined as the average height of the highest one-third number of waves in the indicated time period, while the zero-up-crossing period is defined as the average time interval between two successive up-crossings of the mean sea level (DNV-RP-H103 p.16-17, 2014).

Significant wave heights ranging from 2.5m-5m were considered in the dynamic analyses. For a given H_s the analysis covered zero-up-crossing wave periods, T_z , ranging from (DNV-RP-H103 p.62, 2014):

$$8.9 \cdot \sqrt{\frac{H_s}{g}} \leq T_z \leq 13 \quad (4.1-17)$$

Where:

g	$[m/s^2]$	Acceleration of gravity
H_s	$[m]$	Significant wave height of design seastate
T_z	$[s]$	Zero-up-crossing wave period

Typically the operational limitations are expressed in terms of significant wave height, H_s and peak period, T_p . Spectral peak period is defined as the wave period determined by the inverse of the frequency at which a wave energy spectrum has its maximum value. For JONSWAP wave spectrum, the relation between peak period, T_p , and zero-up-crossing wave period, T_z , can be written as (DNV-RP-H103 p.19, 2014):

$$\frac{T_z}{T_p} = 0.6673 + 0.05037\gamma - 0.006230\gamma^2 + 0.0003341\gamma^3 \quad (4.1-18)$$

Where:

γ	$[-]$	Peak shape parameter
----------	-------	----------------------

In table 4.6 the necessary OrcaFlex input are presented. For each significant wave height the dynamic simulation was run for all the corresponding zero-up-crossing periods.

Table 4.6: Significant wave height and corresponding zero-up-crossing periods and peak periods

Significant wave height, H_s [m]	Zero-up-crossing period, T_z [s]	Peak period, T_p [s]
2.5	4-13	5.1-16,7
3	5-13	6.4-16.7
3.5	5-13	6.4-16.7
4	6-13	7.7-16.7
4.5	6-13	7.7-16.7
5	6-13	7.7-16.7

4.2 Operational Criterion

Operational criteria are important when determining whether a vessel is safe to use for installation operations or not. There are many types of criteria around the world, where some of the most used are set by DNV. These will be used in this thesis.

The main goal of the dynamic analysis is to ensure that the highest and lowest criterion for sling and crane wire loads are within acceptable limits during the whole installation operation, to guarantee that (DNV-RP-H103 p. 69, 2014):

- Snap loads due to slack slings or slack wire shall be avoided
- Static and dynamic loads on the lifted structure, wire and crane shall not exceed the capacity requirements

According to Bøe and Nestegård (2010) the dynamic forces that act on the module and wire during an operation does normally not vary much over the wire length. The total force that acts on the object was therefore in this thesis collected at the end of the wire connecting the structure to the crane tip.

This section is further divided into three sections. Section 4.2.1 deals with the slack sling criterion or lower tension limit. The crane capacity criterion also referred to as upper tension limit is presented in section 4.2.2. The calculated upper and lower tension requirement for each modules level of submergence during the operation is presented in section 4.2.3.

4.2.1 Slack Sling Criterion

Snap forces in slings or hoist line may occur if the hydrodynamic force exceeds the static weight of the object. To ensure no snap load, the forces in the wire and slings shall remain in tension at all times. According to DNV-RP-H103 (2014) section 4.4, the minimum dynamic force in wire shall always be less than or equal to 90% of the static forces:

$$F_{dynamic} \leq 0.9 \cdot F_{static} \quad (4.2-1)$$

Where:

$F_{dynamic}$ [N] Minimum dynamic force in wire

F_{static} [N] Static force in wire when the structure is partly or fully submerged, but the flooding has not yet started

and: $F_{static} = M - \rho_w V g$ (4.2-2)

M [kg] The mass is equal to the mass of object in air

ρ_w [kg/m³] Density of sea water

V [m³] Volume of displaced water during different stages when passing through water surface

g [m/s²] Acceleration of gravity

Hence, the lower limit of tension in slings and crane wire may be expressed as:

$$Lower\ limit = 0.1 \cdot F_{static} \quad (4.2-3)$$

The lifted object will not experience snap forces if the total load in the wire never becomes less than the lower limit. If the tension in the lifting wire is below this limit there are high possibility for impact loads, and the operational criteria is not fulfilled. If the tension in the wire at any point is zero, the lifted structure will experience snap loads.

4.2.2 Capacity Check

The lifted structure and crane wire must be able to withstand the dynamic forces that they are exposed to during the whole installation operation, therefore a capacity check are to be performed.

A Dynamic Amplification Factor (DAF) was used to estimate the maximum allowable tension in the lifting wire. The DAF was calculated for each load case by dividing the maximum total force in the wire by the static weight of the object. In order to understand the meaning of the DAF, the equation of motion is introduced and can be written as (Gudmestad, 2014):

$$m\ddot{z}(t) + c\dot{z}(t) + kz(t) = F(t) = Force \quad (4.2-4)$$

Where m is the object mass and $z = z(t)$ is the dynamic motion measured from static equilibrium position. Further the kz term represents the restoring spring force in the structure, $c\dot{z}$ represents the damping force and $m\ddot{z}$ represents the inertia force.

The solution of equation 4.2-4 is:

$$z(t) = z_h(t) + z_p(t) \quad (4.2-5)$$

Where:

$z_h(t)$	[-]	Solution of the homogeneous equation, $m\ddot{z}(t) + c\dot{z}(t) + kz(t) = 0$
$z_p(t)$	[-]	Solution of the particular equation, $m\ddot{z}(t) + c\dot{z}(t) + kz(t) = F(t)$

The equation of motion is solved as a differential equation hence two solutions are obtained, one homogeneous solution and one particular solution. The homogeneous part of the total solution is defined by the systems initial conditions. This force is not long lasting and is damped out with time, often referred to as the transient solution. When an external force like for example waves are applied to the equation of motion it becomes non-homogeneous, and the particular solution is obtained. The particular solution will last as long as there is external loading.

Hence, the general solution $z(t) = z_h(t) + z_p(t)$ will eventually reduce to the particular solution $z_p(t)$ after the transient period is over, and the solution will thereafter represent the steady state solution.

The excitation force is assumed to be represented by waves that have harmonic oscillation. To determine the particular solution, regular sinusoidal loading is considered and can be written as:

$$F(t) = F_{static} \cdot \sin\omega t \quad (4.2-6)$$

The particular solution becomes (Gudmestad, 2014):

$$z_p(t) = X \cdot \sin(\omega t - \theta) \quad (4.2-7)$$

The amplitude, X, can be written as:

$$X = \frac{F_{static}}{k} \cdot DAF \quad (4.2-8)$$

Where F_{static} represents the static force, ω represents the forcing frequency, t represents time, θ represents the phase angle, k represents the stiffness and DAF is the dynamic amplification factor. The static force over stiffness term represents the deflection resulting from the static force without dynamic effects.

Solve for DAF:

$$DAF = \frac{X \cdot k}{F_{static}} \quad (4.2-9)$$

This relation can be obtained for all single degree of freedom systems that have harmonic oscillation. The dynamic amplification factor states how much the dynamic response is, compared to the static response that is caused by the static loading.

Total load that act on an object may thus be given as the displacement amplitude, X , multiplied by the structural stiffness, k , which is equal to the DAF multiplied by the total static force, F_{static} :

$$F_{total} = X \cdot k = DAF \cdot F_{static} \quad (4.2-10)$$

The equation of motion is now described and it is proven that the total load in a system may be obtained by multiplying the DAF with the static load. This way the total structural loads can be found by applying one variable to account for the dynamic forces acting on the object during the splash zone lifting operation.

Maximum allowable hydrodynamic forces acting on the structure and lifting wire have to be calculated for each specific operation. A limiting DAF shall be obtained, and the upper limit criterion can thus be defined as:

$$Upper\ limit = F_{static} \cdot DAF \quad (4.2-11)$$

If the tension in the lifting wire never exceeds this limit, the structure will never experience forces larger than its capacity.

A lifting analysis shall be performed in order to verify that the upper limit never is exceeded, in this thesis the finite element program OrcaFlex was used for that purpose. The DAF was calculated for each of the simulated load cases according to DNV-RP-H103 section 4.4.4, by dividing the total force in the lifting wire by the static weight of the structure.

$$DAF = \frac{F_{total}}{F_{static}} \quad (4.2-12)$$

Where:

F_{total}	[N]	Total force on the partly or fully submerged object. $F_{total} = F_{dynamic} + F_{static}$
F_{static}	[N]	Static weight of the partly or fully submerged object

From equation 4.2-12 it is seen that when the DAF is equal to 1.0 there are no dynamic loads present, and when the DAF is equal to 2.0 the hydrodynamic forces are equal to the static weight of the structure, which is unacceptable. Therefore, the DAF must be larger than 1.0 and smaller than 2.0.

DNV-OS-H205 (2014) section 3.2.2 specifies DAF for offshore lifts (for structures weighing from 100-1000t) to 1.2, however the definition for an offshore lift are in this standard limited to lift in air from a barge/ship to a fixed platform. For subsea lifts the DAF must be calculated separately, and no specifications are given in the DNV standard. During a subsea lift the dynamic loads acting on the object are increased compared to lifts in air as, and according to Subsea 7 (2010) most lifts through the splash zone have a requirement of $DAF_{static} < 2$. After discussions with fellow students and a person at Subsea 7, the limiting DAF was in the analyses set to $DAF=1.75$ with respect to the static weight of the object

4.2.3 Operational Criterion Dynamic Analysis

During a splash zone lowering operation the object is exposed to the transition from lift in air to lift in water and static and dynamic forces are present. The static force in the crane wire during lowering through the wave zone has a nearly linear relation, while the dynamic force has a nonlinear variation as illustrated in figure 4.8.

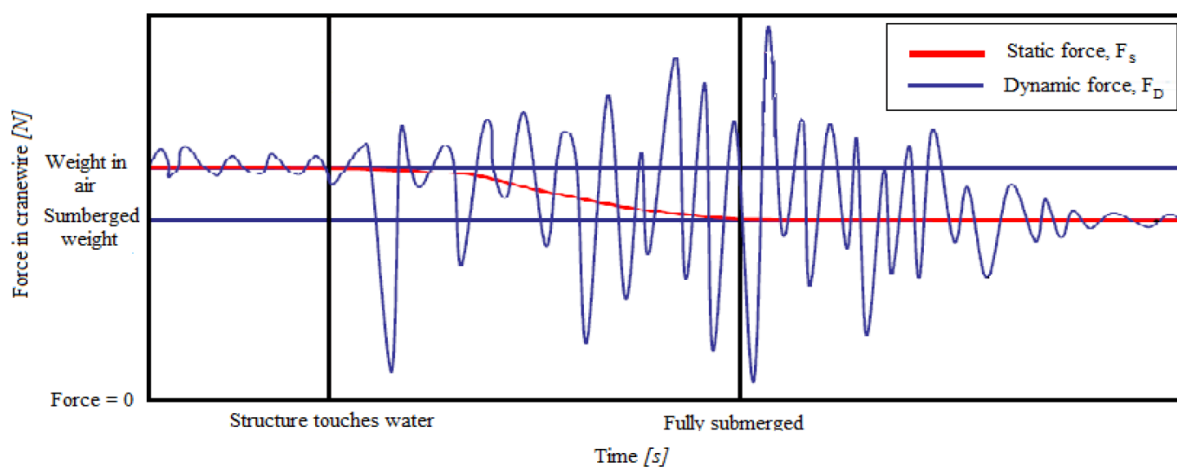


Figure 4.8: Lifting through the splash zone (Subsea 7, 2010)

When the structure is fully submerged, the static weight will be constant for the rest of the lowering operation. Due to this, the highest and lowest allowable dynamic force during a splash zone lifting operation will vary with the depth of submergence of the structure.

Accept criterion for highest and lowest sling and crane wire loads were calculated for each level of submergence according to the lower and upper limit criterion, described in section 4.2.1 and section 4.2.2. The range of acceptable effective tension during installation of the three modules is presented in tables 4.7-4.9 below. Depth of submergence of the 10 meter high modules is defined

as the distance from the bottom of the module to the mean water level. Hence, if depth of submergence is set to $z = -5\text{m}$, half of the module is submerged.

Table 4.7: Highest and lowest allowable effective tension for installation of a module weighing 289t

Depth of submergence [m]	Lowest allowable effective tension [kN]	Highest allowable effective tension [kN]
$z = 1$	284	4961
$z = 0$	283	4955
$z = -1$	280	4897
$z = -5$	265	4638
$z = -10$	247	4314
$z = -15$	247	4314

Table 4.8: Highest and lowest allowable effective tension for installation of a module weighing 400t

Depth of submergence [m]	Lowest allowable effective tension [kN]	Highest allowable effective tension [kN]
$z = 1$	392	6867
$z = 0$	392	6858
$z = -1$	387	6777
$z = -5$	367	6418
$z = -10$	341	5970
$z = -15$	341	5970

Table 4.9: Highest and lowest allowable effective tension for installation of a module weighing 600t

Depth of submergence [m]	Lowest allowable effective tension [kN]	Highest allowable effective tension [kN]
$z = 1$	589	10301
$z = 0$	588	10287
$z = -1$	581	10166
$z = -5$	550	9628
$z = -10$	512	8956
$z = -15$	512	8956

These are the accept criterions that were used in the dynamic analyses for installation of the three modules. As the module increase in weight, it is noticed that both the upper and lower limit criterion increase for all levels of submergence. If the highest and lowest tension in the lifting wire obtained from OrcaFlex were within the acceptable limits during the whole installation operation, the operation may be executed safely. It is guaranteed that snap loads are avoided and that the capacity requirements are not exceeded.

4.3 Dynamic Analysis Result

A presentation of the results obtained from the splash zone analyses is given in this section. The highest and lowest tension in wire close to the crane tip, collected from OrcaFlex, are presented as tabulated values for all load cases (wave heading, significant wave height, level of submergence and zero-up-crossing period) in Appendix B.

This section has been divided into four sub-sections. Section 4.3.1 presents effective tension in lifting wire with respect to wave direction. Effective tension in lifting wire with respect to significant wave height is presented in section 4.3.2. Highest and lowest tension in lifting wire during installation of the three modules is presented in section 4.3.3. Section 4.3.4 provides an overview of the operable seastates for installing the subsea structures.

4.3.1 Effective Tension in Different Wave Direction

The highest and lowest effective tension in the lifting wire in heading 165°, 180° and 195° are presented in figure 4.9 and figure 4.10, when installing one of the subsea structures in one wave height; the module weighing 289t in $H_s=2.5\text{m}$. The blue line in the figures represents wave heading 165°, the red line represents wave heading 180° and the green line represents wave heading 195°. Wave direction with respect to vessel is illustrated in figure 4.2. Results of the other load cases can be seen in Appendix B, however, the affect of applied wave heading proved to be very similar for installation of the other modules.

The highest effective tension in the lifting wire increased steadily from $z = 1\text{m}$ to its maximum at $z = -1\text{m}$. At $z = 1\text{m}$ the structure was not yet lowered into the sea and the acting forces varied between 3201kN-3364kN, depending on wave heading. At $z = 0\text{m}$, the bottom of the module was located right on the sea surface, and the maximum force was in the range of 3662kN- 862kN. For the submergence level where the largest forces occurred, at $z = -1\text{m}$, the highest force was experienced in heading 165°, with effective tension equal to 4298kN. As the structure was lowered more into the sea, the effective tension in the wire decreased. When of half the module was submerged, at $z = -5\text{m}$, the highest force was again experienced in heading 165°. At $z = -10\text{m}$ and $z = -15\text{m}$ the whole module was submerged and the effective tension ranged from 3267kN-3428kN, and 2827kN-2947kN respectively. The highest effective tension during the installation operation in heading 165°, 180° and 195° is presented in figure 4.9, for the mentioned load case. The zero-up-crossing period, T_z , for each level of submergence that resulted in the highest force in the crane wire during the operation was taken as the highest force.

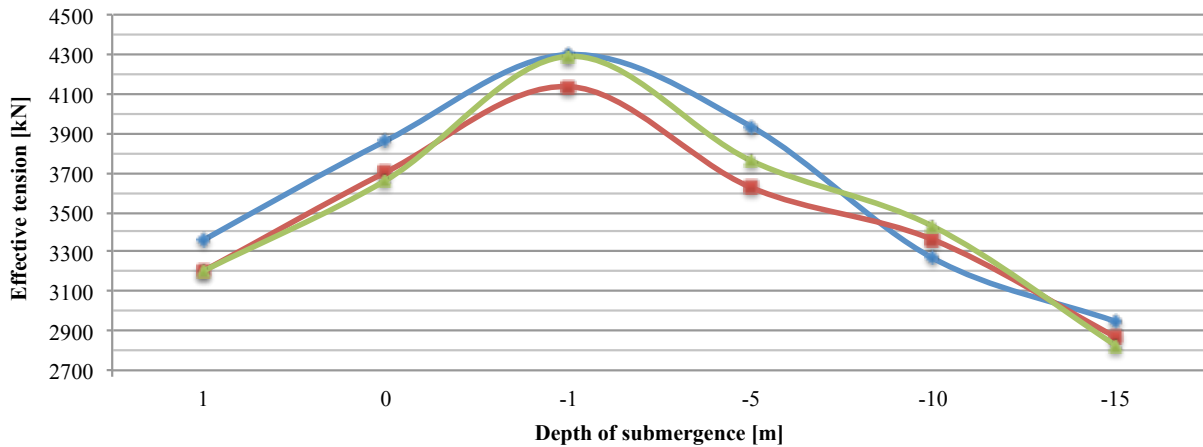


Figure 4.9: Highest effective tension versus depth of submergence when installing a module weighing 289t in $H_s=2.5\text{m}$, in heading 165° , 180° and 190°

The lowest effective tension in the lifting wire has shown to decrease steadily from $z = 1\text{m}$ to its minimum at $z = -1\text{m}$. At $z = 1\text{m}$ the structure was not yet lowered into the sea and the force varied between 2096kN-2194kN depending on the heading. At $z = 0\text{m}$, the bottom of the module was located right on the oscillating sea surface, and the lowest force was in the range of 950kN-1250kN. For the submergence level where the lowest force occurred, at $z = -1\text{m}$, the minimum force was experienced in heading 165° with effective tension equal to 742kN. As the structure was lowered more into the sea, the effective tension in the lifting wire increased again, and when half of the module was submerged, at $z = -5\text{m}$, the lowest force was about the same in all headings. At $z = -10\text{m}$ and $z = -15\text{m}$, the whole module was submerged and the effective tension ranged from 1855kN-1873kN, and 2015kN-2114kN respectively. The lowest effective tension during the installation operation in heading 165° , 180° and 195° is presented in figure 4.10 below. The zero-up-crossing period, T_z , for each level of submergence that resulted in the lowest force in the crane wire during the operation in heading 165° (blue line), 180° (red line) and 195° (green line) was taken as the lowest force.

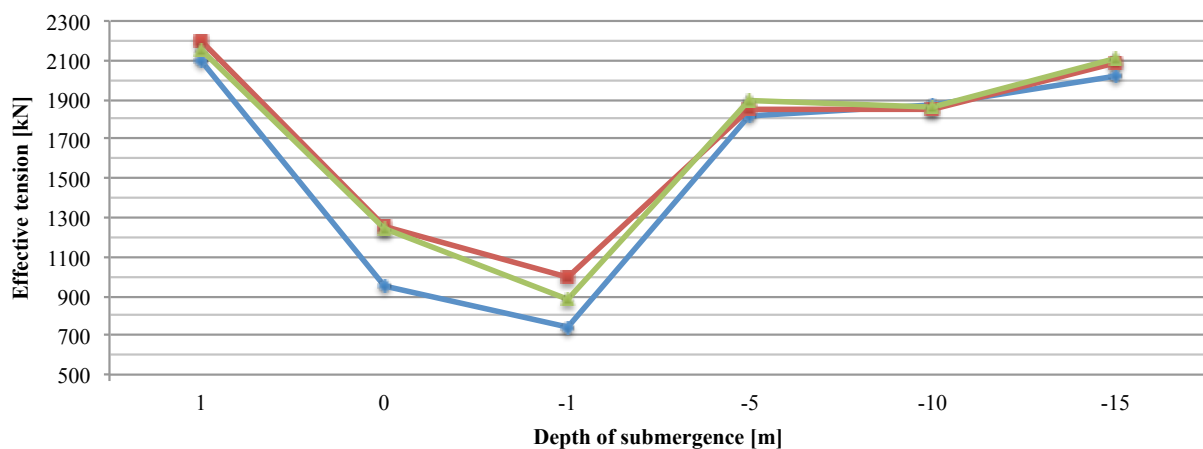


Figure 4.10: Lowest effective tension versus depth of submergence when installing a module weighing 289t in $H_s=2.5\text{m}$, in heading 165° , 180° and 190°

4.3.2 Effective Tension in Different Significant Wave Height

The highest and lowest effective tension in the lifting wire in significant wave heights, $H_s=2.5\text{m}$, $H_s=3\text{m}$, $H_s=3.5\text{m}$, $H_s=4\text{m}$, $H_s=4.5\text{m}$ and $H_s=5\text{m}$ are presented in figure 4.11 and figure 4.12, when installing one of the subsea structures in one wave direction; the module weighing 289t in heading 165° . Results of the other load cases can be seen in Appendix B, however, the affect of increased wave height proved to be very similar for installation of the other subsea structures.

The highest effective tension in the lifting wire occurred when the bottom of the module was located one meter below mean water level, at $z = -1\text{m}$, for all the considered wave heights. In $H_s=2.5\text{m}$, the highest force in the lifting wire was equal to 4298kN. When the wave height increased to $H_s=3\text{m}$, the highest force in the lifting wire raised to 4528kN. As the wave height was increased from $H_s=3\text{m}$ to $H_s=3.5\text{m}$, the effective tension in the lifting wire increased with 124kN. In $H_s=4\text{m}$ and $H_s=4.5\text{m}$ the tension in the lifting wire reached 4786kN and 4879kN respectively. The greatest wave height that was included in the simulations, $H_s=5\text{m}$, resulted in the maximum forces with effective tension equal to 5352kN. Effective tension in lifting wire in significant wave heights, $H_s=2.5\text{m}$, $H_s=3\text{m}$, $H_s=3.5\text{m}$, $H_s=4\text{m}$, $H_s=4.5\text{m}$ and $H_s=5\text{m}$ are presented in figure 4.11 below, for the mentioned load case. The zero-up-crossing period, T_z , for each level of submergence that resulted in the highest force in the crane wire during the operation was taken as the highest force.

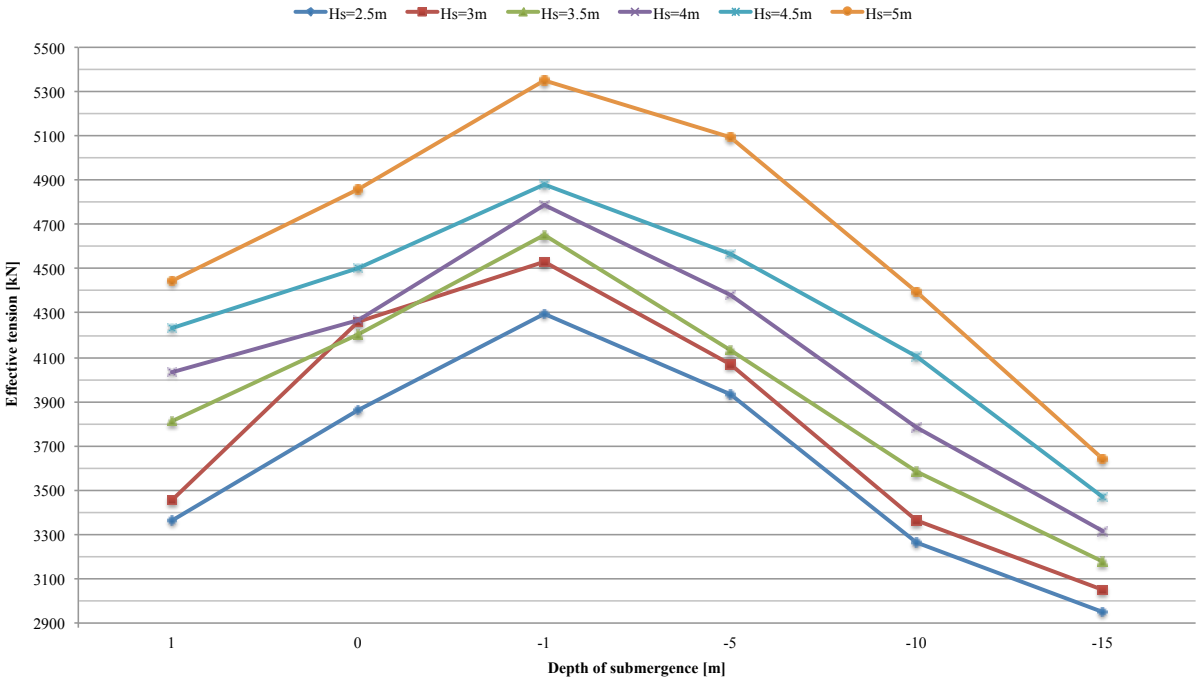


Figure 4.11: Highest effective tension versus depth of submergence for all significant wave heights in heading 165° , when installing a module weighing 289t

The lowest effective tension in the lifting wire occurred at $z = -1\text{m}$ in $H_s=2.5\text{m}$, $H_s=3.5\text{m}$ and $H_s=4\text{m}$, with effective tension equal to 742kN, 512kN and 362kN respectively. In $H_s=3\text{m}$, the lowest force occurred at $z = 0\text{m}$, with tension in lifting wire equal to 556kN. In $H_s=4.5\text{m}$ and $H_s=5\text{m}$ the lowest force occurred at $z = 0\text{m}$, $z = -1\text{m}$ and $z = -5\text{m}$. In $H_s=4.5\text{m}$, the lowest force was observed at $z = -1\text{m}$, with effective tension in lifting wire equal to 286kN. In $H_s=5\text{m}$ the lowest force in the lifting wire was very close to zero at $z = 0\text{m}$, $z = -1\text{m}$ and $z = -5\text{m}$. Effective tension in lifting wire in significant wave heights, $H_s=2.5\text{m}$, $H_s=3\text{m}$, $H_s=3.5\text{m}$, $H_s=4\text{m}$, $H_s=4.5\text{m}$ and $H_s=5\text{m}$ are presented in figure 4.12 below, for the mentioned load case. The zero-up-crossing period, T_z , for each level of submergence that resulted in the lowest force in the crane wire during the operation was taken as the lowest force.

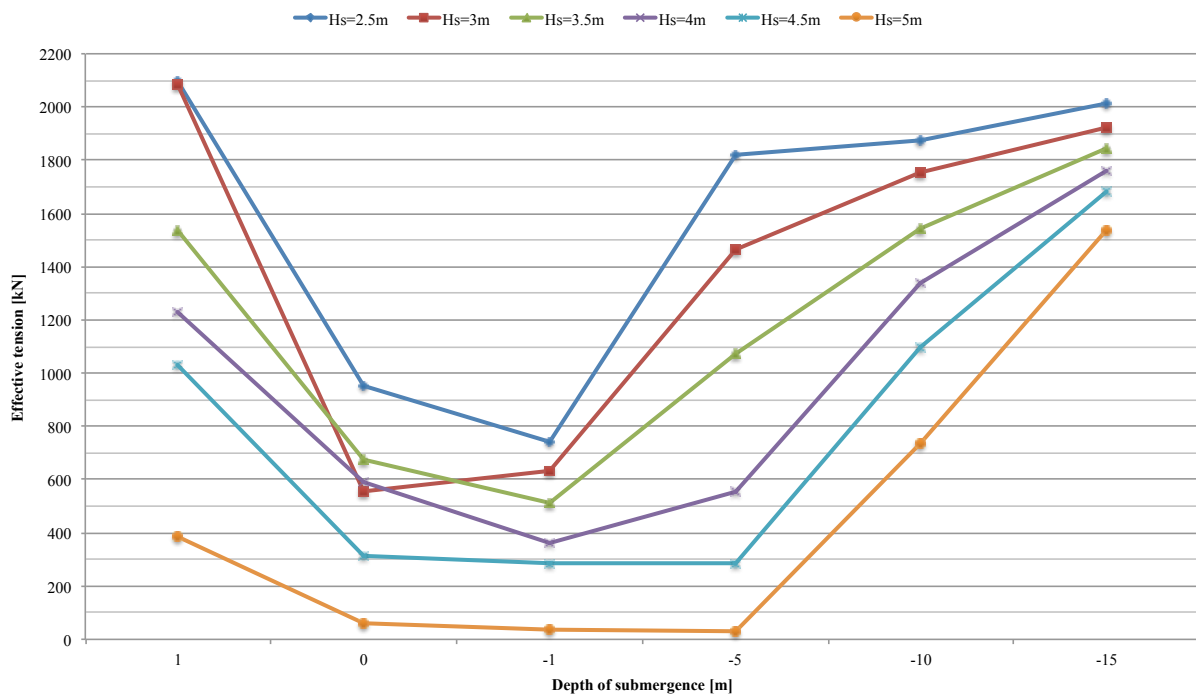


Figure 4.12: Lowest effective tension versus depth of submergence for all significant wave heights at heading 165° , when installing a module weighing 289t

4.3.3 Highest and Lowest Effective Tension in Lifting Wire

In this section, the highest and lowest effective tension in the lifting wire during the three installation operations are presented for wave zero-up-crossing periods, T_z , significant wave heights, $H_s = 2.5\text{m}-5\text{m}$, and wave headings 165° , 180° and 195° . The level of submergence for the zero-up-crossing period that resulted in the highest/lowest force in the crane wire was taken as the highest/lowest value.

Tables presented in this section are based on the effective tension criteria presented in section 4.2.3, and a coloring system is introduced:

= Highest/lowest effective tension for all depths of submergence, within operational requirements

= Highest/lowest effective tension, not within operational requirements

= Seastate outside the considered T_z - range

This section is further divided into three sub-sections. Section 4.3.3.1 includes the results for installing the module weighing 289t. Section 4.3.3.2 includes the result for installing the module weighing 400t and lastly section 4.3.3.3 includes the results for installing the module weighing 600t.

4.3.3.1 Module 289 tons

Results from the dynamic analyses revealed that the highest force in the wire during a splash zone lifting operation of a module weighing 289t, did not exceed the accept criterion in the five first wave heights, in any of the wave headings. In the last wave height considered, $H_s = 5$ m, this was not the case. The force in the lifting wire exceeded the operational criterion in heading 165° in $T_z = 6$ s with an effective tension equal to 5352kN, in $T_z = 7$ s with an effective tension equal to 5130kN and in $T_z = 8$ s with an effective tension equal to 5076kN. In heading 180° and 195° the accept criterion was exceeded in $T_z = 6$ s and $T_z = 7$ s with an effective tension equal to 5524kN and 5635kN, and 5377kN and 4732kN respectively. This can be seen in table 4.10 below.

Table 4.10: Upper limit criterion, highest effective tension in lifting line [kN] - module 289t

Hs [m]	Wave direction [deg]	Tz [s]									
		4	5	6	7	8	9	10	11	12	13
2,5	165	4298	4092	3559	3552	3418	3347	3204	3092	3076	3164
3		N/A	4528	4117	3772	3629	3435	3318	3118	3127	3180
3,5		N/A	4652	4233	4068	3835	3632	3468	3166	3213	3194
4		N/A	N/A	4786	4686	4246	3883	3700	3334	3310	3214
4,5		N/A	N/A	4879	4652	4469	4180	3883	3552	3402	3253
5		N/A	N/A	5352	5130	5076	4383	3996	3690	3502	3337
2,5	180	4136	4048	3653	3441	3362	3205	3148	3077	3111	3151
3		N/A	4523	3997	3572	3539	3330	3273	3084	3122	3167
3,5		N/A	4683	4411	4047	3731	3467	3414	3146	3147	3182
4		N/A	N/A	4696	4554	3940	3626	3569	3229	3226	3195
4,5		N/A	N/A	4765	4531	4191	3826	3750	3308	3310	3208
5		N/A	N/A	5524	5377	4568	4030	3960	3405	3399	3229
2,5	195	4289	4157	3684	3405	3222	3183	3139	3060	3106	3153
3		N/A	4402	3988	3526	3376	3318	3256	3070	3111	3166
3,5		N/A	4593	4279	3663	3596	3469	3390	3128	3128	3182
4		N/A	N/A	4797	4252	3802	3628	3547	3201	3175	3197
4,5		N/A	N/A	4813	4265	3913	3796	3697	3285	3244	3210
5		N/A	N/A	5635	4732	4285	4007	3819	3363	3317	3217

With regards to the lowest allowable tension in the lifting wire when performing a splash zone lifting operation of a module weighing 289t, the results revealed that the accept criterion was not exceeded in $H_s = 2.5$ m, $H_s = 3$ m, $H_s = 3.5$ m, $H_s = 4$ m and $H_s = 4.5$ m, in any of the wave headings. In the last wave height considered, $H_s = 5$ m, this was not the case. The force was below the operational criterion in heading 165° in $T_z = 6$ s with an effective tension equal to 53kN, $T_z = 7$ s with an effective tension equal to 42kN, $T_z = 8$ s with an effective tension equal to 29kN and $T_z = 9$ s with effective tension equal to 36kN. In heading 180° the accept criterion was exceeded in $T_z = 6$ s and $T_z = 7$ s with an effective tension equal to 60kN and 36kN. When heading 195° was applied the

accept criterion was exceeded in $T_z = 6s$ with an effective tension equal to 153kN. This can be seen in table 4.11 below.

Table 4.11: Lower limit criterion, lowest effective tension in lifting line [kN] - module 289t

Hs [m]	Wave direction [deg]	Tz [s]									
		4	5	6	7	8	9	10	11	12	13
2,5	165	742	1050	1572	1484	1824	1958	1968	2095	2126	2193
3		N/A	556	944	804	1441	1547	2026	2044	2106	2198
3,5		N/A	532	512	790	898	1071	1818	2038	2044	2171
4		N/A	N/A	362	490	586	587	1617	1795	2042	2126
4,5		N/A	N/A	286	293	306	790	1362	1797	1995	2060
5		N/A	N/A	53	42	29	36	1084	1590	1847	1951
2,5	180	993	1468	1936	1925	2027	2150	2174	2173	2737	2169
3		N/A	1262	1596	1407	1855	1858	2138	2145	2113	2182
3,5		N/A	670	1052	956	1568	1660	2022	2101	2103	2197
4		N/A	N/A	361	517	1185	1423	1807	2004	2094	2169
4,5		N/A	N/A	315	297	533	956	1589	1829	2002	2122
5		N/A	N/A	60	36	355	560	1246	1539	1827	2054
2,5	195	880	1464	2099	1978	2046	2158	2177	2215	2152	2203
3		N/A	925	1755	1830	1901	2088	2039	2197	2142	2197
3,5		N/A	284	1444	1476	1720	2014	2015	2114	2156	2198
4		N/A	N/A	777	1110	1322	1821	1875	2004	2121	2174
4,5		N/A	N/A	293	846	1005	1673	1655	1926	2104	2156
5		N/A	N/A	153	481	505	1486	1414	1481	1893	1991

4.3.3.2 Module 400 tons

Results from the dynamic analyses revealed that the highest force in the wire during a splash zone lifting operation of a module weighing 400t, did not exceed the accept criterion in the four first wave heights in any of the wave headings. In $H_s = 4.5m$, the highest tension was not within the operational criterion in $T_z = 6s$ in heading 165° and heading 195° with an effective tension equal to 7181kN and 7711kN respectively. In $H_s = 5m$, the allowable tension was exceeded for all headings. Heading 165° resulted in wire tension equal to 7868kN in $T_z = 6s$, and 7529kN in $T_z = 7s$. Highest allowable tension experienced in heading 180° and heading 195° was exceeded in $T_z = 6s$ with tension equal to 7934kN and 7586kN respectively. This can be in table 4.12 below.

Table 4.12: Upper limit criterion, highest effective tension in lifting line [kN] - module 400t

Hs [m]	Wave direction [deg]	Tz [s]									
		4	5	6	7	8	9	10	11	12	13
2,5	165	6430	6373	4816	4625	4517	4603	4368	4255	4213	4337
3		N/A	6582	5374	4886	4787	4638	4521	4265	4285	4357
3,5		N/A	6638	5682	5352	5000	4809	4680	4339	4379	4372
4		N/A	N/A	6753	5631	5231	5064	4899	4549	4496	4392
4,5		N/A	N/A	7181	6161	5646	5485	5030	4824	4572	4408
5		N/A	N/A	7868	7529	6318	5927	5285	5065	4719	4510
2,5	180	6384	5157	4731	4516	4493	4379	4292	4213	4250	4330
3		N/A	5732	5112	4836	4649	4528	4431	4224	4261	4350
3,5		N/A	6676	5434	5255	4865	4678	4611	4285	4308	4370
4		N/A	N/A	6552	5540	5091	4872	4808	4365	4389	4386
4,5		N/A	N/A	6373	5799	5406	4986	5006	4481	4485	4399
5		N/A	N/A	7934	6355	5665	5228	5210	4660	4587	4410
2,5	195	6427	5630	4803	4629	4416	4390	4296	4227	4247	4335
3		N/A	6072	5027	4886	4591	4530	4430	4260	4253	4354
3,5		N/A	6323	5183	5089	4879	4771	4593	4311	4297	4375
4		N/A	N/A	6607	5592	5118	4961	4737	4349	4363	4397
4,5		N/A	N/A	7711	5413	5037	4982	4922	4432	4439	4415
5		N/A	N/A	7586	6353	5264	5170	5115	4541	4526	4443

With regards to the lowest allowable tension in the lifting wire when performing a splash zone lifting operation of a module weighing 400t, the results revealed that the accept criterion was not

exceeded in $H_s = 2.5\text{m}$, $H_s = 3\text{m}$, $H_s = 3.5\text{m}$, $H_s = 4\text{m}$, in any of the wave headings. In heading 165° , the force in the wire was zero in $T_z = 6\text{s}$ and $T_z = 7\text{s}$ in $H_s = 4.5\text{m}$ and $H_s = 5\text{m}$. For $T_z = 8\text{s}$ and $T_z = 9$, the force was below the operational criterion with an effective tension of 38kN and 109kN. In heading 180° and heading 195° , the accept criterion was exceeded for $T_z = 6\text{s}$ with an effective tension equal to 255kN. This can be seen in table 4.13 below.

Table 4.13: Lower limit criterion, lowest effective tension in lifting line [kN] - module 400t

Hs [m]	Wave direction [deg]	Tz [s]									
		4	5	6	7	8	9	10	11	12	13
2,5	165	1151	2090	2448	2423	2730	2900	3025	2963	3015	3108
3		N/A	1145	1878	1726	2358	2460	2978	2893	2993	3109
3,5		N/A	692	1138	858	1839	1918	2725	2870	2866	3067
4		N/A	N/A	408	420	1183	1405	2486	2812	2807	2925
4,5		N/A	N/A	0	0	580	782	2226	2692	2806	2930
5		N/A	N/A	0	0	38	109	1956	2470	2653	2791
2,5	180	1844	2361	2801	2842	2981	3019	3067	3016	3029	3108
3		N/A	2125	2509	2579	2765	2814	2999	3027	3015	3110
3,5		N/A	1431	2040	2130	2436	2575	2928	2987	2990	3109
4		N/A	N/A	1475	1581	2030	2490	2715	2877	2978	3060
4,5		N/A	N/A	981	881	1514	2234	2448	2770	2839	2985
5		N/A	N/A	255	591	854	1326	2130	2475	2652	2927
2,5	195	1236	2487	3044	2776	2926	3022	3047	3092	3055	3109
3		N/A	2044	2803	2690	2753	2937	2968	3080	3044	3106
3,5		N/A	1278	2290	2475	2597	2859	2874	3046	3030	3100
4		N/A	N/A	1807	2080	2304	2667	2800	2796	3017	3073
4,5		N/A	N/A	1108	1676	1917	2563	2604	2819	2982	2975
5		N/A	N/A	255	1219	1496	2419	2369	2692	2880	2895

4.3.3.3 Module 600 tons

Results from the dynamic analyses revealed that the highest allowable force in the wire during a splash zone lifting operation of a module weighing 600t, was exceeded for several seastates. For heading 165° , in $H_s = 3.5\text{m}$ and $T_z = 5\text{s}$ and $T_z = 6\text{s}$, the effective tension was exceeded with values equal to 12326kN and 10364kN respectively. In $H_s = 4\text{m}$ and $H_s = 4.5\text{m}$, the tension was not within the operational criterion for $T_z = 6\text{s}$ and $T_z = 7\text{s}$, with an effective tension equal to 13229N and 11823kN, and 14926 and 12365 respectively. In $H_s = 5\text{m}$ allowable tension was exceeded for $T_z = 6\text{s}$, $T_z = 7\text{s}$, $T_z = 8\text{s}$ and $T_z = 9\text{s}$.

For heading 180° the highest tension was not within the operational criterion in $H_s = 4\text{m}$ with an effective tension in the wire equal to 13248kN. In $H_s = 4.5\text{m}$ and $H_s = 5\text{m}$ for $T_z = 6\text{s}$ and $T_z = 7\text{s}$, the highest allowable effective tension was exceeded, the values were equal to 13926kN and 13023kN, and 16785kN and 12365kN respectively.

Heading 195° resulted in exceeded acceptance criterion in $H_s = 4\text{m}$ and $H_s = 4.5\text{m}$ for $T_z = 6\text{s}$ and $T_z = 7\text{s}$ with effective tension equal to 11694kN and 10530kN, and 12695kN and 11849kN respectively. Lastly in $H_s = 5\text{m}$ allowable tension was exceeded for $T_z = 6\text{s}$, $T_z = 7\text{s}$, $T_z = 8\text{s}$ and $T_z = 9\text{s}$. This can be seen in table 4.14 below.

Table 4.14: Upper limit criterion, highest effective tension in lifting line [kN] - module 600t

Hs [m]	Wave direction [deg]	Tz [s]									
		4	5	6	7	8	9	10	11	12	13
2,5	165	8230	7795	6946	6694	6707	6831	6461	6297	6240	6393
3		N/A	8984	7477	7000	6977	6856	6646	6359	6342	6421
3,5		N/A	12326	10364	7333	7328	7008	6853	6494	6484	6446
4		N/A	N/A	13229	11823	7562	7301	7075	6695	6593	6502
4,5		N/A	N/A	14926	12365	9555	7720	7349	6994	6731	6592
5		N/A	N/A	16532	15684	14965	10846	9291	7272	6859	6726
2,5	180	8153	7382	6747	6634	6591	6501	6406	6227	6264	6393
3		N/A	8612	7208	6937	6827	6699	6579	6315	6309	6427
3,5		N/A	8993	8979	7282	7061	6904	6759	6405	6413	6465
4		N/A	N/A	13284	7679	9352	7118	6926	6497	6511	6505
4,5		N/A	N/A	13926	13023	7511	7303	7131	6662	6602	6544
5		N/A	N/A	16785	12365	9201	7455	7405	6908	6718	6582
2,5	195	8185	7699	6795	6602	6633	6573	6401	6350	6257	6401
3		N/A	8794	7106	6937	6923	6776	6559	6421	6340	6430
3,5		N/A	8956	8620	7147	7205	7059	6755	6426	6451	6461
4		N/A	N/A	11694	10530	7381	7382	7002	6511	6526	6488
4,5		N/A	N/A	12695	11849	7694	7428	7207	6616	6607	6562
5		N/A	N/A	15623	14685	11656	11349	7427	6719	6728	6668

With regards to the lowest allowable tension in lifting wire when performing a splash zone lifting operation of a module weighing 600t, the results revealed that the accept criterion was not exceeded in $H_s = 2.5\text{m}$ and $H_s = 3\text{m}$ for any of the wave headings. The force was zero at several values of T_z when $H_s = 4\text{m}$, $H_s = 4.5\text{m}$ and $H_s = 5\text{m}$. In heading 165° and $H_s = 3.5\text{m}$, the lowest force in the wire was below the requirement for effective tension in lifting wire, with tension equal to 274kN. This and other values can be seen in table 4.15 below.

Table 4.15: Lower limit criterion, lowest effective tension in lifting line [kN] - module 600t

Hs [m]	Wave direction [deg]	Tz [s]									
		4	5	6	7	8	9	10	11	12	13
2,5	165	2041	3689	4187	4146	4331	4552	4498	4566	4599	4755
3		N/A	1516	3482	3287	3940	4049	4499	4565	4556	4752
3,5		N/A	274	1986	2432	3413	3511	4265	4461	4442	4664
4		N/A	N/A	0	262	0	2875	4001	4409	4303	4577
4,5		N/A	N/A	0	252	0	2234	3739	4165	4308	4452
5		N/A	N/A	0	0	73	325	0	2008	4094	4361
2,5	180	1993	4287	4630	4401	4504	4567	4628	4646	4625	4748
3		N/A	2040	4344	4294	4308	4457	4537	4607	4585	4744
3,5		N/A	1682	3691	3711	4025	4349	4435	4562	4546	4696
4		N/A	N/A	369	0	3502	3965	4336	4435	4507	4635
4,5		N/A	N/A	29	0	3040	1098	4024	4315	4382	4573
5		N/A	N/A	0	241	2401	3203	3672	4185	4147	4508
2,5	195	1705	2452	4688	4324	4496	4570	4612	4689	4633	4746
3		N/A	2067	4583	4261	4336	4351	4518	4666	4591	4739
3,5		N/A	0	1268	4169	4133	4319	4307	4603	4556	4691
4		N/A	N/A	259	2046	3859	3975	4313	4485	4550	4618
4,5		N/A	N/A	79	52	1005	3772	4209	4339	4498	4532
5		N/A	N/A	0	0	85	0	1536	4234	4443	4392

4.3.4 Limiting Seastates

By combining the upper and lower limit criterion for lifting the three modules through the splash zone, limiting seastates for the installation operations were obtained. The results are shown in table 4.16 to table 4.18, following coloring system is applied:

	= Operable seastate
	= Non-operable seastate
N/A	= Seastate outside the considered T_z - range

The result revealed that a module weighing 289t can be installed from the considered OCV in H_s ranging from 2.5m-4.5m. For the highest significant wave height considered, $H_s = 5m$, both the upper and lower limit criterion were exceeded for zero-up-crossing periods, $T_z = 6s$, $T_z = 7s$, $T_z = 8s$ and $T_z = 9s$. This can be seen in table 4.16 below.

Table 4.16: Limiting design seastates – installation module weighing 289t

Hs [m]	Wave direction [deg]	Tz [s]										
		4	5	6	7	8	9	10	11	12	13	
2,5	180 ± 15											
3		N/A										
3,5		N/A										
4		N/A	N/A									
4,5		N/A	N/A									
5		N/A	N/A									

The dynamic analyses revealed that a 400t subsea structure can be installed from the considered OCV in H_s ranging from 2.5m-4m. In $H_s = 4.5m$ and $H_s = 5.0m$ both the highest and lowest effective tension were beyond the operational requirement for several zero-up-crossing periods. $H_s = 4.5m$ resulted in limiting seastates for $T_z = 6s$ and $T_z = 7s$, while $H_s = 5m$ resulted in limiting seastates for $T_z = 6s$, $T_z = 7s$, $T_z = 8s$ and $T_z = 9s$. This can be seen in table 4.17 below.

Table 4.17: Limiting design seastates – installation module weighing 400t

Hs [m]	Wave direction [deg]	Tz [s]										
		4	5	6	7	8	9	10	11	12	13	
2,5	180 ± 15											
3		N/A										
3,5		N/A										
4		N/A	N/A									
4,5		N/A	N/A									
5		N/A	N/A									

The dynamic analyses revealed that a 600t subsea structure can be installed from the considered OCV in $H_s = 2.5m$ and $H_s = 3m$. For significant wave heights beyond $H_s = 3m$, both the upper and lower tension limit exceeded the operational criterion for several zero-up-crossing periods. $H_s = 3.5m$ resulted in limiting seastates for $T_z = 5s$ and $T_z = 6s$. $H_s = 4m$ resulted in limiting seastates for $T_z = 6s$, $T_z = 7s$ and $T_z = 8s$. $H_s = 4.5m$ resulted in limiting seastates for $T_z = 6s$, $T_z = 7s$, and $T_z = 8s$. $H_s = 5m$ resulted in limiting seastates for $T_z = 6s$, $T_z = 7s$, $T_z = 8s$, $T_z = 9s$ and $T_z = 10s$. This can be seen in table 4.18 below.

Table 4.18: Limiting design seastates – installation module weighing 600t

Hs [m]	Wave direction [deg]	Tz [s]										
		4	5	6	7	8	9	10	11	12	13	
2,5	180 ± 15											
3		N/A										
3,5		N/A										
4		N/A	N/A									
4,5		N/A	N/A									
5		N/A	N/A									

4.4 Vessel Operability

The total operability of the vessel was calculated by comparing limiting seastates obtained from the dynamic analyses to an annual wave scatter diagram for the North Sea. The scatter diagram can be seen in Appendix C1.

The dynamic analyses did not cover all the seastates in the wave scatter diagram. Seastates included in the simulations were significant wave heights, H_s , ranging from 2.5m-5m, and its corresponding zero-up-crossing periods, T_z . Due to this, it was assumed that the vessel was capable of installing the module in all seastates less than $H_s = 2.5$ m. Further it has been assumed that the vessel was not capable of installing the module in any seastates beyond $H_s = 5$ m. This assumption is considered reasonable, due to the result from the dynamic analyses which revealed that all three modules could be installed in $H_s = 2.5$ m, while in $H_s = 5$ m none of the modules could be installed.

By adding the number of waves occurring in non-operable seastates compared to the total number of waves, the expected vessel uptime is calculated to be 94.6% for the vessel to perform installation of a module weighing 289t. The operable seastates for installing the 289t module are presented in table 4.19, the lower envelope in the scatter diagram represents the non-operable seastates.

Table 4.19: Operable seastates in the North Sea for installation of a module weighing 289t

Hs [m]	Tz [s]													
	0	4	5	6	7	8	9	10	11	12	13	14	14	15
0,0 - 0,5	22	18	9	2	0	0	0	0	0	0	0	0	0	0
0,5 - 1,0	729	755	328	98	19	3	0	0	0	0	0	0	0	0
1,0 - 1,5	725	1600	873	365	70	7	3	0	0	0	0	0	0	0
1,5 - 2,0	83	1151	1106	607	198	39	7	0	0	0	0	0	0	0
2,0 - 2,5	0	310	1010	744	283	72	18	3	0	0	0	0	0	0
2,5 - 3,0	0	16	640	642	304	97	15	2	0	0	0	0	0	1
3,0 - 3,5	0	0	187	514	293	78	16	0	0	0	0	0	0	0
3,5 - 4,0	0	0	33	407	263	101	9	0	0	0	0	0	0	0
4,0 - 4,5	0	0	1	235	271	75	28	2	0	0	0	0	0	0
4,5 - 5,0	0	0	0	79	256	86	16	1	0	0	0	0	0	0
5,0 - 5,5	0	0	0	7	194	75	17	0	1	0	0	0	0	0
5,5 - 6,0	0	0	0	0	117	91	14	1	0	0	0	0	0	0
6,0 - 6,5	0	0	0	0	31	91	7	3	0	0	0	0	0	0
6,5 - 7,0	0	0	0	0	8	61	16	1	0	0	0	0	0	0
7,0 - 7,5	0	0	0	0	3	30	14	1	0	0	0	0	0	0
7,5 - 8,0	0	0	0	0	0	19	27	5	0	0	0	0	0	0
8,0 - 8,5	0	0	0	0	0	6	22	3	0	0	0	0	0	0
8,5 - 9,0	0	0	0	0	0	0	13	5	0	0	0	0	0	0
9,0 - 9,5	0	0	0	0	0	0	10	4	1	0	0	0	0	0
9,5 - 10,0	0	0	0	0	0	0	2	3	1	0	0	0	0	0
10,0 - 10,5	0	0	0	0	0	0	0	1	0	0	0	0	0	0
10,5 - 11,0	0	0	0	0	0	0	0	2	0	0	0	0	0	0
11,0 - 11,5	0	0	0	0	0	0	0	1	0	0	0	0	0	0
11,5 - 12,0	0	0	0	0	0	0	0	1	0	0	0	0	0	0

The expected vessel uptime is calculated to be 92.6% for the vessel to perform installation of a module weighing 400t in the North Sea. The operable seastates for installing the 400t module can be seen in table 4.20.

Table 4.20 Operable seastates in the North Sea for installation of a module weighing 400t

Hs [m]	Tz [s]													
	0	4	5	6	7	8	9	10	11	12	13	14	14	15
0,0 - 0,5	22	18	9	2	0	0	0	0	0	0	0	0	0	0
0,5 - 1,0	729	755	328	98	19	3	0	0	0	0	0	0	0	0
1,0 - 1,5	725	1600	873	365	70	7	3	0	0	0	0	0	0	0
1,5 - 2,0	83	1151	1106	607	198	39	7	0	0	0	0	0	0	0
2,0 - 2,5	0	310	1010	744	283	72	18	3	0	0	0	0	0	0
2,5 - 3,0	0	16	640	642	304	97	15	2	0	0	0	0	0	1
3,0 - 3,5	0	0	187	514	293	78	16	0	0	0	0	0	0	0
3,5 - 4,0	0	0	33	407	263	101	9	0	0	0	0	0	0	0
4,0 - 4,5	0	0	1	235	271	75	28	2	0	0	0	0	0	0
4,5 - 5,0	0	0	0	79	256	86	16	1	0	0	0	0	0	0
5,0 - 5,5	0	0	0	7	194	75	17	0	1	0	0	0	0	0
5,5 - 6,0	0	0	0	0	117	91	14	1	0	0	0	0	0	0
6,0 - 6,5	0	0	0	0	31	91	7	3	0	0	0	0	0	0
6,5 - 7,0	0	0	0	0	8	61	16	1	0	0	0	0	0	0
7,0 - 7,5	0	0	0	0	3	30	14	1	0	0	0	0	0	0
7,5 - 8,0	0	0	0	0	0	19	27	5	0	0	0	0	0	0
8,0 - 8,5	0	0	0	0	0	6	22	3	0	0	0	0	0	0
8,5 - 9,0	0	0	0	0	0	0	13	5	0	0	0	0	0	0
9,0 - 9,5	0	0	0	0	0	0	10	4	1	0	0	0	0	0
9,5 - 10,0	0	0	0	0	0	0	2	3	1	0	0	0	0	0
10,0 - 10,5	0	0	0	0	0	0	0	1	0	0	0	0	0	0
10,5 - 11,0	0	0	0	0	0	0	0	2	0	0	0	0	0	0
11,0 - 11,5	0	0	0	0	0	0	0	1	0	0	0	0	0	0
11,5 - 12,0	0	0	0	0	0	0	0	1	0	0	0	0	0	0

The expected vessel uptime is calculated to be 86.2% for the vessel to perform installation of a module weighing 600t. The operable seastates for installing the 600t module can be seen in table 4.21 below, the lower envelope in the scatter diagram represent the non-operable seastates.

Table 4.21: Operable seastates in the North Sea for installation of a module weighing 600t

Hs [m]	Tz [s]													
	0	4	5	6	7	8	9	10	11	12	13	13	14	15
0,0 - 0,5	22	18	9	2	0	0	0	0	0	0	0	0	0	0
0,5 - 1,0	729	755	328	98	19	3	0	0	0	0	0	0	0	0
1,0 - 1,5	725	1600	873	365	70	7	3	0	0	0	0	0	0	0
1,5 - 2,0	83	1151	1106	607	198	39	7	0	0	0	0	0	0	0
2,0 - 2,5	0	310	1010	744	283	72	18	3	0	0	0	0	0	0
2,5 - 3,0	0	16	640	642	304	97	15	2	0	0	0	0	0	1
3,0 - 3,5	0	0	187	514	293	78	16	0	0	0	0	0	0	0
3,5 - 4,0	0	0	33	407	263	101	9	0	0	0	0	0	0	0
4,0 - 4,5	0	0	1	235	271	75	28	2	0	0	0	0	0	0
4,5 - 5,0	0	0	0	79	256	86	16	1	0	0	0	0	0	0
5,0 - 5,5	0	0	0	7	194	75	17	0	1	0	0	0	0	0
5,5 - 6,0	0	0	0	0	117	91	14	1	0	0	0	0	0	0
6,0 - 6,5	0	0	0	0	31	91	7	3	0	0	0	0	0	0
6,5 - 7,0	0	0	0	0	8	61	16	1	0	0	0	0	0	0
7,0 - 7,5	0	0	0	0	3	30	14	1	0	0	0	0	0	0
7,5 - 8,0	0	0	0	0	0	19	27	5	0	0	0	0	0	0
8,0 - 8,5	0	0	0	0	0	6	22	3	0	0	0	0	0	0
8,5 - 9,0	0	0	0	0	0	0	13	5	0	0	0	0	0	0
9,0 - 9,5	0	0	0	0	0	0	10	4	1	0	0	0	0	0
9,5 - 10,0	0	0	0	0	0	0	2	3	1	0	0	0	0	0
10,0 - 10,5	0	0	0	0	0	0	0	1	0	0	0	0	0	0
10,5 - 11,0	0	0	0	0	0	0	0	2	0	0	0	0	0	0
11,0 - 11,5	0	0	0	0	0	0	0	1	0	0	0	0	0	0
11,5 - 12,0	0	0	0	0	0	0	0	1	0	0	0	0	0	0

4.5 Evaluation of Weather Window

Subsea installation operations must be carefully planned and limiting operational criteria must be determined so that the operation can be executed safely. The operational criterion is often determined by the duration of the operation and the weather conditions that will cause abortion of the operation (Haver, 1999).

This section is further divided into three sections. Section 4.5.1 explains the difference between a weather restricted and unrestricted operation. Section 4.5.2 describes what is meant by operation reference period. The probability of experiencing a sufficiently long weather window for the operation to be performed for all twelve months will be presented in section 4.5.3.

4.5.1 Weather Restricted and Unrestricted Operation

According to DNV-OS-H101 (2011) section 4, a marine operation may be classified as either weather restricted or unrestricted, depending on the length of the operation. If the planned duration of the operation, T_{POP} , is within the range of what can be forecasted with reasonable confidence (normally 72 hours) it is classified as a weather restricted operation. A proper weather window must be present before an operation can be executed. Hence, prior to the execution of a weather restricted operation, a forecasted weather window of suitable length with acceptable weather is necessary (DNV-OS-H101 p. 29, 2011).

Weather unrestricted operations are operations of duration longer than what can be based on forecasts. Design weather conditions are based on statistical weather data from the actual site and season. It is necessary to design for the most extreme weather conditions, as for example extreme loads caused by waves, winds and currents for 100 and 1000-year return period. The return period selected for the design weather condition is mainly based on the length of operation (DNV-OS-H101 p. 21, 2011).

Subsea installation operations will normally be conducted within 3 days. They are therefore usually classified as weather restricted operations that can be dimensioned according to the weather forecast.

4.5.2 Operation Reference Period

An operation reference period, T_R , is introduced to indicate the duration of the installation operation and is defined as (DNV-OS-H101 p. 28, 2011):

$$T_R = T_{POP} + T_C \quad (4.5-1)$$

Where:

T_R [h] Operation reference period

T_{POP}	[h]	Planned operation period
T_C	[h]	Estimated maximum contingency time

The planned operation period, T_{POP} , should normally be based on a detailed schedule for the operation to be executed. Estimated maximum contingency time, T_C , shall be added to cover general uncertainty in the operation time and possible contingency situations (DNV-OS-H101 p. 28, 2011).

T_{POP} is in this thesis defined as the time from the operation is started until the module is landed on the seabed. It includes lift off from deck, lift in air and maneuvering object clear of transportation vessel, lowering through wave zone, further lowering down to sea bed, and finally positioning and landing. The subsea installation operations were assumed to have operation time, T_{POP} , of 5 hours. According to DNV-OS-H101 section 4B, the required contingency time should normally be at least twice as long as the planned operation time if there are any uncertainties related to the planned operation time and required contingency time. Therefore it was assumed that T_C was equal to the planned operation period, and operation reference period $T_R = 5 \text{ hours} + 5 \text{ hours} = 10 \text{ hours}$.

4.5.3 Probability of Acceptable Weather Window

By combining the limiting seastate for the operation and statistical wave data from the North Sea, the probability of experiencing a sufficiently long weather window for operation reference period, $T_R = 10 \text{ hours}$ in all twelve months of the year were found. It should be noted that the design H_s obtained from the dynamic analyses for lowering the module through the splash zone was assumed to be the operation limit for the whole installation operation.

The evaluation is based on hindcast wave data from areas outside the middle of Norway collected from the years 1955 – 1995. The mean duration of weather windows below the threshold was collected from linear interpolation for each month of the year, and used in order to find the probability of a given weather window being greater than 10 hours. Hindcast datasheets and mean duration of weather windows can be found in Appendix C2 and Appendix C3 respectively.

It is assumed that the distribution function for good weather follow an exponential distribution, and the probability of a weather window with duration greater than the required 10 hours can be calculated by the equation (Haver, 1999):

$$P(d) = \exp\left\{-\frac{d}{\beta}\right\} \quad (4.5-2)$$

Where:

$P(d)$	[-]	Probability of a weather window greater than the duration of the operation
d	[h]	Duration of the operation
β	[h]	Mean duration of weather window below threshold

This section is further divided into two sub-sections. Section 4.5.3.1 presents the results for when limiting weather conditions for the operation were taken as the result obtained from the dynamic analyses. Section 4.5.3.2 introduces the alpha factor and presents the results when uncertainty in the weather is included.

4.5.3.1 Not Including Uncertainty in Weather Forecast

By combining the limiting seastate obtained from the dynamic analyses and statistical wave data from the North Sea, the probability of experiencing an acceptable weather window for operation reference period, $T_R = 10$ hours, in all twelve months were found. If the wave height was less than the limiting design seastate for the whole duration of the installation operation, the operation was assumed to be authorized.

The results revealed that the probability of experiencing $H_s < 4.5\text{m}$ for a period of 10 hours, so that installation of a module weighing 289t can be performed is over 99% from May to July. During winter months, with more harsh weather the chance is somewhat lower, the worst month is December where the probability is about 91%.

With a module weight of 400 tons, the results revealed that the probability of experiencing $H_s < 4\text{m}$ for a period of 10 hours so that installation of the module can be performed is still quite high throughout the year. In December, 88% chance for a sufficient weather window is calculated.

The results revealed that the probability of experiencing $H_s < 3\text{m}$ for a period of 10 hours, so that installation of a module weighing 600t could be performed is 97% in the summer months. From November to February it is calculated to be from 84% to about 88% chance of a sufficient weather window in order to execute the operation in North Sea environment. This can be seen in figure 4.13. Calculated values for the probability may be found in Appendix C4.

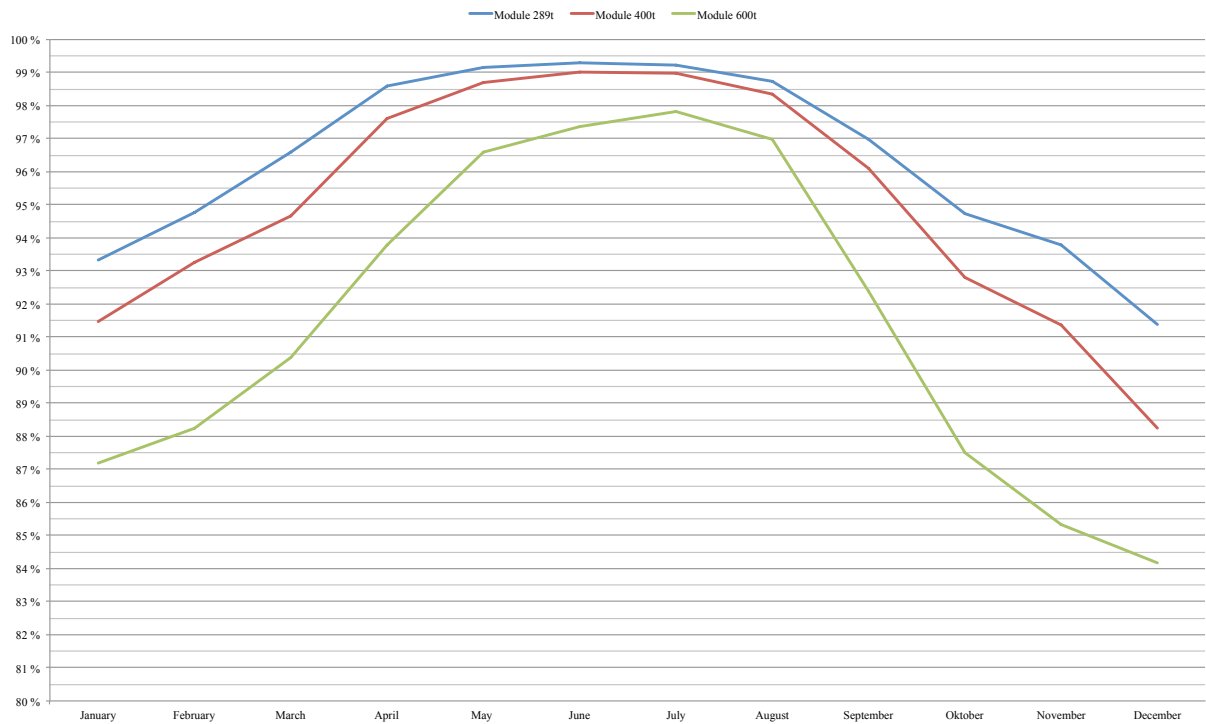


Figure 4.13: Probability of acceptable weather window for installing the different modules through out the year, not included uncertainty in weather

4.5.3.2 Including Uncertainty in Weather Forecast

It will always be uncertainty related to weather forecasting that have to be accounted for. For operations that have a planned operation period of less than 72 hours, a safety factor shall be included (DNV-OS-H101 p 29, 2011).

Figure 4.14 below illustrates the operation periods from start to finish for a marine operation, including, T_C , to account for unplanned events. An α -factor is selected based on the planned period when the operation is going to take place in order to account for uncertainty in the weather forecast.

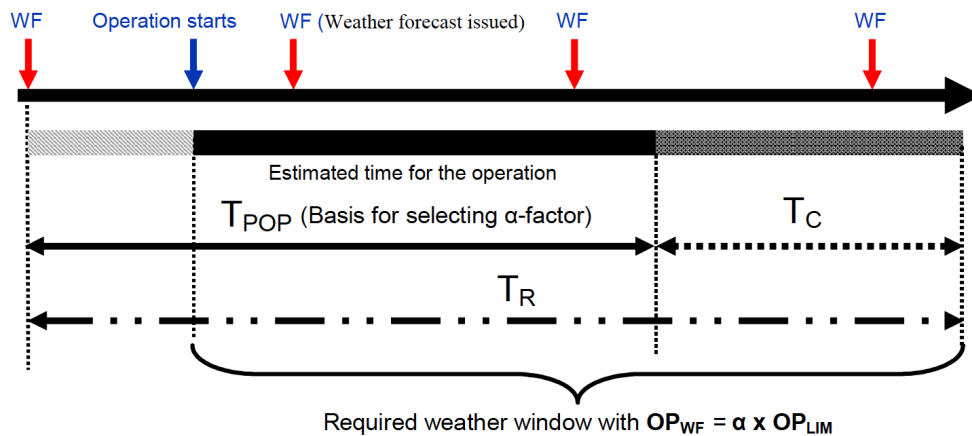


Figure 4.14: Operation periods (DNV-OS-H101 p. 29, 2011)

The α -factor represents a relationship between the operational criteria and the design criteria. The α -factor is multiplied by the design criteria for the operation, and the operational criteria are therefore reduced.

The formula for operational criteria may be expressed as (DNV-OS-H101 p. 29, 2011):

$$OP_{WF} \leq \alpha \cdot OP_{LIM} \quad (4.5-3)$$

Where:

OP_{WF}	[m]	Operational criteria
OP_{LIM}	[m]	Design criteria
α	[-]	Alpha factor

The design criteria, OP_{LIM} , were here assumed to be equal to the design H_s obtained from the dynamic analyses. For waves in the North Sea and the Norwegian Sea where available weather forecast is regarded as level B, the α -factor may be found from table 4.22 below. Level B applies to environmentally sensitive operations like offshore lifting and subsea installation (DNV-OS-H101 p. 34, 2011).

Table 4.22: α -factors for waves, level B highest forecast (DNV-OS-H101 p. 32, 2011)

Operational Period [h]	Design Wave Height [m]						
	$H_s = 1$	$1 < H_s < 2$	$H_s = 2$	$2 < H_s < 4$	$H_s = 4$	$4 < H_s < 6$	$H_s \geq 6$
$T_{POP} \leq 12$	0.68	Linear Interpolation	0.80	Linear Interpolation	0.83	Linear Interpolation	0.84
$T_{POP} \leq 24$	0.66		0.77		0.80		0.82
$T_{POP} \leq 36$	0.65		0.75		0.77		0.80
$T_{POP} \leq 48$	0.63		0.71		0.75		0.78
$T_{POP} \leq 72$	0.58		0.66		0.71		0.76

In table 4.23 below design significant wave heights, α -factors and calculated operational criterion for the three considered cases are given.

Table 4.23: Design significant wave height, α -factor factor and operational criteria

Operation	Limiting H_s [m]	Alpha factor [-]	Operational Criteria [m]
Install module weighing 289t	4.5	0.8325	3.75
Install module weighing 400t	4	0.830	3.32
Install module weighing 600t	3	0.815	2.45

In order to compare the result to the case when the probability of an acceptable weather window was calculated solely on the operational limitation of the dynamic analyses, statistics of episodes from the North Sea were used instead of a weather forecast. If the significant wave height was less than the operational criteria given in table 4.23, for the whole duration of the installation operation, $T_R = 10$ hours, the operation was assumed to be authorized.

Probability that the period of suitable weather is greater than 10 hours, and the modules can be installed according to the defined operational criteria in all twelve months are shown in figure 4.15 below. Calculated values for the probability can be found in Appendix C4.

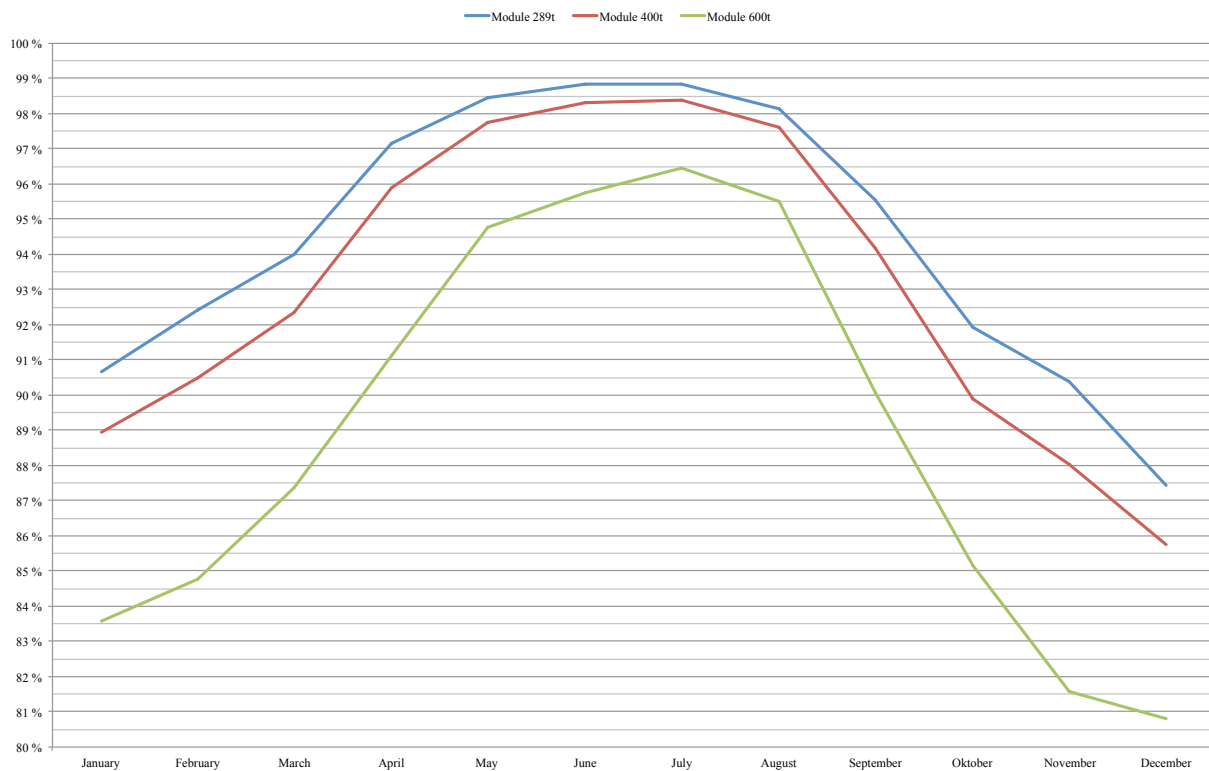


Figure 4.15: Probability of acceptable weather window for installing the different modules through out the year, included uncertainty in weather

The results revealed that the probability of experiencing $H_s < 3.75\text{m}$ for a period of 10 hours, so that installation of a module weighing 289t can be performed is over 98% from May to July. During winter months with more harsh weather the chance is somewhat lower, the worst month is December where the probability is about 88%.

With a module weight of 400 tons, the results revealed that the probability of experiencing $H_s < 3.32\text{m}$ for a period of 10 hours so that installation of the module can be performed is still quite high through out the year. In December, 86% chance for a sufficient weather window is calculated.

The results revealed that the probability of experiencing $H_s < 2.45\text{m}$ for a period of 10 hours, so that installation of a module weighing 600t can be performed is calculated to 96% in July, and during the rest of the summer months the probability is above 94%. From November to February it is calculated to be from 80% to about 84% chance of a sufficient weather window in order to execute the operation in North Sea environment.

4.6 Discussion and Main Findings Feasibility Study

Results from the dynamic analyses revealed that the effective tension in the lifting wire during the installation operation does not vary significantly in wave headings, 165° , 180° and 195° . However, a clear tendency that wave heading 165° results in both the highest and lowest forces is observed. This is considered reasonable as that this is the same side as the module was being lowered into the water, thus the module was more exposed to the whole waves from trough to crest, resulting in larger force in the wire and an increased risk for snap loads. It is important to account for some vessel drifting during the operation, as this may result in somewhat larger forces acting on the module.

The dynamic analyses revealed that the highest and lowest effective tension in the crane wire during the installation operation is highly dependent on the wave height, as expected. As the wave height was increased, maximum effective tension in the lifting wire increased. At the same time the minimum effective tension in the wire decreased, and the chance for slack in sling or crane wire increased.

The dynamic analyses revealed that the 289t subsea module can be installed from the OCV in $H_s = 4.5\text{m}$ given that the vessel is kept within 15° head sea. The 400t module can be installed from the OCV in $H_s = 4\text{m}$. Further, the analyses revealed that the 600t subsea structure can be installed from the OCV in $H_s = 3\text{m}$. For all modules, the most critical situation occurred for short wave zero-up-crossing periods. The reason for this is that it is in the shortest waves the water particle motion and slam forces are largest.

Evaluation of vessel operability in North Sea environment revealed that the vessel uptime varies with the module that is being installed. The vessel operability is high for installation of the 289t and the 400t subsea structure, with total uptime of 94.6% and 92.6% respectively. Operability of the vessel for installing the 600t subsea structure is lower, with an all year operability of 86.2%.

Probability of experiencing a sufficiently long weather window for the installation operation to be performed for the three modules is high during the summer months. Calculated probability for a sufficient weather window from May – July for the module weighing 289t, 400t and 600t, is equal to 99%, 98% and 97% respectively. The month with the lowest probability of experiencing a sufficient weather window for installing the modules is December. The probability is in this month reduced to 91%, 88% and 84% for the module weighing 289t, 400t and 600t respectively. This is considered reasonable, as the weather is harsher in this month of the year.

The results revealed that when uncertainty in the weather statistics is accounted for, the operational wave height for installing the module weighing 289t is reduced to $H_s = 3.75\text{m}$, while for installing the module weighing 400t and 600t the operational wave height reduced to $H_s = 3.32\text{m}$ and $H_s = 2.45\text{m}$ respectively. Furthermore, the probability of experiencing a sufficiently long weather window to perform the operation is also reduced in all twelve months of the year. The probability is reduced by about one percent in the summer months, and from 2-4% in December, when comparing to the result when the probability of a sufficient weather window were based solely on the limiting wave height obtained from the dynamic analysis.

5 Qualitative Comparison - Monohull vs. Twin-Hull

In this chapter, a qualitative comparison of monohull and twin-hull vessels is performed. In the installation and construction vessel industry, there has been a trend in the last years of gradually increasing the size of monohull vessels. The aim of the qualitative comparison is to look into whether the increase in size of monohulls is so high, that the cost to build them is becoming comparable to building medium-size semi-submersibles. An evaluation based on the motion behavior and lightship weight of monohulls and semi-submersibles is performed, to get an indication of whether medium-size semi-submersibles can compete in this market segment.

This chapter is divided into three sections. In section 5.1 motion behavior and operability of the two vessel types are described. Section 5.2 compares lightship weight of some specific monohull and twin-hull vessels. A discussion of the result of the analysis is presented in section 5.3.

5.1 Motion Behavior and Operability

Vessel motion is essential when performing marine operations in environments like the North Sea. Heave and roll are important response variables for offshore vessels (Faltinsen, 1990). Ships have a large waterline area to displacement ratio, as a result of this they follow the waves with relatively high heave and roll response amplitudes compared to column stabilized semi-submersibles. The twin-hull vessels motion characteristics are therefore favorable compared to monohulls as they have lower waterline area to displacement ratio and thus are able to achieve low dynamic response to wave action (Clauss et al., 1992).

Most semi-submersibles have a natural period in heave around 20s. This exceeds the dominant survival wave period of a 100-year wave, and semi-submersibles are usually outside the range of the high energy wave periods in harsh weather (Clauss et al., 1992). The monohull vessels have smaller natural periods, usually within the range of 4-16s depending on mainly the size of the ship (Faltinsen, 1990).

When the period of the waves is equal to the natural period of the vessel, resonance may occur. A vessel with good motion characteristic will avoid the possibility of resonance with larger waves (Gudmestad, 2014). For semi-submersibles, natural heave oscillations can be excited by swells. For monohull vessels the dominating excitation mechanism around the natural heave period are linear wave forces. For both vessel types change in buoyancy forces can cause heave resonance, which is directly related to the vessels waterplane area (Faltinsen, 1990).

To compare motion characteristics of the two vessel types, results of a study performed by Moss Maritime (2002) are introduced as an example. The study covered two monohull vessels and one semi-submersible. The smallest monohull vessel had a length of 94m and a displacement of 8000t. The largest monohull had a length of 128m and a displacement of 15500t, and can be compared to a vessel that is larger than Edda Fauna and smaller than Skandi Acergy. The semi-

submersible had a deck structure with length of 63m and breadth of 62m. This vessel had a displacement of 26600t, which similar to the GVA 4000 design. Transfer functions in heave for waves approaching head sea can be seen in figure 5.1 below for the three vessels.

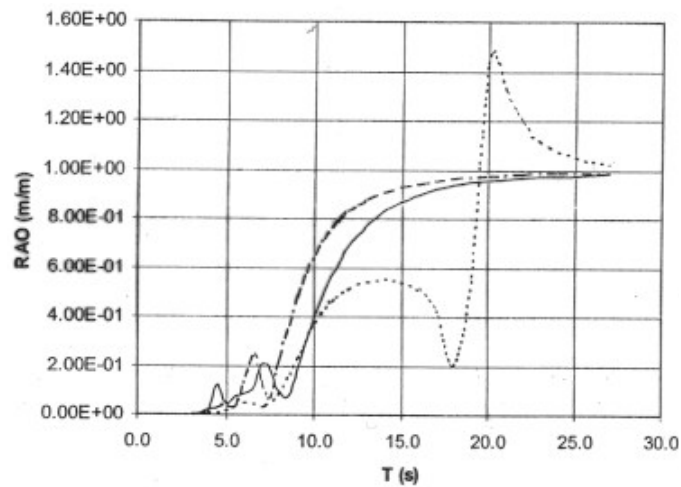


Figure 5.1: RAO for heave, wave heading 0° (Moss Maritime, 2002)

The curve with a dotted line in figure 5.1 represents the semi-submersible, the curve with a dashed line represents the smallest monohull vessel, and the solid line represent the largest monohull vessel. For the smallest monohull vessel it can be seen that the transfer function has a peak at about 6.5s, this corresponds to the vessels natural period in heave. For the largest monohull vessel the natural period is about 7s and for the semi-submersible the natural period is just above 20s.

In figure 5.2 below, the wave energy versus period of waves can be seen for various weather conditions in the North Sea.

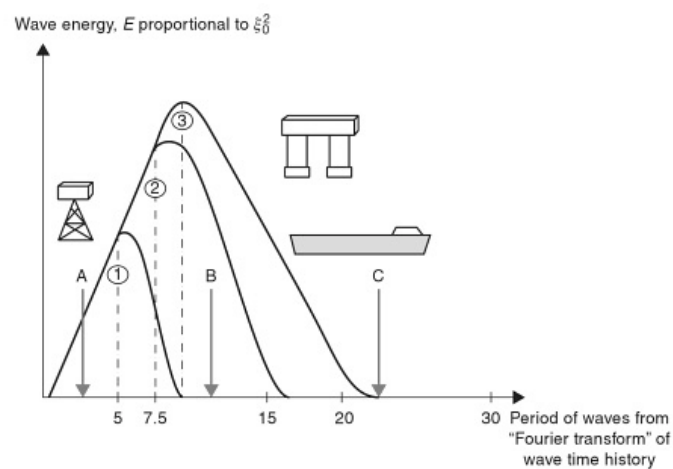


Figure 5.2: Wave energy versus wave period North Sea (Gudmestad, 2014)

Graph 1 represent a calm day, graph 2 represent a normal situation and graph 3 represent a storm situation. Case A represent a structure with low period interacting with short waves with little energy, case B represent a structure that is normally in resonance with energetic waves, and case C represent a structure that is normally not in resonance with waves, although the individual waves are powerful (Gudmestad, 2014). Subsea installation operations are only performed when the weather is acceptable, and never in storm situations.

For lifting operations through the splash zone from a large monohull construction vessel, the wave forces that act on the module limit the operation, the vessel motions being of less significance (Hovland, 2007). Large monohull construction vessels therefore have very similar limiting seastates as medium-size semi-submersibles for performing installation operations of subsea modules. This favors the monohull concepts.

Further, monohull vessels generally have higher transit speed than semi submersibles. Semi-submersibles can reach about 10 knots, while large monohull construction vessels can reach about 16 knots. The semi-submersible has large deck area available for working area or storage of equipment. Due to the semi-submersibles small waterplane area and large lightship weight it has limited deck load capability. Monohull vessels have larger deck load capability and a limited available deck area (Clauss et al., 1992).

5.2 Lightship Weight Comparison

The total weight or displacement of a vessel can be divided in two: lightship weight (LSW) and deadweight (DWT). A vessels lightship weight gives a good indication of the vessel cost. Lightship weight is obtained for several monoulls and semi-submersibles in order to compare the cost of the two vessel types. The lightship weight is the total weight of the vessel steel, machinery and outfit (Couch et al., 1974).

The deadweight provides information about how much weight a vessel is carrying or can safely carry. It is the sum of the weight of cargo, ballast water and payloads like consumables, crew, fuel, extra equipment etc. Deadweight is obtained for several monoulls and semi-submersibles in order to compare displacement versus lightship weight for the two vessel types. Figure 5.3 illustrates the vessel displacement weight breakdown.

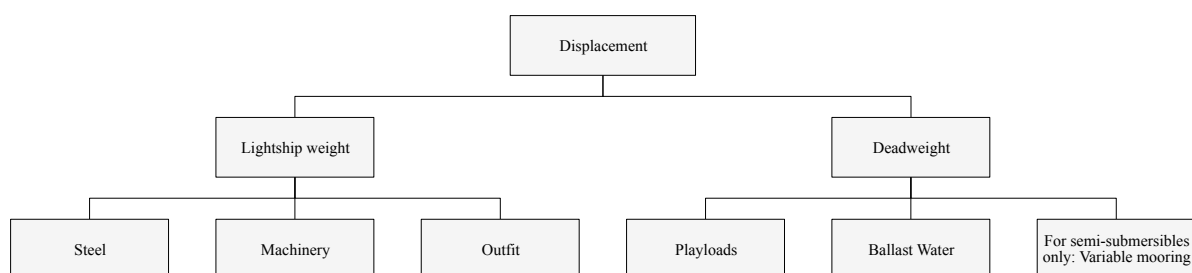


Figure 5.3: Vessel displacement weight breakdown

This section is divided into two sub-sections. Section 5.2.1 presents the lightship weight of seven monohull construction/installation vessels. Section 5.2.2 presents lightship weight for some specific medium-size semi-submersible designs.

5.2.1 Monohull

The weight of the steel is the largest contributor to the lightship weight for monohull vessels. Watson and Gilfillan (1976) presented a simple method for estimating the hull and superstructure weights of monohull vessels and can be expressed as (Watson & Gilfillan, 1976):

$$W_s = C_b^{1/2} L \cdot B \left[K_1 L \cdot \frac{L}{D} \div K_2 D \right] \quad (5.2-1)$$

Where:

W_s	[t]	Steel weight
C_b	[-]	Block coefficient
L	[m]	Length of the underwater form of vessel
B	[m]	Vessel breadth
D	[m]	Vessel depth
$K_{1,2}$	[-]	Constant for specific ship type

When comparing ship forms, displacement and dimensions, a number of coefficients are required for the specific vessel type. The coefficients can be found based on previous successful design for similar vessels.

Hovland (2007) performed a comparison study of a total of 12 construction vessels where he calculated the steel weight based on Watson and Gilfillan's method. He calculated machinery weight based on similar vessels, while outfit weight was based on numbers from vendors.

Monohull vessels considered in the qualitative comparison are: Edda Fauna, Seven Viking, Viking Neptun, Skandi Acergy, Skandi Arctic, Seven Arctic and Normand Maximus. Due to lack of available data on these vessels, interpolation and extrapolation of lightship weight based on vessel length from Hovland's (2007) study was used to estimate the lightship weight of the monohull vessels considered in this thesis. Equation used for the calculation can be found in Appendix D1. The lightship weight versus ship length for the mentioned vessels is shown in figure 5.4.

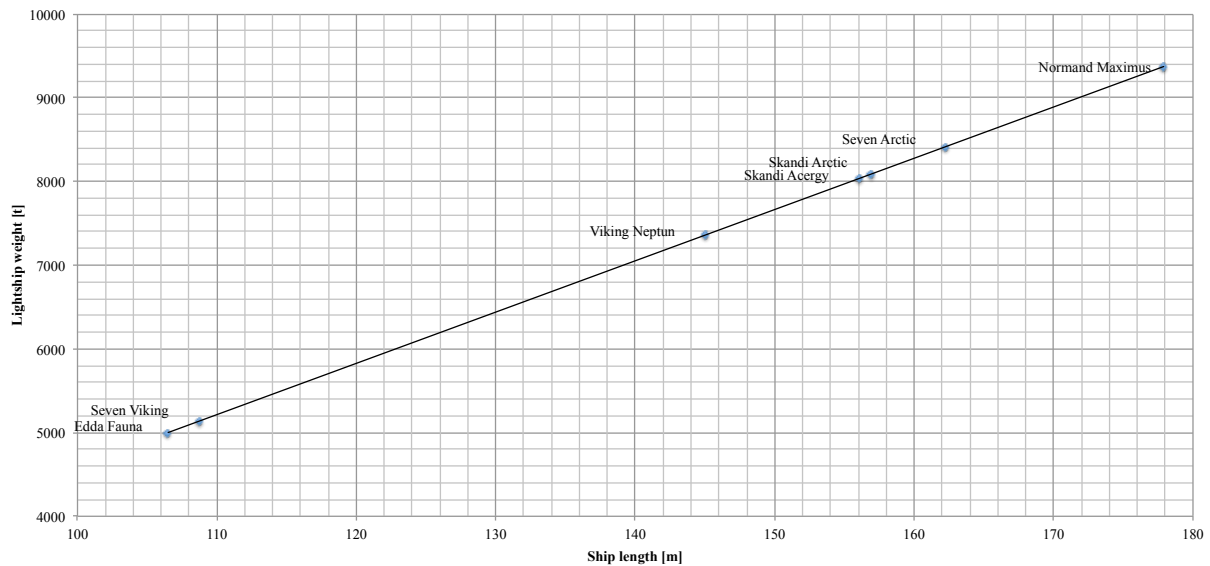


Figure 5.4: Lightship weight versus ship length based on Hovland's (2007) curve, monohull vessels

If the DWT is added to the LSW, the displacement of the vessel is found. Calculated LSW and collected DWT for all considered vessels are presented in figure 5.5 below. For vessels that are not on the market yet, Seven Arctic and Normand Maximus, the approximate DWT was based on extrapolation of DWT collected from the other vessels.








Name: Edda Fauna Delivered: 2008 DWT: 6200t LSW: 5153t	
Name: Skandi Acergy Delivered: 2008 DWT: 11500t LSW: 8032t	
Name: Skandi Arctic Delivered: 2009 DWT: 11000t LSW: 8087t	
Name: Seven Viking Delivered: 2013 DWT: 5125t LSW: 5000t	
Name: Viking Neptun Delivered: 2014 DWT: 13500t LSW: 7358t	
Name: Seven Arctic Delivery: 2016 DWT: 13043t LSW: 8418t	
Name: Normand Maximus Delivery: 2016 DWT: 15060t LSW: 9373t	

Figure 5.5: DWT and LSW monohull vessels (Marinetraffic.com, 2015), (Subsea 7, 2014), (Solstad, 2015), (Hovland, 2007)

5.2.2 Twin-hull

Semi-submersibles are considered in the twin hull vessel category. For semi-submersibles the lightship weight consist of the weight of vessel steel, machinery and outfitting. Clauss, Lehmann and Ostergaard (1992) calculated the lightship weight and operation displacement of several medium-size semi-submersible designs that were developed from the 1960's to 1980's: Sedco 135, Pentagone, Sedco 700, Ocean Victory, Pacesetter, Aker H-3 and GVA 4000. These vessels were used in the comparison study. In addition, semi 1 and Semi 2 were included, this design was developed in 1987 to fill the gap between a large monohull and a semi-submersible vessel for offshore IMR and construction/installation work (Schepman & Santen, 1991). The lightship weight and displacement of the different vessel designs can be seen in figure 5.6 below.

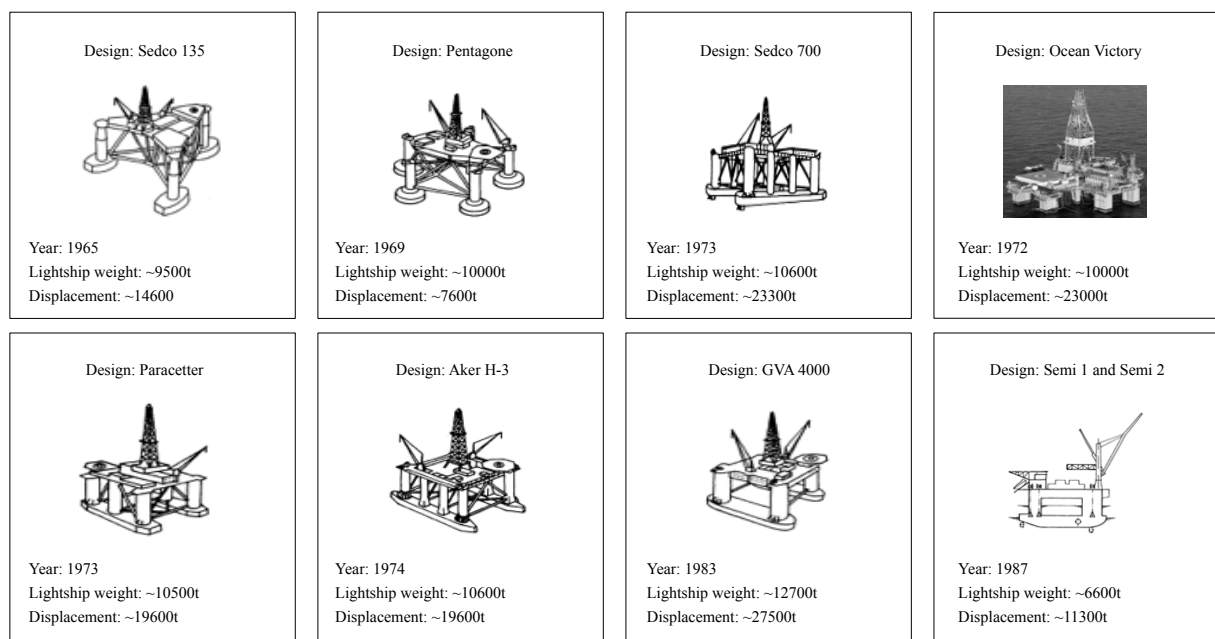


Figure 5.6: Some typical small semi-submersible design with lightship weight and displacement (Clauss et al., 1992), (Kaltvedt, 2014), (Diamond Offshore, 2014), (Schepman & Santen, 1991)

Displacement versus lightship weight for these vessels is presented in figure 5.7, under section 5.3.

There are some semi-submersibles built especially for the purpose of maintenance and construction that have similar designs. Seaway Swan is an Aker H-3 design, while Regalia is a GVA 3000 design, which is similar to the GVA 4000 design. Regalia has a displacement of about 20000t (Gudmestad, 2014). These vessels are shown in figure 3.8.

5.3 Discussion and Main Findings Qualitative Comparison

The installation and construction vessels operability is claimed to be more dependent on the seastate than the motion behavior of the vessel, when performing subsea installation operations (Hovland, 2007). The wave forces that act on the module as it is lowered through the splash zone are the main limiting factor. Although the semi-submersible has favorable motion characteristics, the seastate will limit the operation and a semi-submersible will not obtain a higher operability than a comparable monohull vessel. Considering this fact, the 145m long construction vessel that was analyzed in the feasibility study, and a medium-size semi-submersible are believed to have comparable limiting seastates for performing installation of heavy subsea modules.

The vessels lightship weight gives a good indication of the vessel cost. Figure 5.4 shows that the lightship weight of monohull construction vessels have increased with size considerably the last 10 years. Skandi Acergy and Skandi Arctic that was built in 2008 and 2009 had a lightship weight just above 8000t, and were at the time the largest vessels of their kind. The newly ordered 177.9m long construction vessel, Normand Maximus, has an estimated lightship weight of 9400t. That is 2000t higher than Viking Neptun that was built in 2015.

Figure 5.7 below shows the displacement versus lightship weight of all the vessels considered in the comparison study. Blue and red lines are drawn in the figure to indicate the upper and lower envelope of the two vessel types.

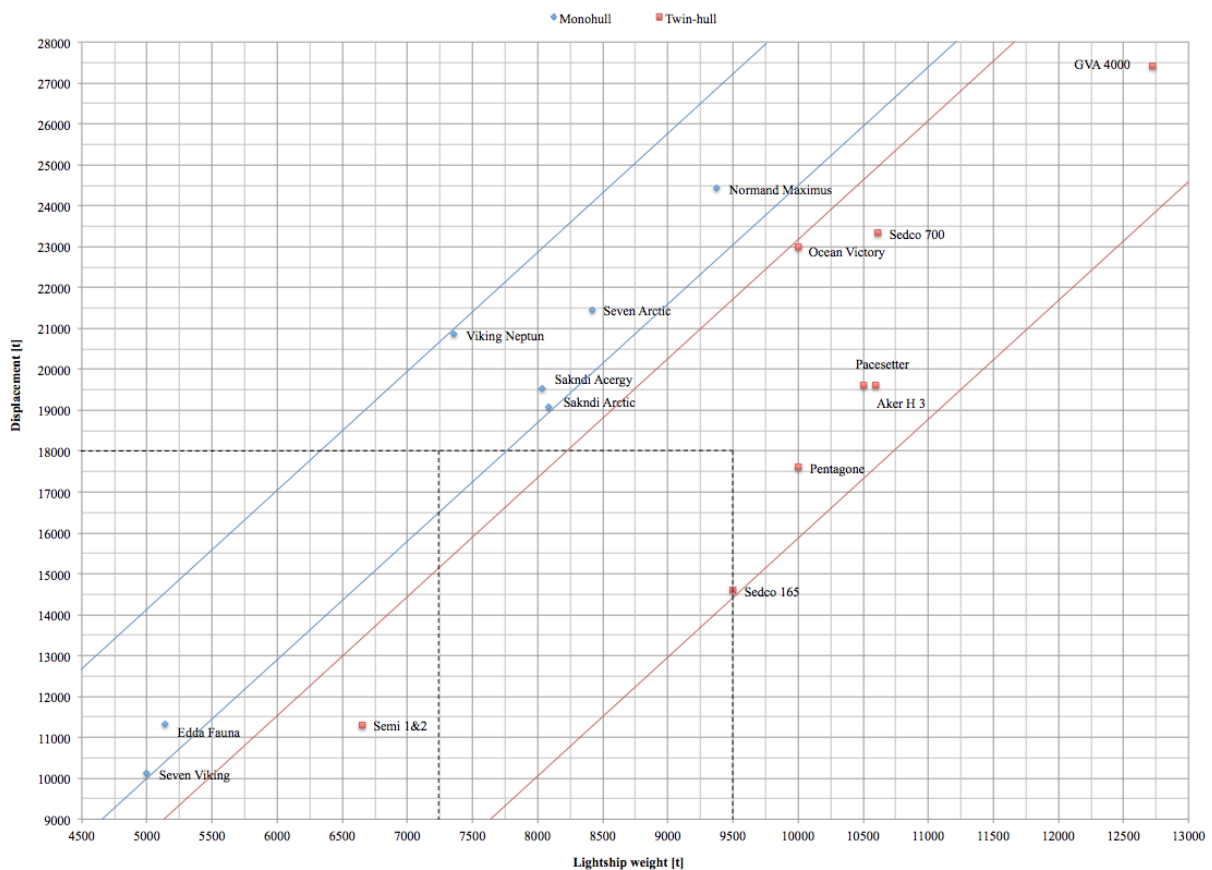


Figure 5.7 Displacement versus lightship weight, monohull and twin-hull vessels

Figure 5.7 shows that the largest monohull vessel, Normand Maximus, has 1200t lower lightship weight than the well known Aker H-3 semi-submersible design, and 3300t lower lightship weight than the GVA 4000 design. A smaller monohull vessel, Skandi Arctic, has 2500t lower lightship weight than the Aker H-3 semi-submersible design, and 4600t lower lightship weight than the GVA 4000 design.

The dotted lines in figure 5.7 indicate that for a vessel with displacement of 18000t, the monohull vessel has a lightship weight around 2250t lower than a comparable semi-submersible. Another example to be made is for monohull Skandi Acergy and twin-hull Aker H-3, they have a lightship weight of about 8000t and 10600t respectively. Both vessels have displacement of 19500t.

For ships and semi-submersibles with equal displacement, it is seen from figure 5.7 that semi-submersibles generally have a considerably higher lightship weight, which again gives a higher cost from the shipyard. Furthermore, semi-submersibles are more expensive to build than monohull vessels (Hovland, 2007). They have a more complex structure when compared to monohulls, which results in a higher cost per unit lightship weight than ships.

Study of transit speeds revealed that a typical Aker H-3 design is limited to about 8 knots (Diamond Offshore, 2014), while Skandi Acergy transits at about 15 knots (Hovland, 2007). It is noticed that the semi-submersibles transit speed is around half the speed of a comparable monohull vessel. As efficiency and speed are very important with regards to offshore activities (Hovland, 2007), the semi-submersible may therefore not be optimal if there is a long travel distance between each job.

6 Conclusion

The feasibility study revealed that the 145 meter long OCV has a high operability for installing the module weighing 289 tons. Installation of the module can be performed in $H_s = 4.5$ meters, and the vessel can operate in 94.6% of the seastates, which corresponds to an uptime of 345 days of the year. The probability of experiencing seastates below the limiting operational seastate, $H_s = 4.5$ meters, for the whole duration of the installation operation is in the best month, June, equal to 99.3% and in the worst month, December, equal to 91.4%.

With a module weight of 400 tons, the vessel operability was somewhat reduced, but still good. Installation of the module can be performed in $H_s = 4$ meters and the vessel has a total operability of 92.6%, which corresponds to an uptime of 338 days of the year. The probability of experiencing seastates below the limiting operational seastate, $H_s = 4$ meters, for the whole duration of the installation operation is in the best month, June, equal to 99% and in the worst month, December, equal to 88.2%.

The heaviest module considered had a weight of 600 tons. The analyses revealed that the OCV has reduced operability for installing this module. Installation of the module can be performed in $H_s = 3$ meters and the vessel can operate in 86.2% of the seastates, which corresponds to an uptime of 314 days of the year. The probability of experiencing seastates below the limiting operational seastate, $H_s = 3$ meters, for the whole duration of the installation operation is in the best month, June, equal to 97.4% and in the worst month, December, equal to 84.2%.

When uncertainty in the weather is accounted for, the operational wave height decreases considerably. The probability of experiencing a sufficiently long weather window to perform the operation is also reduced, especially in the winter months.

The comparison study revealed that the seastate is the main limiting factor when performing subsea installation operations, and that motion behavior of the vessel are of less significance. Although semi-submersibles have favorable motion characteristics, they will not obtain a higher operability than comparable monohull vessels. Furthermore, semi-submersibles generally have a higher lightship weight and a more complex structure compared to monohulls, which results in a higher cost of lightship weight per unit from the shipyard. Semi-submersibles also have a transit speed that is around half the speed of comparable monohull vessels. According to the comparison study, it is not considered likely that semi-submersibles will have a breakthrough in the subsea installation and construction market segment.

7 Further Work

This thesis covered lowering subsea modules through the splash zone, recommendations for further work are to study all phases of a subsea installation operation.

For future analysis it is recommended to obtain accurate data on added mass, slamming force, drag force etc. of the subsea structure. This may be done by CFD studies or model tests.

A different simulation program, for example SIMA/SIMO, may be applied for the dynamic analysis, and results can be compared to the results obtained from OrcaFlex. The influence of swells should be studied as it may affect the vessel operability.

Furthermore, it would also be of interest to perform an additional dynamic analysis utilizing a medium-sized non-drilling semi-submersible for the subsea installation operations.

8 References

- Annual Offshore Support Journal. (2014). *Unique vessels wins support ship award*. London, England
- Birk, L., & Clauss, G.F. (1998). *Design of Optimum Offshore Structures Based on Longterm Wave Statistics*. OMAE'98 Conference, Lisbon, Portugal.
- Bøe, T., & Nestegård, T. (2010). *Dynamic Forces during Deepwater Lifting Operations*. 20th International Offshore and Polar Engineering Conference, Beijing, China.
- Carbon Trust. (2006). *Ocean waves and wave energy device design*. London, UK.
- Clauss, G., Lehmann, E., & Ostergaard, C. (1992). *Offshore Structures Volume 1 Conceptual Design and Hydromechanics*. Germany: Springer
- Couch, R.B., Forrest, M.G., Oakley O.H., Robinson H.F., & Russo, V.L. (1974). *Principles of Naval Architecture*. USA: The Society of Naval Architects and Marine Engineers
- Davies, S., Ramberg, R.M., Bakke, W., & Jensen, R.O. (2010). *OTC 20616. Experience to Date and Future Opportunities for Subsea Processing in Statoil*. Paper presented at Offshore Technology Conference, Houston, Texas, USA.
- Davies, S., Ramberg, R.M., Økland, O., & Rognhø, H. (2013). *OTC 24307. Steps to the Subsea Factory*. Paper presented at Offshore Technology Conference, Rio de Janeiro, Brasil.
- Diamond Offshore. (2014). *Ocean Baroness*. Retrieved 07.05.2015, from <http://www.diamondoffshore.com/Documents/Full%20Binder%20Spec%20Sheets%20.pdf>
- DNV. (2014). *Introduction to Subsea Production Systems*. Retrieved 26.02.2015, from <http://www.uio.no/studier/emner/matnat/math/MEK4450/h14/undervisningsmateriale/module-2/mek4450-dnvg1-02-what-is-subsea.pdf>
- DNV. (2014). *Lifting Operations (VMO Standard - Part 2-5)*. Technical Report DNV-OS-H205. Det Norske Veritas, Høvik, Oslo, Norway.
- DNV. (2011). *Marine Operations, General*. Technical Report DNV-OS-H101. Det Norske Veritas, Høvik, Oslo, Norway.
- DNV. (2014). *Modelling and Analysis of Marine Operations*. Technical Report DNV-RP-H103. Det Norske Veritas, Høvik, Oslo, Norway.

- DNV. (2014). *Subsea Facilities – Technology Developments, Incidents and Future Trends*. Technical Report nr. 2014-0113, Rev 03. Det Norske Veritas, Høvik, Oslo, Norway.
- Faltinsen, O.M. (1990). *Sea Loads on Ships and Offshore Structures*. United Kingdom: Cambridge University Press.
- Gcaptain. (2013). *Singapores Jurong Shipyard Firms Contract to Build Q7000 Well Intervention Rig for Helix*. Retrieved 06.03.2015, from <http://gcaptain.com/singapores-jurong-shipyard-to-build-q7000-well-intervention-rig-for-helix/>
- Gudmestad, O.T. (2014). *Marine Technology and Operations*. University of Stavanger, Norway.
- Gusto MSC. (2009). *Semi-1 and Semi-2*. Retrieved 07.05.2015, from <http://www.gustomsc.com/index.php/zoo/product-sheets-8233/construction-semis>
- Hallin. (2014). *CSS Derwent*. Retrieved 06.03.2015, from <http://www.hallinmarine.com/vessels/css-derwent/>
- Haver, S. (1999). *Weather windows for marine operations*. Lecture notes, University of Stavanger, Norway.
- Hedne, P. (2013). *Subsea processing and transportation of hydrocarbon*. Retrieved 20.02.2015, from <http://www.ipt.ntnu.no/~jsg/undervisning/prosessering/gjester/LysarkHedne2013.pdf>
- Helix Energy Solutions. (2013). *2013 Annual Report. Built for Success. Positioned for Growth*.
- Helix Energy Solutions. (2013). *MODU Q4000*. Retrieved 05.03.2015, from <http://www.helixesg.com/well-intervention/intervention-assets/q4000/>
- Helix Energy Solutions. (2013). *MODU Q5000*. Retrieved 05.03.2015, from <http://www.helixesg.com/well-intervention/intervention-assets/q5000/>
- Helix Energy Solutions. (2015). *Raymond James 36th Annual Institutional Investors Conference*, Orlando, Florida, USA.
- Hovland, E. (2007). *Evaluation of Vessel Concepts for Subsea Operations in North Sea*. (PhD Thesis, University of Stavanger), Faculty of Science and Technology, Department of Mechanical and Structural Engineering and Material Science, Stavanger.
- Infield. (2011). *Subsea Market Report To 2015*.

- Intecsea. (2014). Subsea Processing Poster 2014. Retrieved 23.02.2015, from <http://www.intecsea.com/images/Publications/Posters/2014%20Subsea%20Boosting.pdf>
- Jahnsen, O.F. (2015). *Subsea Processing – Technology to Increase Recovery*. Retrieved 28.04.2015, from <http://hniforum.no/cmsAdmin/uploads/fmc.pdf>
- Journee, J.M.J., & Maissie, W.W. (2001). *Introduction in offshore hydromechanics*. Delft University of Technology
- Kaltvedt, E.C. (2014). *A Parametric study of Variable Deck Load for Drilling Vessels*. (Master Thesis, University of Stavanger), Faculty of Science and Technology, Department of Mechanical and Structural Engineering and Material Science, Stavanger.
- Marinetraffic. (2015). *Edda Fauna*. Retrieved 04.05.2015, from <https://www.marinetraffic.com/no/ais/details/ships/259665000>
- Marinetraffic. (2015). *Regalia*. Retrieved 07.05.2015, from <http://www.marinetraffic.com/ais/details/ships/shipid:729641/mmsi:565086000/imo:8308549/vessel:REGALIA>
- Marinetraffic. (2015). *Seven Viking*. Retrieved 04.05.2015, from <https://www.marinetraffic.com/no/ais/details/ships/257973000>
- Marinetraffic. (2015). *Skandi Acergy*. Retrieved 04.05.2015, from http://www.marinetraffic.com/ais/details/ships/shipid:193762/mmsi:235065411/imo:9387217/vessel:SKANDI_ACERGY
- Marinetraffic. (2015). *Skandi Arctic*. Retrieved 04.05.2015, from <http://www.marinetraffic.com/no/ais/details/ships/311023800>
- Marinetraffic. (2015). *Skandi Arctic*. Retrieved 04.05.2015, from http://www.marinetraffic.com/ais/details/ships/shipid:370343/mmsi:309704000/imo:7529902/vessel:UNCLE_JOHN
- Marinetraffic. (2015). *Viking Neptun*. Retrieved 04.05.2015, from http://www.marinetraffic.com/ais/details/ships/shipid:1241803/mmsi:311000347/imo:9664902/vessel:VIKING_NEPTUN
- Marinetraffic. (2015). *Q4000*. Retrieved 05.03.2015, from <http://www.marinetraffic.com/ais/details/ships/shipid:456713/mmsi:369550000/imo:8767123/vessel:Q4000>

- Moreno-Trejo, J. (2012). *Subsea Production Systems and Services*. (PhD thesis, University of Stavanger), Faculty of Science and Technology, Department of Mechanical and Structural Engineering and Material Science, Stavanger.
- Moss Maritime. (2002). *Operability comparison*. Confidential document.
- Nielsen, G. (2012). *Subsea lifting operations - Hydrodynamic properties of subsea structures*. Retrieved 02.04.2015, from http://www.ivt.ntnu.no/imt/courses/tmr4225/literature/12_sub_sea_lifting_oper.pdf
- Nordhal, T.H. (2002). *Far Saga – spesialutstyrt for undervannsoverasjoner*. FFU Nytt. Retrieved 07.03.2015, from <http://www.ffu.no/uploads/magasinet/2002nr2.pdf>
- Norsk Kystfart. (2002). *Offshorefartøy fra Hauglandet - Stolt Comex Seaway AS*. Retrieved 04.05.2015, from <http://visekar.diskusjonsforum.no/visekar-about99.html>
- Norwegian Petroleum Directorate. (2015). *The Shelf in 2014*. Retrieved 04.03.2015, from http://www.npd.no/Global/Engelsk/1-Whats-new/News/The-shelf-in-2014/Presentasjon_engelsk_utgave.pdf
- OrcaFlex Manual, version 9.8a. (2014). Orchina Ltd. U.K.
- Rawson, K.J., & Tupper, E.C. (2001). *Basic Ship Theory: Volume 1* (5). Oxford: Butterworth – Heinemann.
- Rawson, K.J., & Tupper, E.C. (2001). *Basic Ship Theory: Volume 2* (5). Oxford: Butterworth – Heinemann.
- Reachsubsea. (2015). *Viking Neptun*. Retrieved 23.03.2015, from <http://reachsubsea.com/assets/viking-neptun/#>
- Sarkar, A., & Gudmestad, O.T. (2010). *Splash Zone Lifting Analysis of Subsea Structures*. 29th International Conference on Ocean Offshore and Arctic Engineering, Changhai, China. Doi: 10.1115/ OMAE2010-20489.
- Schepman, G.J., & Santen, J.A. (1991). *Design of the Compact Semisubmersibles Rockwater Semi 1 and 2*. Society of Petroleum Engineers. doi:10.2118/19212-PA.
- Sea Ship News. (2014). *PaxOcean buys CSS Derwent in Hallin Marine settlement*. Retrieved 07.03.2015, from <http://www.seashipnews.com/News/PaxOcean-buys-CSS-Derwent-in-Hallin-Marine-settlement/3w3c3038.html>

- Solstad. (2015). *2014 Annual Report*. Retrieved 01.06.2015, from https://www.google.com/url?sa=t&rct=j&q=&esrc=s&source=web&cd=10&ved=0CGUQFjAJ&url=http%3A%2F%2Fwww.newsweb.no%2Fnewsweb%2Fattachment.do%3Fname%3D%2FAnnualReport_2014.pdf%26attId%3D135599&ei=JXxtVdTtG4HwUPPBgKAJ&usq=AFQjCNGRa1prGqaR97GCL65tf00F-cgoTA&sig2=HRUKHXEqN7ANhslTTcrTJA&bvm=bv.94911696,d.d24
- Statoil. (2012). *IMR in Statoil-next level*. Retrieved 23.03.2015, from http://ffu.no/uploads/Presentasjoner_etter_seminar_2012/FFU_seminar_-_Statoil_IMR_presentation_revised.pdf
- Subsea World News. (2015). *Helix, BP Agree to Delay Q5000 Contract*. Retrieved 05.03.2015, from <http://subseaworldnews.com/2015/02/27/helix-bp-agree-to-delay-q5000-contract/>
- Subsea 7. (2010). *Engineering optimization by using the Simplified Method for Lifting through the Splash Zone*. Retrieved 10.04.2015, from http://www.google.com/url?sa=t&rct=j&q=&esrc=s&source=web&cd=1&ved=0CCUQFjAA&url=http%3A%2F%2Fwww.aakp.no%2Fdownload.aspx%3Fobject_id%3D8AF7D37F88774AD8B5F6E908ECD054DB.pdf&ei=ctgnVYGWecWxsAHL_YKwDQ&usq=AFQjCNEXAo1YwdeXAU9x3uMG49omG_6yow&sig2=AZAlhGXOQ4xY92xPunO9A&bvm=bv.90491159,d.bGg
- Subsea 7. (2014). *Seven Arctic*. Retrieved 23.03.2015, from <http://www.subsea7.com/content/dam/subsea7/documents/whatwedo/fleet/constructionvertical/Seven%20Arctic.pdf>
- Tupper, E.C. (2004). *Introduction to Naval Architecture* (4). Oxford: Elsevier Butterworth – Heinemann.
- Wang, A., Yang, Y., Zhu, S., Li, H., Xu, J., & He, M. (2012). *Latest progress in Deepwater Installation Technologies*. Paper presented at the International Offshore and Polar Engineering Conference, Rhodes, Greece.
- Watson, D.G.M., Gilfillan, A.W. (1976). *Some Ship Design Methods*. Transactions RINA p. 279-234, 1976.

Appendix A - Input OrcaFlex

A1: Input OrcaFlex: Subsea structures

A summary of the parameters plotted into OrcaFlex for the three subsea modules is presented in table A1-1 below. The parameters are calculated as described in section 4.2.1.

Table A1 - 1: Summary subsea modules input OrcaFlex

	Module 289t	Module 400t	Module 600t
Height of module, z	10	10	10
Hydrodynamic added mass fully submerged x-direction, A_{33x}	304t	304t	304t
Hydrodynamic added mass fully submerged y-direction, A_{33y}	399t	399t	399t
Hydrodynamic added mass fully submerged z-direction, A_{33z}	345t	345t	345t
Hydrodynamic added mass coefficient x-direction, C_{Ax}	0,607	0,607	0,607
Hydrodynamic added mass coefficient y-direction, C_{Ay}	0,6042	0,6042	0,6042
Hydrodynamic added mass coefficient z-direction, C_{Az}	0,635	0,635	0,635
Hydrodynamic inertia coefficient x-direction, C_{Mx}	1,607	1,607	1,607
Hydrodynamic inertia coefficient y-direction, C_{My}	1,6042	1,6042	1,6042
Hydrodynamic inertia coefficient z-direction, C_{Mz}	1,635	1,635	1,635
Drag area x-direction, A_{px}	90m ²	90m ²	90m ²
Drag area y-direction, A_{py}	110m ²	110m ²	110m ²
Drag area z-direction, A_{pz}	99m ²	99m ²	99m ²
Mass moment of inertia x-axis, I_x	4359kg/m ²	6033kg/m ²	9050kg/m ²
Mass moment of inertia y-axis, I_y	5322kg/m ²	7366kg/m ²	11050kg/m ²
Mass moment of inertia z-axis, I_z	4864kg/m ²	6733kg/m ²	10100kg/m ²
Displaced volume of water, ∇	36,8m ³	51m ³	76,4m ³
Drag coefficient x, y and z-direction, C_{Dx}, C_{Dy}, C_{Dz}	2,5	2,5	2,5
Slam coefficient, C_s	5	5	5
Slam area z-direction, A_{Sz}	69,3m ²	69,3m ²	69,3m ²

Appendix B - Highest and Lowest Effective Tension in Lifting Wire Obtained from OrcaFlex

B1: Effective tension in lifting wire for installation of a module weighing 289t

The highest and lowest effective tension in lifting wire are presented in table B1-1 – table B1-18 for wave heading 165°, 180° and 190°, significant wave heights, H_s , ranging from 2,5 – 5m, corresponding zero-up-crossing wave periods, T_z , and submergence levels $z = 1m, 0m, -1m, -5m, -10m, -15m$.

Table B1- 1: Maximum and minimum effective tension in lifting for wave heading 165° and $H_s = 2,5m$

Wave direction: 165°													
Sea state		Wire tension [kN] z = 1		Wire tension [kN] z = 0		Wire tension [kN] z = - 1		Wire tension [kN] z = - 5		Wire tension [kN] z = - 10		Wire tension [kN] z = - 15	
H _s [m]	T _z [s]	Max	Min	Max	Min	Max	Min	Max	Min	Max	Min	Max	Min
2,5	4	3364	2096	3862	950	4298	742	3935	1819	3267	1873	2861	2078
2,5	5	3221	2473	3653	1525	4092	1050	3616	2135	3263	1879	2802	2164
2,5	6	3111	2661	3559	2030	3543	1572	3467	1947	3094	1991	2816	2114
2,5	7	3075	2605	3403	1984	3552	1484	3283	1844	2960	1956	2947	2015
2,5	8	3192	2573	3300	1934	3418	2060	3213	1824	2977	1993	2909	2082
2,5	9	3213	2604	3347	2383	3310	1958	3086	2232	2877	2107	2824	2146
2,5	10	3072	2632	3113	2555	3204	2218	2994	2353	2944	1968	2866	2143
2,5	11	3012	2629	3092	2592	3091	2470	2915	2351	2759	2095	2800	2257
2,5	12	2963	2679	3046	2557	3076	2533	2893	2327	2704	2126	2678	2126
2,5	13	2984	2720	3164	2680	3114	2589	2969	2418	2803	2202	2726	2193

Table B1- 2: Maximum and minimum effective tension in lifting wire for wave heading 165° and $H_s = 3m$

Wave direction: 165°													
Sea state		Wire tension [kN] z = 1		Wire tension [kN] z = 0		Wire tension [kN] z = - 1		Wire tension [kN] z = - 5		Wire tension [kN] z = - 10		Wire tension [kN] z = - 15	
H _s [m]	T _z [s]	Max	Min	Max	Min	Max	Min	Max	Min	Max	Min	Max	Min
3	5	3456	2087	4263	556	4528	635	4065	1891	3363	1956	2844	2145
3	6	3363	2552	4032	1705	4117	944	3751	1646	3185	1849	2908	2079
3	7	3294	2548	3772	1569	3770	804	3520	1507	3117	1754	3050	1925
3	8	3303	2500	3401	1441	3629	1794	3405	1465	3159	1860	3042	1963
3	9	3322	2547	3422	2140	3435	1547	3237	2063	2965	2015	2969	2029
3	10	3115	2583	3194	2486	3318	2026	3109	2255	2844	2103	2887	2106
3	11	3054	2585	3096	2595	3118	2363	3026	2211	2802	2044	2810	2207
3	12	2997	2644	3127	2543	3081	2439	2959	2331	2734	2106	2719	2109
3	13	3020	2699	3180	2651	3123	2509	2986	2427	2808	2202	2716	2198

Table B1- 3: Maximum and minimum effective tension in lifting wire for wave heading 165° and $H_s = 3,5m$

Wave direction: 165°													
Sea state		Wire tension [kN] z = 1		Wire tension [kN] z = 0		Wire tension [kN] z = - 1		Wire tension [kN] z = - 5		Wire tension [kN] z = - 10		Wire tension [kN] z = - 15	
H _s [m]	T _z [s]	Max	Min	Max	Min	Max	Min	Max	Min	Max	Min	Max	Min
3,5	5	3813	1535	4203	673	4652	532	4135	1450	3581	1885	2954	2093
3,5	6	3655	2269	4118	1379	4233	512	3979	1307	3281	1702	3031	2009
3,5	7	3660	2361	3975	1097	4068	790	3897	1071	3394	1541	3167	1846
3,5	8	3377	2436	3588	898	3829	1401	3835	1079	3235	1616	3157	1924
3,5	9	3322	2518	3525	1848	3632	1071	3381	1849	3414	1810	3175	1928
3,5	10	3167	2538	3291	2320	3468	1818	3220	2119	3239	1921	3103	1926
3,5	11	3153	2544	3166	2532	3165	2206	3084	2125	2873	2038	2793	2176
3,5	12	3034	2607	3213	2530	3122	2323	3033	2307	2913	2081	2805	2044
3,5	13	3059	2679	3194	2621	3130	2425	2985	2372	2797	2171	2744	2192

Table B1- 4: Maximum and minimum effective tension in lifting wire for wave heading 165° and $H_s = 4\text{m}$

Wave direction: 165°													
Sea state		Wire tension [kN] z = 1		Wire tension [kN] z = 0		Wire tension [kN] z = - 1		Wire tension [kN] z = - 5		Wire tension [kN] z = - 10		Wire tension [kN] z = - 15	
H _s [m]	Tz [s]	Max	Min	Max	Min	Max	Min	Max	Min	Max	Min	Max	Min
4	6	4034	1253	4269	630	4786	362	4379	765	3418	1495	3038	1937
4	7	3866	1232	4213	600	4686	490	4027	553	3784	1335	3316	1762
4	8	3573	2259	3918	592	4162	889	4246	586	3467	1437	3296	1853
4	9	3339	2493	3626	1649	3883	587	3582	1588	3343	1723	3239	1842
4	10	3238	2497	3367	2056	3700	1617	3352	1923	3427	1787	3194	1852
4	11	3334	2506	3257	2422	3230	2028	3177	1973	3155	1795	3041	2048
4	12	3069	2570	3310	2449	3177	2196	3171	2192	2861	2042	2808	2095
4	13	3099	2659	3214	2589	3181	2328	2990	2298	2820	2126	2762	2194

Table B1- 5: Maximum and minimum effective tension in lifting wire for wave heading 165° and $H_s = 4,5\text{m}$

Wave direction: 165°													
Sea state		Wire tension [kN] z = 1		Wire tension [kN] z = 0		Wire tension [kN] z = - 1		Wire tension [kN] z = - 5		Wire tension [kN] z = - 10		Wire tension [kN] z = - 15	
H _s [m]	Tz [s]	Max	Min	Max	Min	Max	Min	Max	Min	Max	Min	Max	Min
4,5	6	4234	1032	4506	312	4879	286	4469	286	3666	1332	3164	1868
4,5	7	3927	1603	4265	325	4652	354	4566	293	4102	1095	3470	1683
4,5	8	3734	2101	4074	386	4469	582	4312	306	3793	1133	3449	1783
4,5	9	3360	2465	3868	1133	4180	790	3816	1252	3564	1609	3212	1808
4,5	10	3335	2455	3431	1719	3883	1362	3523	1757	3274	1760	3196	1894
4,5	11	3552	2470	3359	2283	3312	1841	3292	1797	3095	1919	2890	2068
4,5	12	3104	2534	3402	2327	3248	2043	3225	2116	2956	1995	2856	2061
4,5	13	3136	2640	3235	2505	3253	2211	3006	2205	2890	2060	2852	2142

Table B1- 6: Maximum and minimum effective tension in lifting wire for wave heading 165° and $H_s = 5\text{m}$

Wave direction: 165°													
Sea state		Wire tension [kN] z = 1		Wire tension [kN] z = 0		Wire tension [kN] z = - 1		Wire tension [kN] z = - 5		Wire tension [kN] z = - 10		Wire tension [kN] z = - 15	
H _s [m]	Tz [s]	Max	Min	Max	Min	Max	Min	Max	Min	Max	Min	Max	Min
5	6	4445	383	4860	123	5352	53	5009	69	3919	1004	3208	1821
5	7	4089	1200	4436	59	5130	42	5095	75	4397	738	3629	1536
5	8	3858	1808	4467	63	4845	188	5076	29	4084	836	3642	1699
5	9	3521	2411	4003	930	4383	36	4002	907	4113	1341	3386	1653
5	10	3357	2476	3523	1334	3996	1084	3676	1532	3312	1566	3354	1695
5	11	3690	2436	3456	2074	3407	1599	3471	1590	3128	1790	3000	2025
5	12	3131	2507	3502	2162	3351	1879	3314	2016	3041	1847	2919	2001
5	13	3168	2621	3238	2401	3337	2071	3085	2090	3188	1951	2917	2053

Table B1- 7: Maximum and minimum effective tension in lifting wire for wave heading 180° and $H_s = 2,5\text{m}$

Wave direction: 180°													
Sea state		Wire tension [kN] z = 1		Wire tension [kN] z = 0		Wire tension [kN] z = - 1		Wire tension [kN] z = - 5		Wire tension [kN] z = - 10		Wire tension [kN] z = - 15	
H _s [m]	Tz [s]	Max	Min	Max	Min	Max	Min	Max	Min	Max	Min	Max	Min
2,5	4	3201	2194	3703	1250	4136	993	3626	1855	3361	1855	2857	2090
2,5	5	3134	2452	3695	1844	4048	1468	3519	1987	3115	2049	2825	2217
2,5	6	3005	2655	3653	1936	3458	1941	3284	2178	3094	1953	2752	2195
2,5	7	3065	2624	3337	2103	3441	1925	3275	2074	2964	1954	2839	2117
2,5	8	3081	2589	3243	2307	3362	2189	3153	2069	2978	2027	2869	2138
2,5	9	3076	2649	3147	2534	3205	2275	3071	2191	2819	2180	2774	2150
2,5	10	3056	2644	3057	2553	3148	2368	2945	2305	2744	2174	2787	2186
2,5	11	2971	2660	3052	2559	3077	2486	2926	2344	2737	2173	2782	2253
2,5	12	2953	2685	3053	2581	3111	2574	2859	2339	2693	2137	2686	2146
2,5	13	2976	2712	3151	2677	3105	2597	2962	2416	2783	2169	2747	2201

Table B1- 8: Maximum and minimum effective tension in lifting wire for wave heading 180° and $H_s = 3\text{m}$

Wave direction: 180°													
Sea state		Wire tension [kN] z = 1		Wire tension [kN] z = 0		Wire tension [kN] z = - 1		Wire tension [kN] z = - 5		Wire tension [kN] z = - 10		Wire tension [kN] z = - 15	
H_s [m]	T_z [s]	Max	Min	Max	Min	Max	Min	Max	Min	Max	Min	Max	Min
3	5	3570	2181	4035	1293	4523	1262	3955	2074	3304	1955	2849	2197
3	6	3043	2619	3997	1730	3916	1596	3909	2031	3035	2067	2819	2119
3	7	3159	2580	3506	1695	3572	1407	3381	1821	2979	1912	2934	2059
3	8	3123	2539	3389	2008	3539	1959	3360	1855	3021	1941	2984	2100
3	9	3136	2607	3258	2370	3330	2091	3188	1858	2889	2089	2843	2085
3	10	3102	2602	3120	2522	3273	2223	3045	2148	2802	2162	2851	2138
3	11	3002	2623	3066	2556	3084	2361	3000	2294	2808	2145	2789	2225
3	12	2978	2654	3075	2581	3122	2495	2924	2323	2745	2113	2690	2134
3	13	3006	2689	3167	2648	3114	2526	2966	2422	2785	2182	2745	2198

Table B1- 9: Maximum and minimum effective tension in lifting wire for wave heading 180° and $H_s = 3,5\text{m}$

Wave direction: 180°													
Sea state		Wire tension [kN] z = 1		Wire tension [kN] z = 0		Wire tension [kN] z = - 1		Wire tension [kN] z = - 5		Wire tension [kN] z = - 10		Wire tension [kN] z = - 15	
H_s [m]	T_z [s]	Max	Min	Max	Min	Max	Min	Max	Min	Max	Min	Max	Min
3,5	5	3810	1538	4344	802	4683	670	4201	1887	3475	1905	2832	2108
3,5	6	3310	2439	4305	1052	4411	1163	3951	1884	3266	1911	2905	2072
3,5	7	3416	2326	3759	1251	4047	956	3718	1459	3205	1733	3022	1997
3,5	8	3369	2299	3561	1647	3731	1609	3631	1568	3094	1765	3112	2023
3,5	9	3189	2566	3368	2159	3467	1862	3409	1660	2955	1963	2935	2017
3,5	10	3146	2558	3182	2391	3414	2023	3161	2022	2866	2120	2935	2074
3,5	11	3035	2588	3119	2517	3146	2222	3027	2243	2860	2101	2803	2181
3,5	12	3003	2623	3147	2565	3133	2396	3001	2311	2803	2103	2732	2121
3,5	13	3036	2666	3182	2614	3122	2438	2970	2413	2778	2197	2742	2201

Table B1- 10: Maximum and minimum effective tension in lifting wire for wave heading 180° and $H_s = 4\text{m}$

Wave direction: 180°													
Sea state		Wire tension [kN] z = 1		Wire tension [kN] z = 0		Wire tension [kN] z = - 1		Wire tension [kN] z = - 5		Wire tension [kN] z = - 10		Wire tension [kN] z = - 15	
H_s [m]	T_z [s]	Max	Min	Max	Min	Max	Min	Max	Min	Max	Min	Max	Min
4	6	3602	2168	4464	361	4696	941	4446	1565	3318	1792	2925	2018
4	7	3696	1950	4000	824	4211	517	4554	1141	3416	1632	3111	1924
4	8	3463	2011	3698	1185	3940	1270	3811	1191	3213	1550	3210	1976
4	9	3233	2529	3488	1891	3626	1423	3551	1465	3089	1819	2997	1947
4	10	3193	2513	3239	2178	3569	1807	3280	1871	2996	2035	3018	2005
4	11	3125	2555	3186	2417	3229	2046	3117	2132	2928	2004	2817	2137
4	12	3029	2591	3226	2512	3144	2307	3066	2235	2865	2094	2777	2107
4	13	3068	2644	3195	2580	3131	2336	2994	2339	2806	2169	2759	2194

Table B1- 11: Maximum and minimum effective tension in lifting wire for wave heading 180° and $H_s = 4,5\text{m}$

Wave direction: 180°													
Sea state		Wire tension [kN] z = 1		Wire tension [kN] z = 0		Wire tension [kN] z = - 1		Wire tension [kN] z = - 5		Wire tension [kN] z = - 10		Wire tension [kN] z = - 15	
H_s [m]	T_z [s]	Max	Min	Max	Min	Max	Min	Max	Min	Max	Min	Max	Min
4,5	6	4075	1815	4465	315	4765	362	4593	1229	3453	1695	3028	1954
4,5	7	3984	1455	3926	365	4295	297	4531	604	3661	1461	3203	1850
4,5	8	3605	1724	3801	533	4191	894	4158	641	3399	1327	3394	1905
4,5	9	3271	2490	3615	1664	3826	956	3736	1525	3295	1650	3129	1856
4,5	10	3244	2467	3335	1889	3750	1591	3429	1589	3067	1950	3123	1929
4,5	11	3246	2523	3274	2306	3308	1829	3223	1980	3010	1877	2870	2093
4,5	12	3056	2560	3310	2403	3181	2183	3164	2180	2947	2002	2828	2107
4,5	13	3098	2621	3208	2537	3169	2222	3041	2275	2836	2122	2804	2180

Table B1- 12: Maximum and minimum effective tension in lifting wire for wave heading 180° and $H_s = 5m$

Wave direction: 180°													
Sea state		Wire tension [kN] z = 1		Wire tension [kN] z = 0		Wire tension [kN] z = - 1		Wire tension [kN] z = - 5		Wire tension [kN] z = - 10		Wire tension [kN] z = - 15	
H _s [m]	Tz [s]	Max	Min	Max	Min	Max	Min	Max	Min	Max	Min	Max	Min
5	6	4465	1133	5524	60	5299	76	5491	801	3760	1603	3008	1900
5	7	4576	900	4245	36	4414	66	5377	56	3927	1175	3327	1751
5	8	3711	1444	4333	365	4468	355	4568	568	3662	1090	3563	1821
5	9	3307	2438	3693	1397	3921	560	4030	1333	3611	1491	3216	1775
5	10	3300	2423	3439	1548	3960	1317	3544	1246	3228	1762	3231	1852
5	11	3353	2439	3368	2181	3405	1539	3344	1852	3119	1802	2928	2043
5	12	3081	2530	3399	2270	3243	1999	3241	2039	3005	1827	2876	2071
5	13	3132	2598	3222	2449	3229	2095	3067	2146	2903	2054	2844	2147

Table B1- 13: Maximum and minimum effective tension in lifting wire for wave heading 195° and $H_s = 2,5m$

Wave direction: 195°													
Sea state		Wire tension [kN] z = 1		Wire tension [kN] z = 0		Wire tension [kN] z = - 1		Wire tension [kN] z = - 5		Wire tension [kN] z = - 10		Wire tension [kN] z = - 15	
H _s [m]	Tz [s]	Max	Min	Max	Min	Max	Min	Max	Min	Max	Min	Max	Min
2,5	4	3205	2156	3662	1247	4289	880	3762	1892	3428	1862	2824	2114
2,5	5	3067	2557	3643	1681	4157	1464	3516	2122	3083	2020	2739	2154
2,5	6	3018	2655	3603	2218	3684	2099	3270	2294	2955	2148	2751	2196
2,5	7	3085	2618	3405	2414	3318	2138	3117	2214	2946	1978	2767	2185
2,5	8	3174	2535	3222	2404	3197	2302	3049	2168	2982	2046	2827	2163
2,5	9	3174	2627	3134	2558	3183	2393	3048	2316	2864	2188	2763	2158
2,5	10	3088	2633	3083	2540	3139	2423	2941	2334	2754	2211	2774	2177
2,5	11	2989	2631	3055	2557	3060	2555	2880	2347	2728	2215	2775	2252
2,5	12	2963	2674	3045	2561	3106	2599	2893	2370	2701	2152	2705	2173
2,5	13	2992	2702	3153	2673	3125	2613	2938	2400	2745	2203	2756	2203

Table B1- 14: Maximum and minimum effective tension in lifting wire for wave heading 195° and $H_s = 3m$

Wave direction: 195°													
Sea state		Wire tension [kN] z = 1		Wire tension [kN] z = 0		Wire tension [kN] z = - 1		Wire tension [kN] z = - 5		Wire tension [kN] z = - 10		Wire tension [kN] z = - 15	
H _s [m]	Tz [s]	Max	Min	Max	Min	Max	Min	Max	Min	Max	Min	Max	Min
3	5	3258	2208	3952	1078	4402	925	3854	2054	3344	1864	2793	2100
3	6	3093	2619	3706	1891	3988	1755	3774	2103	3106	2042	2809	2139
3	7	3141	2563	3423	2206	3526	1830	3331	2030	3015	1909	2831	2120
3	8	3240	2495	3376	2140	3328	2048	3149	2001	3005	1901	2970	2092
3	9	3277	2556	3259	2514	3318	2238	3138	2228	2912	2088	2839	2098
3	10	3139	2589	3131	2527	3256	2265	2996	2291	2960	2039	2844	2112
3	11	3028	2587	3065	2556	3070	2461	2896	2338	2770	2205	2773	2197
3	12	2992	2640	3075	2550	3111	2576	2883	2370	2723	2142	2711	2174
3	13	3028	2676	3166	2650	3135	2556	2938	2404	2740	2205	2759	2197

Table B1- 15: Maximum and minimum effective tension in lifting wire for wave heading 195° and $H_s = 3,5m$

Wave direction: 195°													
Sea state		Wire tension [kN] z = 1		Wire tension [kN] z = 0		Wire tension [kN] z = - 1		Wire tension [kN] z = - 5		Wire tension [kN] z = - 10		Wire tension [kN] z = - 15	
H _s [m]	Tz [s]	Max	Min	Max	Min	Max	Min	Max	Min	Max	Min	Max	Min
3,5	5	3722	1784	4329	284	4593	932	4213	1795	3535	1862	2891	1992
3,5	6	3376	2551	4238	1444	4243	1447	4279	1905	3203	1984	2871	2075
3,5	7	3180	2508	3553	1910	3663	1476	3552	1892	3053	1887	2906	2060
3,5	8	3361	2457	3596	1872	3478	1734	3315	1720	3051	1756	3061	2063
3,5	9	3457	2445	3378	2374	3469	2065	3328	2125	3020	2014	2968	2020
3,5	10	3185	2537	3201	2472	3390	2103	3073	2128	2981	2015	3018	2015
3,5	11	3070	2546	3127	2543	3128	2371	2957	2314	2831	2114	2801	2184
3,5	12	3023	2605	3122	2537	3128	2521	2923	2353	2773	2164	2734	2156
3,5	13	3066	2651	3182	2620	3150	2498	2964	2404	2749	2198	2764	2202

Table B1- 16: Maximum and minimum effective tension in lifting wire for wave heading 195° and $H_s = 4\text{m}$

Wave direction: 195°													
Sea state		Wire tension [kN] z = 1		Wire tension [kN] z = 0		Wire tension [kN] z = - 1		Wire tension [kN] z = - 5		Wire tension [kN] z = - 10		Wire tension [kN] z = - 15	
H _s [m]	Tz [s]	Max	Min	Max	Min	Max	Min	Max	Min	Max	Min	Max	Min
4	6	3504	2289	4466	842	4797	777	4435	1840	3596	1904	2930	2020
4	7	3265	2334	3984	1516	3865	1110	4252	1741	3209	1786	2971	2007
4	8	3426	2404	3802	1499	3672	1322	3735	1381	3088	1551	3180	2007
4	9	3574	2375	3439	2183	3628	1893	3404	1914	3287	1821	3080	1905
4	10	3234	2495	3270	2308	3547	1875	3148	1981	2914	2041	3017	1975
4	11	3115	2507	3187	2494	3201	2262	3129	2093	2894	2004	2871	2122
4	12	3056	2570	3175	2505	3133	2439	2976	2306	2824	2123	2773	2121
4	13	3104	2626	3197	2589	3154	2435	2981	2401	2813	2174	2769	2195

Table B1- 17: Maximum and minimum effective tension in lifting wire for wave heading 195° and $H_s = 4,5\text{m}$

Wave direction: 195°													
Sea state		Wire tension [kN] z = 1		Wire tension [kN] z = 0		Wire tension [kN] z = - 1		Wire tension [kN] z = - 5		Wire tension [kN] z = - 10		Wire tension [kN] z = - 15	
H _s [m]	Tz [s]	Max	Min	Max	Min	Max	Min	Max	Min	Max	Min	Max	Min
4,5	6	3970	1907	4249	293	4813	316	3946	1626	3647	1802	3014	1929
4,5	7	3339	2233	4103	1115	4265	846	3908	1340	3380	1640	3073	1941
4,5	8	3499	2204	3913	1088	3840	1005	3820	1026	3173	1332	3309	1925
4,5	9	3609	2391	3567	1980	3796	1673	3653	1809	3210	1762	3334	1872
4,5	10	3297	2459	3377	2119	3697	1655	3256	1775	3037	1938	3126	1896
4,5	11	3200	2473	3232	2363	3285	2101	3200	2014	2940	1926	2918	2060
4,5	12	3089	2534	3244	2459	3142	2343	3040	2237	2964	2104	2876	2119
4,5	13	3140	2602	3210	2559	3174	2350	2971	2339	2846	2156	2817	2176

Table B1- 18: Maximum and minimum effective tension in lifting wire for wave heading 195° and $H_s = 5\text{m}$

Wave direction: 195°													
Sea state		Wire tension [kN] z = 1		Wire tension [kN] z = 0		Wire tension [kN] z = - 1		Wire tension [kN] z = - 5		Wire tension [kN] z = - 10		Wire tension [kN] z = - 15	
H _s [m]	Tz [s]	Max	Min	Max	Min	Max	Min	Max	Min	Max	Min	Max	Min
5	6	3997	1481	4936	153	5591	314	5635	1333	3656	1732	3050	1905
5	7	3558	1942	4311	691	4688	481	4732	1065	3557	1435	3154	1867
5	8	3576	2040	4018	645	3967	505	4285	650	3473	1058	3449	1817
5	9	3687	2429	3716	1641	4007	1486	3791	1616	3287	1602	3372	1803
5	10	3395	2438	3483	1943	3819	1414	3334	1600	3157	1778	3234	1823
5	11	3311	2447	3301	2185	3363	1939	3157	1932	3039	1841	2962	2030
5	12	3124	2497	3317	2326	3174	2248	3133	2118	3103	2019	2901	1893
5	13	3176	2579	3217	2529	3175	2239	3029	2278	2947	1991	2849	2178

B2: Effective tension in lifting wire for installation of a module weighing 400t

The highest and lowest effective tension in lifting wire are presented in table B2-1 – table B2-18 for wave heading 165°, 180° and 190°, significant wave heights, H_s , ranging from 2,5 – 5m, corresponding zero-up-crossing wave periods, T_z , and submergence levels $z = 1m, 0m, -1m, -5m, -10m, -15m$.

Table B2 - 1: Maximum and minimum effective tension in lifting for wave heading 165° and $H_s = 2,5m$

Wave direction: 165°													
Sea state		Wire tension [kN] z = 1		Wire tension [kN] z = 0		Wire tension [kN] z = - 1		Wire tension [kN] z = - 5		Wire tension [kN] z = - 10		Wire tension [kN] z = - 15	
H_s [m]	T_z [s]	Max	Min	Max	Min	Max	Min	Max	Min	Max	Min	Max	Min
2,5	4	4565	3007	5969	1977	6430	1151	5417	2623	4697	2728	3852	3035
2,5	5	4299	3494	5238	2090	6373	2148	4518	2986	4081	2943	3808	2974
2,5	6	4217	3681	4768	3016	4816	2448	4542	2905	3986	2910	3814	3017
2,5	7	4260	3606	4568	2965	4625	2423	4342	2741	3997	2846	3995	2884
2,5	8	4435	3565	4485	2956	4517	3097	4348	2736	3990	2897	4087	2881
2,5	9	4437	3605	4603	3396	4457	2900	4167	3189	3890	2995	3854	3012
2,5	10	4245	3643	4245	3583	4368	3184	4068	3316	3840	3067	3879	3025
2,5	11	4170	3644	4255	3637	4227	3464	3981	3319	3938	2963	3766	3136
2,5	12	4103	3709	4185	3588	4213	3561	3959	3279	3705	3015	3686	3022
2,5	13	4130	3766	4337	3711	4277	3619	4039	3398	3786	3114	3727	3108

Table B2 - 2: Maximum and minimum effective tension in lifting for wave heading 165° and $H_s = 3m$

Wave direction: 165°													
Sea state		Wire tension [kN] z = 1		Wire tension [kN] z = 0		Wire tension [kN] z = - 1		Wire tension [kN] z = - 5		Wire tension [kN] z = - 10		Wire tension [kN] z = - 15	
H_s [m]	T_z [s]	Max	Min	Max	Min	Max	Min	Max	Min	Max	Min	Max	Min
3	5	4791	2987	5531	1590	6582	1145	4847	2837	4358	2795	3819	3018
3	6	4529	3599	5374	2580	5216	1878	4804	2533	4257	2710	3920	2982
3	7	4473	3526	4837	2527	4886	1726	4729	2374	4088	2667	4120	2771
3	8	4602	3443	4686	2374	4787	2759	4530	2358	4118	2694	4086	2864
3	9	4595	3531	4638	3127	4608	2460	4309	3003	4096	2894	4167	2761
3	10	4313	3576	4365	3489	4521	2996	4204	3207	3863	3005	3949	2978
3	11	4233	3584	4265	3596	4234	3325	4055	3216	3867	2893	3798	3090
3	12	4151	3662	4285	3569	4220	3453	4039	3285	3780	3003	3742	2993
3	13	4181	3738	4357	3670	4292	3530	4054	3394	3796	3119	3728	3109

Table B2 - 3: Maximum and minimum effective tension in lifting for wave heading 165° and $H_s = 3,5m$

Wave direction: 165°													
Sea state		Wire tension [kN] z = 1		Wire tension [kN] z = 0		Wire tension [kN] z = - 1		Wire tension [kN] z = - 5		Wire tension [kN] z = - 10		Wire tension [kN] z = - 15	
H_s [m]	T_z [s]	Max	Min	Max	Min	Max	Min	Max	Min	Max	Min	Max	Min
3,5	5	5402	2389	6177	1414	6638	692	5417	2616	4317	2696	4047	2893
3,5	6	4812	3303	5528	2266	5682	1138	5006	2144	4300	2510	3941	2910
3,5	7	4804	3376	5352	2066	5261	858	4875	1963	4399	2401	4281	2676
3,5	8	4749	3351	4892	1839	5000	2372	4816	1909	4272	2478	4240	2753
3,5	9	4631	3477	4738	2835	4809	1918	4500	2778	4276	2657	4180	2669
3,5	10	4389	3512	4446	3270	4680	2725	4327	3051	4389	2741	4163	2759
3,5	11	4339	3525	4305	3539	4322	3144	4169	3053	3926	2870	3817	3030
3,5	12	4201	3611	4379	3540	4277	3316	4125	3236	3992	2866	3836	2981
3,5	13	4234	3711	4372	3628	4310	3442	4054	3322	3850	3067	3778	3118

Table B2 - 4: Maximum and minimum effective tension in lifting for wave heading 165° and $H_s = 4\text{m}$

Wave direction: 165°													
Sea state		Wire tension [kN] z = 1		Wire tension [kN] z = 0		Wire tension [kN] z = - 1		Wire tension [kN] z = - 5		Wire tension [kN] z = - 10		Wire tension [kN] z = - 15	
H_s [m]	T_z [s]	Max	Min	Max	Min	Max	Min	Max	Min	Max	Min	Max	Min
4	6	5314	2808	5659	1669	6753	408	5618	1672	4362	2336	4065	2838
4	7	5068	3030	5631	1255	5564	420	5284	1379	4731	2137	4417	2584
4	8	4930	3227	5070	1183	5227	1914	5231	1445	4513	2223	4414	2620
4	9	4652	3442	4849	2487	5064	1405	4711	2489	4777	2546	4368	2588
4	10	4487	3458	4599	2969	4899	2492	4469	2870	4536	2486	4145	2675
4	11	4549	3463	4398	3406	4406	2948	4268	2894	4139	2875	4070	2812
4	12	4253	3561	4496	3449	4344	3179	4204	3150	4282	2807	3900	2913
4	13	4289	3684	4392	3584	4332	3324	4082	3165	4019	2925	3850	3051

Table B2 - 5: Maximum and minimum effective tension in lifting for wave heading 165° and $H_s = 4,5\text{m}$

Wave direction: 165°													
Sea state		Wire tension [kN] z = 1		Wire tension [kN] z = 0		Wire tension [kN] z = - 1		Wire tension [kN] z = - 5		Wire tension [kN] z = - 10		Wire tension [kN] z = - 15	
H_s [m]	T_z [s]	Max	Min	Max	Min	Max	Min	Max	Min	Max	Min	Max	Min
4,5	6	5780	2115	6236	725	7181	0	6579	945	4724	2046	4190	2759
4,5	7	5167	2517	5930	574	6161	0	5810	701	5114	1818	4607	2481
4,5	8	5201	2920	5378	580	5622	1100	5646	912	4825	1930	4586	2593
4,5	9	4690	3405	5010	1861	5485	782	4960	2169	4741	2379	4359	2585
4,5	10	4590	3411	4683	2651	5030	2226	4664	2661	4564	2409	4323	2628
4,5	11	4824	3408	4509	3273	4479	2726	4374	2692	4164	2753	3972	2922
4,5	12	4303	3514	4572	3314	4418	3024	4326	3039	4011	2806	3926	2908
4,5	13	4339	3658	4408	3535	4405	3189	4081	3116	3938	2930	3894	3016

Table B2 - 6: Maximum and minimum effective tension in lifting for wave heading 165° and $H_s = 5\text{m}$

Wave direction: 165°													
Sea state		Wire tension [kN] z = 1		Wire tension [kN] z = 0		Wire tension [kN] z = - 1		Wire tension [kN] z = - 5		Wire tension [kN] z = - 10		Wire tension [kN] z = - 15	
H_s [m]	T_z [s]	Max	Min	Max	Min	Max	Min	Max	Min	Max	Min	Max	Min
5	6	6266	1924	7128	457	7868	0	7022	0	4988	1709	4208	2674
5	7	5356	2007	7098	0	7529	0	6246	67	5465	1313	4773	2352
5	8	5231	2579	6118	38	5890	377	6318	316	5154	1547	4825	2470
5	9	4740	3383	5262	1408	5927	109	5242	1801	4916	2197	4465	2514
5	10	4679	3397	4864	2315	5285	1956	4799	2389	4671	2461	4528	2538
5	11	5065	3355	4606	3084	4588	2473	4533	2470	4270	2647	4095	2889
5	12	4337	3475	4719	3148	4521	2832	4440	2922	4101	2653	3984	2879
5	13	4387	3633	4433	3411	4510	3036	4154	2978	4089	2791	3997	2911

Table B2 - 7: Maximum and minimum effective tension in lifting wire for wave heading 180° and $H_s = 2,5\text{m}$

Wave direction: 180°													
Sea state		Wire tension [kN] z = 1		Wire tension [kN] z = 0		Wire tension [kN] z = - 1		Wire tension [kN] z = - 5		Wire tension [kN] z = - 10		Wire tension [kN] z = - 15	
H_s [m]	T_z [s]	Max	Min	Max	Min	Max	Min	Max	Min	Max	Min	Max	Min
2,5	4	4625	3149	5934	2258	6384	1844	5716	2475	4279	2819	3798	2959
2,5	5	4210	3532	4951	2709	5157	2361	4581	3025	4034	3036	3758	3111
2,5	6	4162	3676	4731	3064	4727	2801	4304	3158	3885	3068	3734	3080
2,5	7	4239	3633	4516	3074	4473	2942	4258	3062	3888	2842	3885	3013
2,5	8	4269	3589	4398	3275	4493	3148	4259	3009	4002	2981	3953	2994
2,5	9	4253	3664	4333	3531	4379	3269	4131	3142	3844	3079	3805	3019
2,5	10	4227	3659	4230	3585	4292	3333	4028	3254	3749	3086	3817	3067
2,5	11	4112	3684	4198	3588	4213	3517	3941	3284	3771	3016	3795	3159
2,5	12	4089	3717	4194	3616	4250	3584	3919	3290	3716	3029	3663	3034
2,5	13	4119	3754	4330	3712	4258	3627	4029	3392	3737	3108	3735	3111

Table B2 - 8: Maximum and minimum effective tension in lifting wire for wave heading 180° and $H_s = 3\text{m}$

Wave direction: 180°													
Sea state		Wire tension [kN] z = 1		Wire tension [kN] z = 0		Wire tension [kN] z = - 1		Wire tension [kN] z = - 5		Wire tension [kN] z = - 10		Wire tension [kN] z = - 15	
H_s [m]	T_z [s]	Max	Min	Max	Min	Max	Min	Max	Min	Max	Min	Max	Min
3	5	4632	3156	5345	2353	5732	2125	4918	2895	4169	2885	3804	3087
3	6	4211	3627	5112	2509	4962	2522	4576	2956	4181	2840	3882	2907
3	7	4358	3572	4723	2597	4836	2579	4517	2798	3983	2744	4005	2942
3	8	4334	3520	4569	2925	4649	2836	4514	2765	4066	2822	4089	2931
3	9	4331	3606	4431	3335	4528	3046	4259	2814	3942	2987	3901	2940
3	10	4291	3601	4314	3520	4431	3152	4149	3085	3834	3069	3914	2999
3	11	4156	3634	4224	3584	4218	3390	4032	3269	3840	3027	3803	3105
3	12	4123	3674	4225	3602	4261	3482	3989	3271	3784	3015	3713	3017
3	13	4161	3722	4350	3667	4270	3547	4036	3396	3733	3110	3737	3110

Table B2 - 9: Maximum and minimum effective tension in lifting wire for wave heading 180° and $H_s = 3,5\text{m}$

Wave direction: 180°													
Sea state		Wire tension [kN] z = 1		Wire tension [kN] z = 0		Wire tension [kN] z = - 1		Wire tension [kN] z = - 5		Wire tension [kN] z = - 10		Wire tension [kN] z = - 15	
H_s [m]	T_z [s]	Max	Min	Max	Min	Max	Min	Max	Min	Max	Min	Max	Min
3,5	5	5132	2401	6676	1431	6599	1656	5094	2745	4371	2805	3832	3005
3,5	6	4467	3446	5397	2040	5434	2110	4850	2731	4150	2847	3824	3009
3,5	7	4642	3317	5021	2130	5255	2139	4776	2377	4165	2654	4078	2855
3,5	8	4537	3325	4728	2505	4865	2436	4746	2441	4102	2632	4236	2869
3,5	9	4410	3549	4589	3089	4678	2815	4469	2575	4026	2850	3999	2860
3,5	10	4356	3541	4373	3396	4611	2968	4264	2982	3952	3000	4014	2928
3,5	11	4201	3586	4285	3528	4273	3229	4125	3208	3931	2987	3819	3052
3,5	12	4158	3631	4308	3548	4273	3363	4073	3251	3864	3013	3774	2990
3,5	13	4203	3691	4370	3622	4281	3451	4044	3299	3784	3112	3757	3109

Table B2 - 10: Maximum and minimum effective tension in lifting wire for wave heading 180° and $H_s = 4\text{m}$

Wave direction: 180°													
Sea state		Wire tension [kN] z = 1		Wire tension [kN] z = 0		Wire tension [kN] z = - 1		Wire tension [kN] z = - 5		Wire tension [kN] z = - 10		Wire tension [kN] z = - 15	
H_s [m]	T_z [s]	Max	Min	Max	Min	Max	Min	Max	Min	Max	Min	Max	Min
4	6	4872	3151	5948	1475	6552	1729	5262	2515	4200	2759	3917	2943
4	7	4984	2893	5127	1581	5540	1696	5082	2014	4460	2483	4181	2764
4	8	4823	2965	4901	2030	5091	2053	4970	2143	4203	2437	4365	2801
4	9	4488	3489	4765	2810	4872	2597	4712	2490	4146	2687	4109	2767
4	10	4427	3479	4459	3206	4808	2715	4393	2769	4029	2884	4122	2845
4	11	4306	3538	4345	3453	4365	3029	4266	3088	4021	2877	3896	3001
4	12	4195	3587	4389	3494	4296	3223	4159	3185	3951	2990	3825	2978
4	13	4245	3660	4386	3576	4292	3335	4052	3210	3869	3060	3819	3096

Table B2 - 11: Maximum and minimum effective tension in lifting wire for wave heading 180° and $H_s = 4,5\text{m}$

Wave direction: 180°													
Sea state		Wire tension [kN] z = 1		Wire tension [kN] z = 0		Wire tension [kN] z = - 1		Wire tension [kN] z = - 5		Wire tension [kN] z = - 10		Wire tension [kN] z = - 15	
H_s [m]	T_z [s]	Max	Min	Max	Min	Max	Min	Max	Min	Max	Min	Max	Min
4,5	6	5153	2878	6030	981	6373	1399	5862	2168	4401	2711	3951	2882
4,5	7	5459	2378	5443	1040	5799	881	5386	1454	4685	2317	4322	2667
4,5	8	4807	2650	5124	1514	5406	1620	5247	1529	4449	2192	4521	2738
4,5	9	4542	3432	4939	2497	4986	2234	4816	2414	4328	2536	4240	2663
4,5	10	4497	3419	4549	2928	5006	2448	4538	2450	4181	2774	4246	2759
4,5	11	4481	3491	4415	3341	4465	2776	4327	2923	4117	2770	3964	2937
4,5	12	4232	3544	4485	3436	4363	3050	4260	3110	4085	2839	3880	2957
4,5	13	4289	3629	4399	3530	4327	3207	4059	3120	3944	2985	3881	3051

Table B2 - 12: Maximum and minimum effective tension in lifting wire for wave heading 180° and $H_s = 5\text{m}$

Wave direction: 180°													
Sea state		Wire tension [kN] z = 1		Wire tension [kN] z = 0		Wire tension [kN] z = - 1		Wire tension [kN] z = - 5		Wire tension [kN] z = - 10		Wire tension [kN] z = - 15	
H _s [m]	Tz [s]	Max	Min	Max	Min	Max	Min	Max	Min	Max	Min	Max	Min
5	6	5902	2226	6880	255	6325	680	7934	1520	4723	2386	4050	2814
5	7	5662	1807	5640	591	5914	704	6355	718	4996	2074	4446	2620
5	8	4920	2334	5348	854	5665	1108	5463	957	4605	1894	4685	2661
5	9	4577	3381	5098	2210	5228	1326	5178	2075	4593	2361	4370	2571
5	10	4580	3362	4637	2577	5210	2151	4751	2130	4256	2649	4360	2673
5	11	4660	3448	4517	3209	4567	2475	4495	2771	4244	2681	4044	2874
5	12	4266	3503	4587	3311	4433	2887	4357	3048	4114	2652	3957	2931
5	13	4334	3597	4410	3456	4394	3070	4132	3035	3988	2927	3945	3006

Table B2 - 13: Maximum and minimum effective tension in lifting wire for wave heading 195° and $H_s = 2,5\text{m}$

Wave direction: 195°													
Sea state		Wire tension [kN] z = 1		Wire tension [kN] z = 0		Wire tension [kN] z = - 1		Wire tension [kN] z = - 5		Wire tension [kN] z = - 10		Wire tension [kN] z = - 15	
H _s [m]	Tz [s]	Max	Min	Max	Min	Max	Min	Max	Min	Max	Min	Max	Min
2,5	4	4583	3229	5794	2354	6427	1236	5466	2718	4595	2803	3893	3009
2,5	5	4239	3525	5238	2640	5630	2487	4847	3074	4155	2913	3766	3023
2,5	6	4179	3669	4693	3242	4803	3121	4267	3267	3906	3063	3731	3044
2,5	7	4267	3624	4629	3377	4409	3133	4190	3155	3883	2776	3807	3062
2,5	8	4385	3516	4416	3412	4340	3306	4091	3133	3981	2926	3905	3011
2,5	9	4390	3640	4351	3549	4297	3403	4114	3288	3842	3094	3818	3022
2,5	10	4266	3641	4251	3573	4296	3451	3980	3293	3745	3141	3817	3047
2,5	11	4138	3645	4227	3592	4202	3565	3907	3290	3748	3092	3795	3149
2,5	12	4103	3702	4189	3593	4247	3621	3920	3316	3687	3055	3675	3057
2,5	13	4143	3740	4335	3710	4286	3640	4011	3384	3743	3116	3744	3109

Table B2 - 14: Maximum and minimum effective tension in lifting wire for wave heading 195° and $H_s = 3$

Wave direction: 195°													
Sea state		Wire tension [kN] z = 1		Wire tension [kN] z = 0		Wire tension [kN] z = - 1		Wire tension [kN] z = - 5		Wire tension [kN] z = - 10		Wire tension [kN] z = - 15	
H _s [m]	Tz [s]	Max	Min	Max	Min	Max	Min	Max	Min	Max	Min	Max	Min
3	5	4747	3078	5635	2101	6072	2044	5159	2952	4251	2855	3940	2860
3	6	4232	3618	4883	2876	5027	2803	4612	3052	4064	2941	3774	2991
3	7	4342	3548	4886	3139	4663	2838	4381	2937	4116	2690	3893	2982
3	8	4519	3460	4591	3151	4497	3068	4291	2941	4034	2753	4032	2937
3	9	4530	3549	4511	3486	4421	3258	4233	3215	3956	2968	3940	2937
3	10	4336	3580	4318	3533	4430	3288	4067	3233	3843	3070	3911	2968
3	11	4192	3585	4260	3580	4195	3483	3969	3269	3842	3080	3792	3095
3	12	4144	3655	4239	3574	4253	3593	3950	3313	3795	3044	3732	3055
3	13	4193	3705	4354	3669	4300	3578	4016	3385	3743	3119	3748	3106

Table B2 - 15: Maximum and minimum effective tension in lifting wire for wave heading 195° and $H_s = 3,5\text{m}$

Wave direction: 195°													
Sea state		Wire tension [kN] z = 1		Wire tension [kN] z = 0		Wire tension [kN] z = - 1		Wire tension [kN] z = - 5		Wire tension [kN] z = - 10		Wire tension [kN] z = - 15	
H _s [m]	Tz [s]	Max	Min	Max	Min	Max	Min	Max	Min	Max	Min	Max	Min
3,5	5	4826	2789	6295	1278	6323	1431	5712	2934	4513	2856	3888	2909
3,5	6	4503	3567	5070	2308	5183	2290	5060	2832	4237	2836	3835	2921
3,5	7	4404	3473	5089	2819	4861	2475	4631	2757	4082	2658	4004	2895
3,5	8	4714	3375	4879	2847	4707	2740	4543	2661	4064	2597	4152	2880
3,5	9	4771	3411	4595	3395	4564	3098	4451	3009	4053	2889	4034	2859
3,5	10	4398	3510	4416	3460	4593	3086	4153	3052	4160	2927	4015	2874
3,5	11	4251	3528	4311	3519	4257	3379	4031	3251	3938	3049	3817	3046
3,5	12	4187	3608	4297	3518	4263	3543	4008	3296	3832	3035	3769	3030
3,5	13	4245	3670	4375	3621	4326	3506	4018	3390	3797	3115	3750	3100

Table B2 - 16: Maximum and minimum effective tension in lifting wire for wave heading 195° and $H_s = 4$

Wave direction: 195°													
Sea state		Wire tension [kN] z = 1		Wire tension [kN] z = 0		Wire tension [kN] z = - 1		Wire tension [kN] z = - 5		Wire tension [kN] z = - 10		Wire tension [kN] z = - 15	
H _s [m]	Tz [s]	Max	Min	Max	Min	Max	Min	Max	Min	Max	Min	Max	Min
4	6	4662	3335	5582	1829	6607	1807	6207	2765	4560	2727	3888	2802
4	7	4517	3341	5253	2471	5592	2080	4895	2573	4191	2597	4079	2841
4	8	4849	3368	5118	2490	4816	2391	4773	2304	4117	2342	4297	2808
4	9	4961	3313	4689	3200	4767	2872	4548	2823	4498	2667	4317	2721
4	10	4467	3451	4489	3288	4737	2854	4318	2893	4031	2880	4116	2800
4	11	4312	3472	4349	3465	4331	3261	4122	3104	4020	2796	3904	2980
4	12	4232	3559	4363	3463	4283	3462	4085	3258	3920	3029	3822	3017
4	13	4297	3637	4397	3585	4335	3423	4051	3366	3848	3073	3817	3089

Table B2 - 17: Maximum and minimum effective tension in lifting wire for wave heading 195° and $H_s = 4,5m$

Wave direction: 195°													
Sea state		Wire tension [kN] z = 1		Wire tension [kN] z = 0		Wire tension [kN] z = - 1		Wire tension [kN] z = - 5		Wire tension [kN] z = - 10		Wire tension [kN] z = - 15	
H _s [m]	Tz [s]	Max	Min	Max	Min	Max	Min	Max	Min	Max	Min	Max	Min
4,5	6	5194	2909	6389	1306	6195	1108	7711	2577	4578	2528	3959	2742
4,5	7	4586	3133	5233	2036	5378	1676	5413	2194	4394	2469	4176	2767
4,5	8	4794	3116	5037	2058	5021	1947	4922	1917	4271	2087	4520	2748
4,5	9	4970	3312	4791	2963	4982	2642	4704	2669	4590	2563	4405	2610
4,5	10	4552	3401	4594	3088	4922	2604	4388	2692	4163	2756	4263	2719
4,5	11	4388	3422	4432	3366	4426	3111	4251	2963	4052	2819	4021	2899
4,5	12	4277	3509	4439	3404	4293	3362	4182	3162	3998	2982	3869	2989
4,5	13	4350	3604	4415	3542	4357	3328	4034	3310	3983	2975	3869	3085

Table B2 - 18: Maximum and minimum effective tension in lifting wire for wave heading 195° and $H_s = 5m$

Wave direction: 195°													
Sea state		Wire tension [kN] z = 1		Wire tension [kN] z = 0		Wire tension [kN] z = - 1		Wire tension [kN] z = - 5		Wire tension [kN] z = - 10		Wire tension [kN] z = - 15	
H _s [m]	Tz [s]	Max	Min	Max	Min	Max	Min	Max	Min	Max	Min	Max	Min
5	6	5399	2573	7182	587	6665	255	7586	2259	4541	2428	4068	2664
5	7	4713	2974	5450	1582	5798	1219	6353	1790	4620	2274	4291	2684
5	8	4943	2820	5229	1577	5163	1580	5264	1496	4394	1898	4677	2661
5	9	5170	3354	4918	2646	5166	2425	4890	2419	4472	2476	4551	2561
5	10	4662	3369	4704	2854	5115	2369	4494	2532	4310	2608	4362	2622
5	11	4541	3382	4504	3208	4511	2950	4371	2824	4143	2692	4135	2839
5	12	4324	3458	4526	3315	4364	3249	4213	3063	4096	2880	4005	2940
5	13	4400	3573	4443	3500	4377	3208	4079	3241	4015	2895	3964	3050

B3: Effective tension in lifting wire for installation of a module weighing 600t

The highest and lowest effective tension in lifting wire are presented in table B3-1 – table B3-18 for wave heading 165°, 180° and 190°, significant wave heights, H_s , ranging from 2,5 – 5m, corresponding zero-up-crossing wave periods, T_z , and submergence levels $z = 1m, 0m, -1m, -5m, -10m, -15m$.

Table B3 - 1: Maximum and minimum effective tension in lifting for wave heading 165° and $H_s = 2,5m$

Wave direction: 165°													
Sea state		Wire tension [kN] z = 1		Wire tension [kN] z = 0		Wire tension [kN] z = - 1		Wire tension [kN] z = - 5		Wire tension [kN] z = - 10		Wire tension [kN] z = - 15	
H_s [m]	T_z [s]	Max	Min	Max	Min	Max	Min	Max	Min	Max	Min	Max	Min
2,5	4	6664	4865	8055	3823	8230	2041	6943	4680	6315	4422	5586	4530
2,5	5	6422	5325	7619	3689	7795	3761	6430	4705	5737	4622	5581	4711
2,5	6	6267	5319	6946	4766	6808	4187	6111	4655	5698	4607	5597	4619
2,5	7	6438	5398	6662	4719	6694	4146	6288	4388	5822	4316	5885	4418
2,5	8	6693	5279	6693	4789	6707	4832	6300	4390	6255	4331	5881	4444
2,5	9	6629	5394	6831	5212	6561	4625	6108	4868	5797	4580	5730	4552
2,5	10	6349	5463	6344	5407	6461	4952	6015	5037	5854	4512	5881	4498
2,5	11	6258	5482	6297	5480	6243	5267	5895	5033	5670	4566	5592	4737
2,5	12	6159	5568	6240	5445	6223	5407	5874	4998	5567	4658	5521	4599
2,5	13	6196	5653	6393	5565	6335	5467	5936	5162	5575	4786	5489	4755

Table B3 - 2: Maximum and minimum effective tension in lifting for wave heading 165° and $H_s = 3m$

Wave direction: 165°													
Sea state		Wire tension [kN] z = 1		Wire tension [kN] z = 0		Wire tension [kN] z = - 1		Wire tension [kN] z = - 5		Wire tension [kN] z = - 10		Wire tension [kN] z = - 15	
H_s [m]	T_z [s]	Max	Min	Max	Min	Max	Min	Max	Min	Max	Min	Max	Min
3	5	6906	4667	7977	3063	8984	1516	6663	4418	6090	4364	5675	4638
3	6	6516	5437	7477	4309	7039	3482	6340	4315	5985	4252	5769	4549
3	7	6658	5272	6857	4207	7000	3287	6569	3965	5988	4139	6052	4284
3	8	6977	5136	6958	4198	6940	4509	6564	3940	5976	4278	6041	4353
3	9	6832	5282	6856	4938	6726	4049	6312	4674	6172	4167	5930	4421
3	10	6438	5368	6453	5275	6646	4679	6163	4894	5763	4574	5865	4499
3	11	6353	5395	6359	5402	6280	5066	5990	4919	5822	4565	5692	4617
3	12	6230	5499	6342	5382	6256	5287	5963	4975	5640	4637	5604	4556
3	13	6270	5613	6421	5501	6367	5372	5944	5113	5584	4753	5551	4752

Table B3 - 3: Maximum and minimum effective tension in lifting for wave heading 165° and $H_s = 3,5m$

Wave direction: 165°													
Sea state		Wire tension [kN] z = 1		Wire tension [kN] z = 0		Wire tension [kN] z = - 1		Wire tension [kN] z = - 5		Wire tension [kN] z = - 10		Wire tension [kN] z = - 15	
H_s [m]	T_z [s]	Max	Min	Max	Min	Max	Min	Max	Min	Max	Min	Max	Min
3,5	5	7741	3939	11561	274	12326	1603	8317	4191	6133	4296	5767	4506
3,5	6	6837	5147	8109	3736	10364	1986	7555	3914	5992	4156	5804	4522
3,5	7	6956	5157	7174	3707	7333	2432	6825	3348	6221	3806	6244	4177
3,5	8	7159	5024	7328	3472	7209	4147	6816	3413	6175	4062	6233	4214
3,5	9	6976	5198	7008	4613	6967	3511	6560	4401	6116	4276	6106	4222
3,5	10	6545	5274	6590	5034	6853	4337	6321	4732	6054	4459	6135	4265
3,5	11	6494	5300	6425	5324	6363	4838	6142	4745	5817	4461	5711	4594
3,5	12	6307	5427	6484	5297	6356	5133	6093	4930	5817	4442	5719	4504
3,5	13	6351	5574	6446	5439	6387	5260	5957	5036	5674	4664	5636	4686

Table B3 - 4: Maximum and minimum effective tension in lifting for wave heading 165° and $H_s = 4\text{m}$

Wave direction: 165°													
Sea state		Wire tension [kN] z = 1		Wire tension [kN] z = 0		Wire tension [kN] z = - 1		Wire tension [kN] z = - 5		Wire tension [kN] z = - 10		Wire tension [kN] z = - 15	
H _s [m]	Tz [s]	Max	Min	Max	Min	Max	Min	Max	Min	Max	Min	Max	Min
4	6	7190	4515	8614	3089	13229	0	6941	3381	6462	4033	5998	4406
4	7	7253	4784	7373	2805	11823	262	7109	2728	6615	3503	6426	4027
4	8	7235	4620	7562	2808	7431	0	7156	2856	6308	3733	6489	4105
4	9	7006	5141	7301	4229	7196	2875	6683	4101	6267	3926	6263	4137
4	10	6683	5193	6719	4724	7075	4001	6486	4532	6426	4023	6148	4295
4	11	6695	5206	6503	5240	6488	4606	6247	4569	5995	4409	5975	4411
4	12	6386	5355	6593	5205	6453	4946	6202	4785	5971	4303	5887	4529
4	13	6435	5538	6502	5376	6407	5123	6043	4860	5870	4577	5746	4607

Table B3 - 5: Maximum and minimum effective tension in lifting for wave heading 165° and $H_s = 4,5\text{m}$

Wave direction: 165°													
Sea state		Wire tension [kN] z = 1		Wire tension [kN] z = 0		Wire tension [kN] z = - 1		Wire tension [kN] z = - 5		Wire tension [kN] z = - 10		Wire tension [kN] z = - 15	
H _s [m]	Tz [s]	Max	Min	Max	Min	Max	Min	Max	Min	Max	Min	Max	Min
4,5	6	7725	4042	8532	2478	14926	0	8234	2655	6283	3535	5988	4380
4,5	7	7329	4229	8550	1729	12365	252	7623	1879	7025	3164	6798	3879
4,5	8	7816	4317	8007	2115	9555	0	7813	2296	6685	3400	6735	3938
4,5	9	7078	5067	7558	3678	7720	2234	7094	3735	6560	3692	6383	4068
4,5	10	6848	5120	6857	4384	7349	3739	6687	4281	6460	3836	6360	4053
4,5	11	6994	5121	6605	5069	6621	4378	6391	4324	6484	4165	6135	4194
4,5	12	6457	5286	6731	5102	6561	4780	6358	4663	5956	4308	5881	4419
4,5	13	6510	5501	6592	5307	6498	4964	6051	4756	5879	4452	5801	4562

Table B3 - 6: Maximum and minimum effective tension in lifting for wave heading 165° and $H_s = 5\text{m}$

Wave direction: 165°													
Sea state		Wire tension [kN] z = 1		Wire tension [kN] z = 0		Wire tension [kN] z = - 1		Wire tension [kN] z = - 5		Wire tension [kN] z = - 10		Wire tension [kN] z = - 15	
H _s [m]	Tz [s]	Max	Min	Max	Min	Max	Min	Max	Min	Max	Min	Max	Min
5	6	8243	2726	11965	1595	16532	0	12469	1492	6529	3280	6206	4242
5	7	7551	3771	10083	361	15684	0	12312	1690	7440	2795	6889	3716
5	8	7861	4344	8426	1181	14965	73	9120	1665	7026	2997	6959	3857
5	9	7144	5005	7644	2957	10846	325	7255	3356	6675	3599	6604	3878
5	10	7021	5070	7046	4104	9291	0	6937	3983	6586	3811	6567	3862
5	11	7272	5040	6700	4875	6795	2008	6534	4073	6514	4097	6159	4335
5	12	6512	5216	6859	4900	6674	4558	6491	4511	6116	4094	6003	4358
5	13	6586	5462	6726	5245	6618	4780	6131	4595	5968	4379	6034	4361

Table B3 - 7: Maximum and minimum effective tension in lifting for wave heading 180° and $H_s = 2,5\text{m}$

Wave direction: 180°													
Sea state		Wire tension [kN] z = 1		Wire tension [kN] z = 0		Wire tension [kN] z = - 1		Wire tension [kN] z = - 5		Wire tension [kN] z = - 10		Wire tension [kN] z = - 15	
H _s [m]	Tz [s]	Max	Min	Max	Min	Max	Min	Max	Min	Max	Min	Max	Min
2,5	4	6628	5051	8080	3942	8153	1993	7173	4717	6177	4423	5526	4704
2,5	5	6320	5414	7224	4588	7382	4287	6341	4879	5640	4701	5615	4726
2,5	6	6257	5506	6747	4856	6734	4735	6083	4841	5598	4692	5485	4630
2,5	7	6357	5440	6590	4852	6634	4743	6182	4754	5704	4401	5721	4596
2,5	8	6400	5393	6559	5062	6591	4848	6180	4615	5837	4601	5888	4504
2,5	9	6361	5491	6471	5355	6501	5030	6063	4858	5689	4651	5692	4567
2,5	10	6342	5488	6331	5382	6406	5060	5977	4985	5619	4740	5679	4628
2,5	11	6168	5528	6227	5449	6218	5335	5866	4977	5676	4646	5599	4746
2,5	12	6135	5576	6218	5479	6264	5413	5826	5005	5555	4678	5484	4625
2,5	13	6179	5632	6393	5570	6299	5470	5930	5158	5522	4784	5500	4748

Table B3 - 8: Maximum and minimum effective tension in lifting for wave heading 180° and $H_s = 3$

Wave direction: 180°													
Sea state		Wire tension [kN] z = 1		Wire tension [kN] z = 0		Wire tension [kN] z = - 1		Wire tension [kN] z = - 5		Wire tension [kN] z = - 10		Wire tension [kN] z = - 15	
H_s [m]	T_z [s]	Max	Min	Max	Min	Max	Min	Max	Min	Max	Min	Max	Min
3	5	6730	4807	7582	3954	8612	2040	6559	4704	5887	4527	5854	4609
3	6	6328	5430	7208	4440	6997	4344	6359	4615	5686	4577	5585	4588
3	7	6552	5353	6862	4324	6937	4425	6382	4496	5833	4294	5915	4477
3	8	6509	5287	6703	4662	6827	4427	6428	4308	5922	4433	6042	4395
3	9	6483	5403	6633	5146	6699	4718	6245	4558	5810	4523	5830	4457
3	10	6438	5403	6448	5276	6579	4823	6125	4830	5745	4653	5825	4537
3	11	6233	5458	6315	5376	6239	5196	5957	4951	5752	4607	5630	4678
3	12	6188	5512	6309	5399	6275	5279	5912	4978	5656	4667	5560	4585
3	13	6242	5584	6427	5503	6316	5389	5942	5134	5593	4793	5567	4744

Table B3 - 9: Maximum and minimum effective tension in lifting for wave heading 180° and $H_s = 3,5$ m

Wave direction: 180°													
Sea state		Wire tension [kN] z = 1		Wire tension [kN] z = 0		Wire tension [kN] z = - 1		Wire tension [kN] z = - 5		Wire tension [kN] z = - 10		Wire tension [kN] z = - 15	
H_s [m]	T_z [s]	Max	Min	Max	Min	Max	Min	Max	Min	Max	Min	Max	Min
3,5	5	7475	4039	8246	3455	8993	1682	6927	4496	6072	4430	5792	4554
3,5	6	6594	5251	7620	3691	8979	3987	6664	4322	6051	4353	5734	4452
3,5	7	6811	5094	7209	3711	7282	3996	6623	4144	6020	4083	6046	4361
3,5	8	6628	5175	6917	4197	7061	4025	6793	4065	6235	4242	6197	4285
3,5	9	6601	5316	6779	4873	6904	4362	6420	4438	5938	4358	5977	4349
3,5	10	6535	5316	6557	5169	6759	4600	6265	4696	5893	4552	5961	4435
3,5	11	6301	5382	6405	5290	6333	5030	6063	4904	5839	4562	5730	4614
3,5	12	6242	5447	6413	5313	6326	5127	6005	4934	5763	4647	5638	4546
3,5	13	6302	5537	6465	5435	6332	5281	5954	5014	5684	4752	5651	4696

Table B3 - 10: Maximum and minimum effective tension in lifting for wave heading 180° and $H_s = 4$ m

Wave direction: 180°													
Sea state		Wire tension [kN] z = 1		Wire tension [kN] z = 0		Wire tension [kN] z = - 1		Wire tension [kN] z = - 5		Wire tension [kN] z = - 10		Wire tension [kN] z = - 15	
H_s [m]	T_z [s]	Max	Min	Max	Min	Max	Min	Max	Min	Max	Min	Max	Min
4	6	7127	4938	8004	2975	13284	369	6909	3922	6270	4336	5801	4473
4	7	7200	4630	7679	3076	1108	0	6876	3594	6303	3799	6169	4253
4	8	7093	4816	7151	3662	9352	3502	7016	3637	6225	3974	6424	4185
4	9	6729	5221	6986	4537	7118	3965	6615	4395	6102	4189	6118	4244
4	10	6625	5223	6647	5046	6926	4362	6438	4391	6053	4429	6115	4336
4	11	6434	5296	6497	5205	6437	4801	6206	4772	5964	4435	5849	4541
4	12	6298	5383	6511	5225	6415	4941	6106	4849	5873	4546	5716	4507
4	13	6368	5491	6505	5367	6349	5155	5966	4878	5778	4684	5737	4635

Table B3 - 11: Maximum and minimum effective tension in lifting for wave heading 180° and $H_s = 4,5$ m

Wave direction: 180°													
Sea state		Wire tension [kN] z = 1		Wire tension [kN] z = 0		Wire tension [kN] z = - 1		Wire tension [kN] z = - 5		Wire tension [kN] z = - 10		Wire tension [kN] z = - 15	
H_s [m]	T_z [s]	Max	Min	Max	Min	Max	Min	Max	Min	Max	Min	Max	Min
4,5	6	7399	4755	10562	2418	13926	29	7704	3602	6017	4270	5802	4438
4,5	7	7657	4072	8104	2465	13023	0	7145	2942	6619	3550	6319	4154
4,5	8	7260	4374	7380	3059	7511	3040	7451	3224	6408	3698	6582	4063
4,5	9	6877	5121	7188	4195	7303	1098	6853	4100	6263	4014	6264	4146
4,5	10	6720	5131	6717	4772	7131	4104	6611	4024	6148	4286	6261	4235
4,5	11	6662	5208	6591	5121	6556	4528	6399	4610	6093	4315	5948	4463
4,5	12	6351	5318	6602	5134	6506	4739	6218	4684	6010	4382	5800	4469
4,5	13	6432	5445	6544	5297	6413	5016	6031	4753	5874	4609	5827	4573

Table B3 - 12: Maximum and minimum effective tension in lifting for wave heading 180° and $H_s = 5\text{m}$

Wave direction: 180°													
Sea state		Wire tension [kN] z = 1		Wire tension [kN] z = 0		Wire tension [kN] z = - 1		Wire tension [kN] z = - 5		Wire tension [kN] z = - 10		Wire tension [kN] z = - 15	
H _s [m]	Tz [s]	Max	Min	Max	Min	Max	Min	Max	Min	Max	Min	Max	Min
5	6	7672	4353	10603	1539	16785	0	13652	3169	6104	4096	5945	4390
5	7	8227	3425	8135	1876	12365	241	7403	2233	6952	3341	6525	4053
5	8	7238	4038	7768	2401	9201	2528	7698	2573	6690	3389	6861	3948
5	9	7009	5022	7358	3782	7455	3203	7101	3792	6463	3808	6452	4026
5	10	6847	5038	6803	4437	7405	3772	6781	3672	6364	4133	6422	4124
5	11	6908	5121	6687	4994	6675	4191	6494	4417	6250	4185	6067	4397
5	12	6407	5254	6718	5039	6598	4494	6331	4566	6128	4147	5891	4408
5	13	6498	5400	6582	5225	6500	4848	6115	4612	5975	4519	5921	4508

Table B3 - 13: Maximum and minimum effective tension in lifting for wave heading 195° and $H_s = 2,5\text{m}$

Wave direction: 195°													
Sea state		Wire tension [kN] z = 1		Wire tension [kN] z = 0		Wire tension [kN] z = - 1		Wire tension [kN] z = - 5		Wire tension [kN] z = - 10		Wire tension [kN] z = - 15	
H _s [m]	Tz [s]	Max	Min	Max	Min	Max	Min	Max	Min	Max	Min	Max	Min
2,5	4	6736	5123	7811	4091	8185	1705	6968	4711	6161	4376	5676	4631
2,5	5	6396	5399	7699	4419	7112	2452	6516	4904	5691	4582	5657	4601
2,5	6	6273	5498	6722	5069	6795	4950	6135	4882	5620	4700	5532	4688
2,5	7	6394	5433	6602	5189	6437	4920	6146	4771	5708	4324	5713	4598
2,5	8	6633	5302	6625	5238	6483	5119	6100	4769	5810	4547	5808	4496
2,5	9	6573	5473	6543	5361	6401	5180	6033	4963	5737	4672	5710	4570
2,5	10	6383	5458	6366	5397	6401	5287	5937	5028	5631	4721	5700	4612
2,5	11	6209	5478	6350	5454	6219	5370	5845	4993	5646	4689	5572	4746
2,5	12	6160	5555	6252	5442	6257	5487	5800	5012	5530	4708	5491	4633
2,5	13	6217	5612	6401	5562	6333	5470	5910	5153	5522	4796	5506	4746

Table B3 - 14: Maximum and minimum effective tension in lifting for wave heading 195° and $H_s = 3\text{m}$

Wave direction: 195°													
Sea state		Wire tension [kN] z = 1		Wire tension [kN] z = 0		Wire tension [kN] z = - 1		Wire tension [kN] z = - 5		Wire tension [kN] z = - 10		Wire tension [kN] z = - 15	
H _s [m]	Tz [s]	Max	Min	Max	Min	Max	Min	Max	Min	Max	Min	Max	Min
3	5	6572	5012	7515	3872	8794	2067	7041	4694	6134	4360	5798	4502
3	6	6339	5425	7006	4602	7106	4660	6311	4890	5699	4583	5626	4600
3	7	6505	5329	6937	4885	6587	4655	6297	4555	5876	4261	5855	4521
3	8	6923	5127	6833	4942	6668	4845	6254	4518	5852	4336	5973	4387
3	9	6776	5346	6765	5221	6554	5049	6198	4805	6041	4364	5913	4351
3	10	6481	5366	6463	5297	6559	5116	6050	4851	5719	4614	5841	4518
3	11	6290	5390	6421	5373	6248	5268	5914	4969	5753	4666	5633	4673
3	12	6223	5486	6340	5352	6267	5424	5875	5013	5642	4695	5569	4591
3	13	6292	5560	6430	5503	6366	5405	5915	5156	5600	4761	5557	4739

Table B3 - 15: Maximum and minimum effective tension in lifting for wave heading 195° and $H_s = 3,5\text{m}$

Wave direction: 195°													
Sea state		Wire tension [kN] z = 1		Wire tension [kN] z = 0		Wire tension [kN] z = - 1		Wire tension [kN] z = - 5		Wire tension [kN] z = - 10		Wire tension [kN] z = - 15	
H _s [m]	Tz [s]	Max	Min	Max	Min	Max	Min	Max	Min	Max	Min	Max	Min
3,5	5	7618	4143	8846	3173	8956	0	7405	4646	6042	4480	5933	4327
3,5	6	6443	5353	7110	4021	8620	1268	6575	4685	5796	4436	5725	4532
3,5	7	6592	5216	7147	4532	6754	4227	6639	4184	5976	4169	5929	4449
3,5	8	7205	4942	7087	4585	6841	4499	6468	4264	6003	4133	6173	4289
3,5	9	7059	5119	6911	5105	6713	4784	6498	4628	6076	4435	6118	4319
3,5	10	6569	5267	6595	5186	6755	4887	6167	4622	6208	4357	6146	4307
3,5	11	6378	5308	6426	5289	6350	5166	6006	4937	5950	4611	5723	4603
3,5	12	6288	5417	6451	5267	6287	5350	5957	4985	5722	4685	5648	4556
3,5	13	6369	5510	6461	5430	6400	5322	5922	5127	5711	4691	5633	4722

Table B3 - 16: Maximum and minimum effective tension in lifting for wave heading 195° and $H_s = 4\text{m}$

Wave direction: 195°													
Sea state		Wire tension [kN] z = 1		Wire tension [kN] z = 0		Wire tension [kN] z = - 1		Wire tension [kN] z = - 5		Wire tension [kN] z = - 10		Wire tension [kN] z = - 15	
H _s [m]	Tz [s]	Max	Min	Max	Min	Max	Min	Max	Min	Max	Min	Max	Min
4	6	6693	5149	9085	856	11694	259	8965	4429	6098	4292	5797	4414
4	7	6773	5079	7303	2046	10530	3792	6702	4223	6190	4031	6098	4337
4	8	7381	4751	7270	4269	7047	4109	6723	3999	6116	3859	6362	4170
4	9	7382	4917	7008	4926	6886	4524	6509	4406	6509	3975	6222	4083
4	10	6668	5173	6700	5067	7002	4639	6298	4520	5989	4383	6099	4313
4	11	6469	5231	6511	5209	6435	5003	6090	4757	5995	4485	5890	4548
4	12	6351	5345	6526	5180	6363	5235	6037	4864	5843	4621	5755	4550
4	13	6450	5461	6488	5375	6407	5212	5968	5072	5784	4618	5740	4648

Table B3 - 17: Maximum and minimum effective tension in lifting for wave heading 195° and $H_s = 4,5\text{m}$

Wave direction: 195°													
Sea state		Wire tension [kN] z = 1		Wire tension [kN] z = 0		Wire tension [kN] z = - 1		Wire tension [kN] z = - 5		Wire tension [kN] z = - 10		Wire tension [kN] z = - 15	
H _s [m]	Tz [s]	Max	Min	Max	Min	Max	Min	Max	Min	Max	Min	Max	Min
4,5	6	7027	4758	8248	2742	12695	79	8894	4141	6522	4108	5892	4354
4,5	7	6892	4851	7676	3731	11849	52	6982	3805	6343	4030	6285	4210
4,5	8	7584	4809	7694	3838	1005	3680	7054	3583	6253	3548	6543	4066
4,5	9	7428	4896	7229	4779	7142	4345	6723	4147	6443	3772	6476	3953
4,5	10	6793	5109	6833	4824	7207	4358	6427	4307	6101	4216	6242	4209
4,5	11	6562	5164	6616	5117	6542	4841	6241	4579	6117	4339	5972	4427
4,5	12	6416	5271	6607	5085	6447	5095	6116	4784	5942	4558	5865	4498
4,5	13	6529	5414	6562	5309	6447	5089	6041	4992	5870	4532	5834	4604

Table B3 - 18: Maximum and minimum effective tension in lifting for wave heading 195° and $H_s = 5\text{m}$

Wave direction: 195°													
Sea state		Wire tension [kN] z = 1		Wire tension [kN] z = 0		Wire tension [kN] z = - 1		Wire tension [kN] z = - 5		Wire tension [kN] z = - 10		Wire tension [kN] z = - 15	
H _s [m]	Tz [s]	Max	Min	Max	Min	Max	Min	Max	Min	Max	Min	Max	Min
5	6	7454	4289	9852	1050	15623	0	9793	3739	6544	4166	5951	4242
5	7	7094	4555	8672	0	14685	0	7187	3594	6550	3781	6354	4150
5	8	7556	4532	8099	837	11656	85	7382	3157	6443	3245	6747	3986
5	9	7570	4941	7417	2769	11349	0	7090	3918	6960	3523	6638	3934
5	10	6935	5063	6994	4574	7427	1536	6559	4130	6272	4012	6471	4006
5	11	6719	5096	6692	5035	6677	4612	6444	4434	6183	4234	6086	4363
5	12	6483	5196	6728	5003	6538	4960	6265	4706	6191	4443	5920	4483
5	13	6600	5370	6668	5231	6471	4939	6122	4920	5974	4392	5910	4539

Appendix C - Weather Statistics

C1: Wave scatter diagram

Table C1- 1: Wave Scatter Diagram for the Location Haltenbanken in the North Sea (Birk & Clauss, 1998)

Significant wave height Hs [m]	Zero-up-crossing period Tz [s]												
	0	4	5	6	7	8	9	10	11	12	13	14	15
0,0 - 0,5	22	18	9	2	0	0	0	0	0	0	0	0	0
0,5 - 1,0	729	755	328	98	19	3	0	0	0	0	0	0	0
1,0 - 1,5	725	1600	873	365	70	7	3	0	0	0	0	0	0
1,5 - 2,0	83	1151	1106	607	198	39	7	0	0	0	0	0	0
2,0 - 2,5	0	310	1010	744	283	72	18	3	0	0	0	0	0
2,5 - 3,0	0	16	640	642	304	97	15	2	0	0	0	0	1
3,0 - 3,5	0	0	187	514	293	78	16	0	0	0	0	0	0
3,5 - 4,0	0	0	33	407	263	101	9	0	0	0	0	0	0
4,0 - 4,5	0	0	1	235	271	75	28	2	0	0	0	0	0
4,5 - 5,0	0	0	0	79	256	86	16	1	0	0	0	0	0
5,0 - 5,5	0	0	0	7	194	75	17	0	1	0	0	0	0
5,5 - 6,0	0	0	0	0	117	91	14	1	0	0	0	0	0
6,0 - 6,5	0	0	0	0	31	91	7	3	0	0	0	0	0
6,5 - 7,0	0	0	0	0	8	61	16	1	0	0	0	0	0
7,0 - 7,5	0	0	0	0	3	30	14	1	0	0	0	0	0
7,5 - 8,0	0	0	0	0	0	19	27	5	0	0	0	0	0
8,0 - 8,5	0	0	0	0	0	6	22	3	0	0	0	0	0
8,5 - 9,0	0	0	0	0	0	0	13	5	0	0	0	0	0
9,0 - 9,5	0	0	0	0	0	0	10	4	1	0	0	0	0
9,5 - 10,0	0	0	0	0	0	0	2	3	1	0	0	0	0
10,0 - 10,5	0	0	0	0	0	0	0	1	0	0	0	0	0
10,5 - 11,0	0	0	0	0	0	0	0	2	0	0	0	0	0
11,0 - 11,5	0	0	0	0	0	0	0	1	0	0	0	0	0
11,5 - 12,0	0	0	0	0	0	0	0	1	0	0	0	0	0

C2: Hindcast Wave Data

Table C2- 1: Åsgard Field - Duration of seastates (hours) where significant wave height is below specified values. Data: DNMI Hindcast Gridpnt 1221 (1955-1995), (Haver, 1999)

Month	2m				3m			
	Mean (h)	Stdev.(h)	Max (h)	# events	Mean (h)	Stdev.(h)	Max (h)	# events
1	42	44	247	3.4	73	84	425	5.1
2	45	44	323	3.9	80	96	610	4.7
3	54	59	430	4.2	99	124	976	5.1
4	69	60	321	4.9	156	221	1.841	4.7
5	104	106	642	5.3	288	301	1.536	3.5
6	112	122	1.034	5.0	376	414	1.790	2.9
7	136	142	745	4.7	451	451	1.852	2.4
8	131	127	823	4.4	327	274	1.224	2.5
9	71	71	441	4.9	126	138	867	4.9
10	52	55	341	4.2	75	93	771	5.9
11	38	38	255	4.0	63	68	400	6.0
12	38	36	243	3.2	58	65	443	5.6
Year	75	92	1.034	49.5	126	207	1.852	47.0
Month	4m				5m			
	Mean (h)	Stdev.(h)	Max (h)	# events	Mean (h)	Stdev.(h)	Max (h)	# events
1	112	137	759	5.2	178	400	4.984	4.8
2	143	216	2.104	4.2	229	453	4.487	4.0
3	183	282	2.089	4.7	392	717	4.795	3.8
4	414	656	3.852	3.5	996	1.230	4.559	2.2
5	768	909	3.746	2.3	1.614	1.303	3.839	1.6
6	1.028	886	3.137	1.7	1.770	1.036	3.147	1.3
7	981	701	2.579	1.5	1.653	626	2.757	1.1
8	603	430	1.835	1.7	963	516	2.013	1.3
9	252	258	1.595	3.3	403	371	1.784	2.4
10	134	184	1.488	5.3	237	267	1.491	4.0
11	111	130	761	5.4	200	219	1.086	4.0
12	80	93	555	6.7	142	190	1.361	5.5
Year	200	389	3.852	36.5	317	633	4.984	25.4
Month	6m				7m			
	Mean (h)	Stdev.(h)	Max (h)	# events	Mean (h)	Stdev.(h)	Max (h)	# events
1	307	683	5.757	4.0	566	1.144	6.698	2.9
2	549	1.073	5.616	2.9	960	1.614	6.326	2.2
3	882	1.534	5.601	3.0	1.994	2.405	7.759	2.1
4	2.263	1.860	5.246	1.6	3.567	2.029	7.480	1.2
5	2.822	1.298	4.713	1.1	3.299	1.714	6.760	1.2
6	2.531	930	3.969	1.1	3.204	1.093	6.016	1.0
7	2.066	634	3.249	1.0	2.707	825	5.296	1.0
8	1.353	556	2.505	1.1	1.963	825	4.552	1.0
9	653	490	1.804	1.8	1.166	789	3.808	1.3
10	435	376	1.494	2.5	747	623	3.088	1.8
11	328	349	2.175	3.0	566	525	2.344	2.1
12	275	339	1.865	3.8	439	515	2.283	2.7
Year	544	1.030	5.757	15.5	961	1.594	7.759	9.0

C3: Mean duration for weather windows below operational criteria

The mean duration for weather windows below operational criteria for installation of the different modules are found by linear interpolation in the hindcast wave datasheets in Appendix C2, and is given in table C3-1 not including alpha factor, and table C3-2 including alpha factor.

Table C3-1: Mean time below threshold [h] for operational criteria for installing modules, not included alpha factor

Month	Module 289t, $H_s = 4.5m$	Module 400t, $H_s = 4m$	Module 600t, $H_s = 3m$
January	145	112	73
February	186	143	80
March	287,5	183	99
April	705	414	156
May	1191	768	288
June	1399	1028	376
July	1317	981	451
August	783	603	327
September	327,5	252	126
October	185,5	134	75
November	155,5	111	63
December	111	80	58

Table C3-2: Mean time below threshold [h] for operational criteria for installing modules, included alpha factor

Month	Module 289t, $OP_{WF} = 3.75m$	Module 400t, $OP_{WF} = 3.32m$	Module 600t, $OP_{WF} = 2.45m$
January	102.1	85.5	55.8
February	127.0	100.2	60.6
March	161.7	125.9	74.0
April	348.5	238.6	107.7
May	646.1	441.6	185.9
June	862.4	584.6	229.5
July	846.4	620.6	276.2
August	532.9	415.3	218.2
September	220.0	166.3	95.5
October	119.0	93.9	62.2
November	98.8	78.4	49.1
December	74.4	65.0	46.9

C4: Probability that the period of suitable weather is greater than 10 hours

Probability that the period of suitable weather is greater than 10 hours all twelve months of the year are given in table C4-1 not including alpha factor, and table C4-2 including alpha factor. The probability is calculated according to equation 4.5-2.

Table C4- 1: Probability of weather window greater than 10 hours throughout the year, not included alpha factor

Month	Module 289t	Module 400t	Module 600t
January	0,933	0,915	0,872
February	0,948	0,932	0,882
March	0,966	0,947	0,904
April	0,986	0,976	0,938
May	0,992	0,987	0,966
June	0,993	0,990	0,974
July	0,992	0,990	0,978
August	0,987	0,984	0,970
September	0,970	0,961	0,924
October	0,948	0,928	0,875
November	0,938	0,914	0,853
December	0,914	0,882	0,842

Table C4- 2: Probability of weather window greater than 10 hours throughout the year, included alpha factor

Month	Module 289t	Module 400t	Module 600t
January	0.907	0.890	0.836
February	0.924	0.905	0.848
March	0.940	0.924	0.874
April	0.972	0.959	0.911
May	0.985	0.978	0.948
June	0.988	0.983	0.957
July	0.988	0.984	0.964
August	0.981	0.976	0.955
September	0.956	0.942	0.901
October	0.919	0.899	0.852
November	0.904	0.880	0.816
December	0.874	0.857	0.808

Appendix D - Vessel Data Calculation

D1: Interpolation lightship weight monohull vessels

Table D1- 1: Linear interpolation used for calculation of lightship weight monohull vessel

